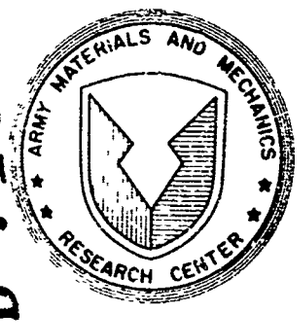

AD

AMMRC CR 70-25

EXPLOSIVE AUTOFRETTAGE OF CANNON BARRELS

February 1971

Jimmy D. Mote, Larry K. W. Ching, Robert E. Knight*,
Richard J. Fay*, and Michael A. Kaplan*

Martin Marietta Corporation
Denver Division
Denver, Colorado 80201

* Denver Research Institute
University of Denver
Denver, Colorado 80210

Final Report - Contract DAAG46-69-C-0061

Prepared for:

ARMY MATERIALS AND MECHANICS RESEARCH CENTER
Watertown, Massachusetts 02172

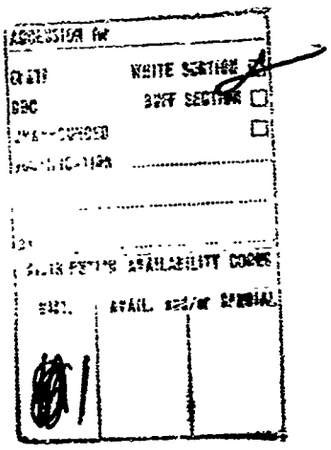

The findings in this report are not to be construed as an official Department of the Army position, unless so designated by other authorized documents.

Mention of any trade names or manufacturers in this report shall not be construed as advertising nor as an official indorsement or approval of such products or companies by the United States Government.

DISPOSITION INSTRUCTIONS

Destroy this report when it is no longer needed.
Do not return it to the originator.

AMMRC CR 70-25

EXPLOSIVE AUTOFRETTAGE OF CANNON BARRELS

Jimmy D. Mote, Larry K. W. Ching, Robert E. Knight*, Richard J. Fay*, and Michael A. Kaplan*

Martin Marietta Corporation
Denver Division
Denver, Colorado 80201

*Denver Research Institute
University of Denver
Denver, Colorado 80210

February 1971

Final Report - DAAG46-69-C-0061

D/A Project 1T062105A328
AMCMS Code 5025.11.29400
Metals Research for Army Materiel

Prepared for

ARMY MATERIALS AND MECHANICS RESEARCH CENTER
Watertown, Massachusetts 02172

Foreword

This work was performed under Contract DAAG46-69-C-0061 for the Army Materials and Mechanics Research Center. The analytical and sub-scale experimental portion of the effort was conducted under a subcontract to the University of Denver. Appreciation is expressed for contributions by Dean John A. Weese of the University of Denver, College of Engineering, during the early stages of the program. The efforts of Mr. D. D. Bouma of the Martin Marietta Corporation, Denver Division, in collecting the residual stress data for process verification are gratefully acknowledged.

ABSTRACT

The object of this program was to determine the feasibility of autofrettaging cannon barrels with explosives. The study involved determining the applicability of, the reliability of, and the scaling laws associated with the process. The results of this study provide the basis for the establishment of specifications and procedures for the explosive autofrettage of 152 mm gun barrels. The study consisted of mutually supportive experimental and analytical programs conducted concurrently.

An experimental process was undertaken to determine the expansion produced at the bore of a tube, which modelled the breech section of the 152 mm gun tube, due to different amounts of explosive material along the bore of the tube. It was found that the explosive process could be controlled to produce the desired residual bore expansion.

Using results of the analysis to make changes in the experimental approach, a method of expanding the tubes explosively was developed which gave acceptable results in both the 20% and 40% models of the breech section and also with a 40% scale model of the entire M81, 152 mm gun tube. The process was scaled up and applied to a breech section of a 105 mm gun tube.

CONTENTS

FIGURES

FIGURES

FIGURES

I. INTRODUCTION

The object of this program was to determine the feasibility of autofrettaging cannon barrels with explosives. The study involved determining the applicability of, the reliability of, and the scaling laws associated with the process. The results of this study provide the basis for the establishment of specifications and procedures for the explosive autofrettage of 152 mm gun barrels. The study consisted of mutually supportive experimental and analytical programs conducted concurrently. The analytical study developed the scaling laws and similitude requirements for scale model testing. Also, a mathematical model of the plastic response of a thick-walled cylinder to an internal impulse was completed. This model shows the effect of elastic unloading and varying pressure loadings of finite duration. The experimental program, conducted primarily with 1/5 scale models of the breech section of the 152 mm gun barrel, was used to determine the requirements of the explosive charge, such as the configuration, method of initiation, and the quantity of explosive material. This program also shows that the residual stress pattern depends on the shape of the pressure pulse.

Verification of the process was determined on a 40% scale model of the M81, 152 mm gun barrel and a breech section of a 105 mm gun tube.

II. SUMMARY

Existing methods of autofrettaging cannon barrels were investigated to determine which control and inspection procedures presently used could be used with explosively autofrettaged pieces. The external die used in the expansion of 152 mm barrels at Watervliet Arsenal was large and heavy, so it was decided to develop the process without using an external die to control expansion. The inspection processes of checking material strength and bore expansion were felt to be applicable to the explosive process.

An experimental process was undertaken to determine the expansion produced at the bore of a tube, which modelled the breech section of the 152 mm gun tube, using different amounts of explosive material along the bore of the tube. While this was under way, a mathematical analysis of the explosive process and an experimental-analytical procedure to determine the residual stresses in the walls of a thick-walled tube were started.

It was found that the explosive process could be controlled to produce the desired residual bore expansion very well. It could even be controlled to the extent that the end effects in a tube were not important. When the residual stress determination was effected, however, the residual stresses at the bore of the tube were found to be lower than desired. Hence, the experimental program was curtailed to await direction from the results of the analysis.

Using results of the analysis to make changes in the experimental methods used to expand the 20% scale tubes, acceptable residual stress

values in the range of 70-75,000 psi at the bore of the tube were obtained. These methods also essentially eliminated end effects in the autofrettaged specimens. This method was then used to autofrettage tubes which were 40% models of the breech of the gun tube. Due to a lack of control over all the pertinent parameters in the scaling process, the residual stresses obtained from the 40% tube were low, i.e., 30-40,000 psi.

Making futher use of the results of the mathematical analysis to modify the process used to expand the tubes, a method of expanding the tubes explosively was developed which gave acceptable results in both the 20% and 40% models of the breech section and also with a 40% scale model of the entire M81, 152 mm gun tube. The process was scaled up and applied to a breech section of a 105 mm gun tube. Optimization of the process was beyond the scope of this contract.

III. MATHEMATICAL ANALYSIS

This section details the mathematical development and the numerical results from the equation developed.

NOMENCLATURE

$F(b/a)$	Reyield Function
G	Shear Modulus
$G(\gamma, \eta)$	Reyield Function
I_n	Substitution Quantity
$K(t)$	A function of time
S_{ij}	Components of the deviatoric stress tensor
a	Inner radius of tube
$\underline{a}$	Acceleration
b	Outer radius of tube
d_{ij}	Components of the strain rate tensor

e	Strain or base of Naperian logarithum
g_{ij}	Components of the metric tensor
$g(r)$, $h(r)$	Substitution Quantities
k	Constant
p	Pressure
p_1	Pressure at which plastic flow ceases
p_s	Pressure required to produce total plastic flow statically
t	Time
u	Displacement
v	Velocity
$x_1 = r$	Radial Coordinate
$x_2 = \theta$	Tangential coordinate
$x_3 = Z$	Longitudinal Coordinate
α	Pressure Decay Constant
$\beta_{1, 2, 3, 4}$	Constants
γ	Ratio of the decay constant, α, to the breathing mode frequence, ω.
η	Ratio of the pressure p_1 to p_s

ρ	Mass density of the tube
ω	Breathing mode frequency of a thick-walled incompressible elastic tube
ω_{ij}	Components of the spin tensor
μ	A positive scalar
σ	Stress

1. Mathematical Model

A. Physical Description of the Process

The simplest configuration for attempting dynamic autofrettage is shown in Figure 1. A line charge is placed along the axis of the tube and held in place by end plugs. The charge is detonated in such a way that the resulting tube expansion is uniform away from the ends. This may be accomplished by simultaneous detonation at several places along the axis or for very high speed explosives, e.g., detasheet or pentolite, merely by initiating detonation at one end. The gap between the explosive and tube wall is filled with air or water. With this configuration there is little which can be done to regulate the pressure decay. However, as will be shown, the residual stresses depend intimately on the pressure-time history. Thus, a configuration affording some degree or pressure control was developed.

In this configuration, as shown in Figure 2, the explosive is placed along the axis of the air filled ductile metal tube which, in turn, is placed along the axis of the thick-walled tube to be autofrettaged. The inner tube is called the radial piston. The region between the radial piston and the outer tube is filled with water. End plugs and a restraining fixture prevent the water from rapidly escaping from the ends.

The large internal pressure, developed after detonation of the explosive, force the piston to accelerate radially. The outward motion of the piston is accompanied by expansion of the internal gases and therefore a decrease in internal pressure. At the same time, the compression of the water results in rapidly increasing cavity pressures. As this process continues, the net force on the piston becomes negative and the piston is slowed down and brought to rest. The combination of high water pressure and low gas pressure acting on the piston at this time produces large negative

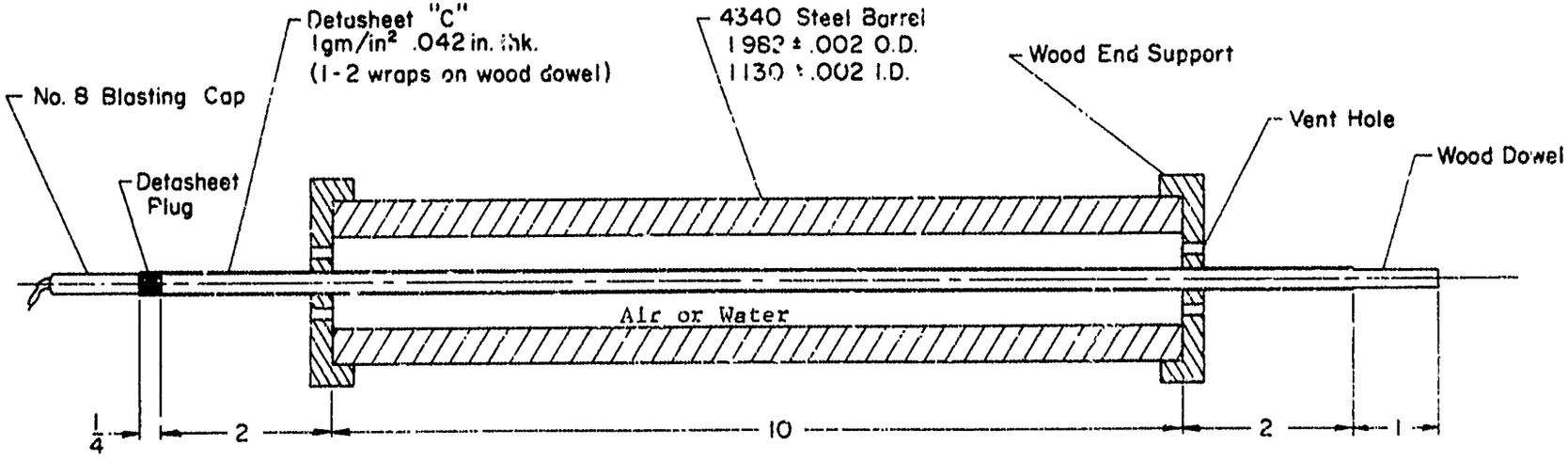

Figure 1 Explosive Charge Configuration for 1/5 Scale Barrels

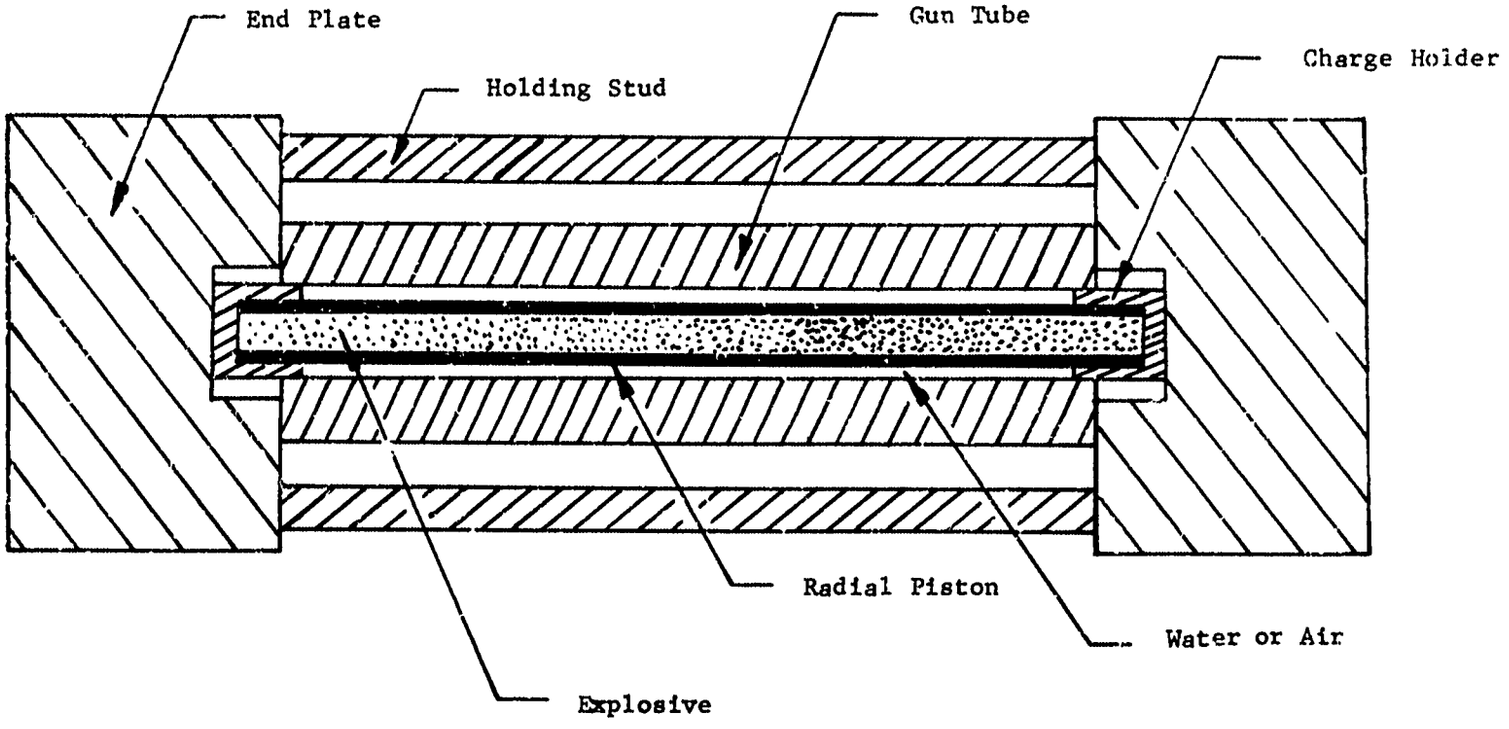

Figure 2 Final Autofrettage Fixture

radial accelerations which drive the piston inward and cause the process to reverse itself. The piston's motion is therefore oscillatory. The peak pressure in the cavity, with proper design, will be sufficient to produce total plastic flow in the outer tube. Because of energy dissipated through plastic work and an increase in the bore of the outer tube, the magnitudes of both cavity pressure and piston velocity decay rapidly with time. The outer tube, after flowing plastically, oscillates about a time dependent equilibrium position. The oscillation is due partly to the release of stored elastic energy and partly to the variation in applied pressure.

Some degree of cavity pressure control can be established by using different quantities and types of explosive, by varying the dimensions of the water gap and radial piston, and by using different materials for the piston. The configuration acts as an attenuator of the rate of energy transfer. The explosive energy released almost instantaneously at detonation is prevented, for the most part, from being rapidly transferred to the outer tube by a series of shock waves. Under these conditions the pressure at the bore of the outer tube, as well as the stress, velocity and other relevant parameters associated with the outer tube, are expected to be essentially continuous in both space and time. Also, the change in any parameter in the time necessary for a wave to travel through the outer tube wall should be small compared to the value of the parameter itself. A state satisfying these conditions will be called a state of dynamic equilibrium.

The physical description provided above becomes more and more inaccurate as the wall of the piston is thinned. The second configuration (Figure 2) then approaches the configuration shown in Figure 1, and the physical process, for short times, is more accurately pictured as a series of shock interactions. In the first configuration, an initial shock wave is produced by detonation which reflects off the inner wall of the tube causing a plastic wave and elastic precursor to begin propagating through the tube wall. The reflected shock travels radially inward until it interacts with an expanding gas bubble. The wave interactions in the cavity become quite complex beyond this point and no attempt will be made to describe them. A correspondingly complex situation exists in the tube wall.

The net result of these wave interactions is that the system is rapidly brought to a state of dynamic equilibrium. Beyond this point, the parameters can be assumed to be continuous in time. If the tube is still flowing plastically when wave processes become unimportant and if the state of stress at this time depends primarily on current conditions (as it does for the model used herein) then the residual stress will be independent of the details of the wave interactions. It is assumed that this is the case*

*Dynamic hoop strains at the outer wall of the tube were measured in one of the tests using the first configuration. In this test, a hardened steel tube, whose ratio of outer to inner wall diameter was 1.75, suffered a 1% permanent expansion at the outer wall. The strain measurements, which were essentially a measure of the radial displacement, indicated that the magnitude of wave effects was negligible at the time of cessation of plastic flow. Rapid changes in the slope of the strain curve had all but disappeared at this time.

so that a single mathematical model for the description of both configurations can be used. The model is one in which the wave speed is infinite and therefore dynamic equilibrium is reached instantaneously.

B. Basic Assumptions

In order to analytically investigate the process, the following assumptions are made:

A1. The axial and tangential velocities and displacements are negligible. The partial derivatives of all quantities with respect to the axial and tangential directions are zero.

A2. The pressure time history at the bore of the outer tube is of the form

$$p(t) = p_o e^{-\alpha t} \qquad 1.1$$

where p_o is sufficiently large to produce total plastic flow, i.e., plastic flow through the wall of the tube.

A3. The tube is composed of an isotropic incompressible elastic-plastic material which does not work harden, is not rate sensitive, and has no Baushinger effect.

Assumption A1 is merely a restatement of the conditions of axial symmetry and plane strain. It follows from A1 that the velocity, displacements, and deformation fields are functions of radial position and time. Assumption A2 is an approximation to the damped oscillatory behavior of the water pressure. The assumption of material incompressibility in A3 eliminates the possibility of wave solutions and substantially simplifies the mathematics.

C. Governing Equations

Standard tensor notation will be used in this section with a semicolon denoting covariant space differentiation and all repeated indices summed from one to three. Circular cylindrical coordinates x^1, x^2, x^3, are used denoting the radial, tangential, and longitudinal directions respectively. In the writing of specific equations, the familiar r, θ, z notation will also be employed.

(1) Kinematics

From A1

$$v_2 = v_3 = u_2 = u_3 = 0 \qquad 1.2$$

where v_i and u_i are the components of the velocity and displacement vectors respectively. The non-vanishing components v_1 and u_1 will be designated simply by v and u, i.e.,

$$v_1 = v(r, t) \tag{1.3}$$

and

$$u_1 = u(r, t). \tag{1.4}$$

The incompressibility equation

$$v^i{}_{;i} = 0 \tag{1.5}$$

reduces to

$$\frac{\partial v}{\partial r} + \frac{v}{r} = 0 \tag{1.6}$$

in view of 1.2 and 1.3. Integration of 1.6 gives

$$v = \frac{1}{r}\,\dot{K}(t) \tag{1.7}$$

where $\dot{K}(t)$ is an unknown function of time. Equation 1.7 is valid whether the tube is totally elastic, totally plastic, or partially elastic and partially plastic. In the latter case, it implies that the radial velocity is continuous across the elastic-plastic interface. The radial acceleration, $\underline{a}$, is the material derivative D/Dt of the radial velocity, where

$$\frac{D(\ )}{Dt} = \frac{\partial(\ )}{\partial t} + v^i\,(\ )_{;i}. \tag{1.8}$$

From 1.8, 1.7, and 1.2 we obtain

$$\underline{a} = \frac{\ddot{K}}{r} - \frac{\dot{K}^2}{r^3} \tag{1.9}$$

where $\ddot{K} = d\dot{K}/dt$. The strain rate tensor d_{ij} is defined as

$$d_{ij} = \frac{1}{2}(v_{i;j} + v_{j;i}). \qquad 1.10$$

Explicit expressions for d_{ij} in terms of $\dot{K}$ are found by using 1.2 and 1.7 in 1.10. The result is

$$d_{11} = -d_{22} = -\frac{K}{r^2} \; ; \quad d_{ij} = 0 \text{ otherwise.} \qquad 1.11$$

During some time interval, Δt, when the tube is not totally plastic, the change in displacements Δu and strains Δe_{ij} will be small and the equation of incompressibility 1.5 may be replaced by

$$\Delta e^{i}_{;i} = 0 \qquad 1.12$$

where the change in the components of strain are expressed in terms of the change in displacements by

$$\Delta e_{ij} = \frac{1}{2}(\Delta u_{i;j} + \Delta u_{j;i}). \qquad 1.13$$

When 1.11 is used in 1.12 along with 1.2 and 1.4, an equation in Δu analogous to 1.6 is obtained. Integration of this equation yields

$$\Delta u = u - \bar{u}(r) = \frac{K}{r} \qquad 1.14$$

where $\bar{u}(r)$ is the initial displacement at the beginning of the time interval Δt. In keeping with the usual assumptions associated with elastic behavior and constrained plastic flow, we shall consider the convective terms in the material derivatives of the components of displacements and velocity to be small compared with the partial time derivatives of these antities. Therefore, the velocity and acceleration associated with the displacements 1.14 are simply

$$v = \frac{\dot{K}}{r} \; ; \quad a = \frac{\ddot{K}}{r} \qquad 1.15$$

where the dots refer to differentiation with respect to time. The components of the change in strain in terms of K(t) are found to be

$$\Delta e_{11} = -\Delta e_{22} = -\frac{K}{r^2} \quad ; \quad \Delta e_{ij} = 0 \quad \text{otherwise} \tag{1.16}$$

by the use of 1.14 in 1.13. Equations 1.7 and 1.9 will be used during total plastic flow while equations 1.14 and 1.15 will be used for elastic and constrained plastic behavior.

Constitutive Equations

The constitutive equations for an incompressible, isotropic, linear elastic solid are

$$S_{ij} = 2Ge_{ij} \tag{1.17}$$

where G is the shear modulus and S_{ij} are the components of the deviatoric stress tensor. The components σ_{ij} of stress and the deviatoric stress are related by

$$S_{ij} = \sigma_{ij} - \frac{1}{3} g^{km} \sigma_{km} \; g_{ij} \tag{1.18}$$

where the g_{ij} are the components of the metric tensor. Equations 1.17 is valid for deformation from an initially unstressed, unstrained state. If elastic behavior is initiated from a non-zero stress state, as in the elastic unloading following plastic flow, then 1.17 must be written as

$$\Delta S_{ij} = 2 G \Delta e_{ij}. \tag{1.19}$$

Here, ΔS_{ij} and Δe_{ij} represent the changes in the initial stress and strain states produced by elastic deformation. The changes in the deviatoric stress components, obtained by using 1.16 in 1.19 are

$$\Delta S_{11} = -\Delta S_{22} = -\frac{2G}{r^2} K \quad ; \quad \Delta S_{ij} = 0 \text{ otherwise.} \tag{1.20}$$

When these are substituted into 1.18 (written in terms of Δs_{ij} and $\Delta \sigma_{ij}$), it is found that

$$\Delta\sigma_{33} = \frac{1}{2} (\Delta \sigma_{11} + \frac{1}{r^2} \Delta \sigma_{22}) \tag{1.21}$$

and

$$\frac{1}{r^2}\,\Delta\sigma_{22} - \Delta\sigma_{11} = \frac{4G}{r^2}\,K. \qquad 1.22$$

The physical components of radial and hoop stress, σ_r and σ_θ respectively, are related to the tensorial components of stress by

$$\sigma_r = \sigma_{11} \quad ; \quad \sigma_\theta = \frac{1}{r^2}\,\sigma_{22}. \qquad 1.23$$

Thus, 1.22 can be written as

$$\Delta\sigma_\theta - \Delta\sigma_r = \frac{4G}{r^2}\,K \qquad 1.24$$

The complete stress state is simply the sum of the initial stresses $\bar{\sigma}_{ij}$ and the change in stresses $\Delta\sigma_{ij}$ so that

$$\sigma_{ij} = \bar{\sigma}_{ij} + \Delta\sigma_{ij}. \qquad 1.25$$

Material behavior during plastic flow will be described by the Prandtl-Reuss equations,

$$d_{ij} = \mu S_{ij} + \frac{1}{2G}\,\dot{S}_{ij} \qquad 1.26$$

where μ is a positive scalar and the dot over the deviatoric stress denotes the Jaumann time derivative. The Jaumann derivative reduces to the material derivative when the components ω_{ij} of the spin tensor are zero, where

$$\omega_{ij} = \frac{1}{2}\,(v_{i;j} - v_{j;i}). \qquad 1.27$$

It is easily demonstrated that $\omega_{ij} = 0$ under the velocity field given by 1.2 and 1.15. Therefore, 1.8 may be used to evaluate S_{ij}. The resulting equations can be written

$$\dot{S}_{ij} = \frac{\partial S_{ij}}{\partial t} + v_1\,S_{ij;1} \qquad 1.28$$

when 1.2 is used. Evaluation of 1.26 for i = 1, j = 2 gives

$$\frac{d\,S_{12}}{dt} + (\mu - \frac{\dot{K}}{r^2})S_{12} = 0 \qquad 1.29$$

when 1.11, 1.15, and 1.28 are used, and where

$$\frac{d\,S_{ij}}{dt} = \frac{\partial S_{ij}}{\partial t} + v_1\frac{\partial S_{ij}}{\partial r} \qquad 1.30$$

is the time rate of change of S_{ij} along a particle path. The solution of 1.29 is

$$S_{12} = A\left[e^{-\mu t} + \int_{t_o}^{t} \dot{K}(\tau)/r(\tau, r_o)\,d\tau\right] \qquad 1.31$$

where A is a function of the position r_o of a particle at time t_o when plastic flow is initiated, and $r(r_o, t)$ is the particle path. The tube is unstressed prior to the application of pressure and the change in shear stress during elastic loading is zero (from 1.20). Therefore, $S_{12} = 0$ following elastic loading. The evaluation of 1.31 at $t = t_o$ shows that A = 0 and therefore

$$S_{12} = 0. \qquad 1.32$$

A continuation of the above argument for subsequent elastic and plastic behavior shows that 1.32 is valid for all times. In a similar way, we can show that S_{33} as well as all the other components of shear stress vanish. Thus

$$S_{ij} = \sigma_{ij} = 0 \quad \text{for } i \neq j, \qquad 1.33$$

and

$$S_{33} = 0. \qquad 1.34$$

The remaining independent equation of 1.26 is

$$\mu S_{11} + \frac{1}{2G} \dot{S}_{11} = -\frac{1}{r^2} \dot{K}. \qquad 1.35$$

The use of 1.34 and 1.18 yields, in terms of the physical components of stress

$$\sigma_z = \frac{1}{2} (\sigma_r + \sigma_\theta) \qquad 1.36$$

and when this is used to evaluate S_{11} and S_{22} we obtain

$$S_{11} = -S_{22} = \frac{1}{2} (\sigma_r - \sigma_\theta). \qquad 1.37$$

The Von-Mises yield condition

$$S^i_j S^j_i = \frac{1}{2} k^2 \qquad 1.38$$

will be used as the condition for plastic flow. Since the material does not work harden, k is a constant. Its value is $2\sigma_y/\sqrt{3}$, where σ_y is the yield strength of the material in tension. The yield condition simplifies to

$$\sigma_\theta - \sigma_r = \pm k \qquad 1.39$$

when 1.33, 1.34, and 1.37 are substituted into 1.38. It follows from 1.39 and 1.37 that $\dot{S}_{11} = 0$. With this result, 1.36 is written as

$$\mu = \frac{2\dot{K}}{r^2 (\sigma_\theta - \sigma_r)} . \qquad 1.40$$

Since μ is always positive during plastic flow, $\sigma_\theta - \sigma_r$ must have the same sign as $\dot{K}$. This determines the sign of k in the yield condition, 1.39. Thus

$$\sigma_\theta - \sigma_r = k \quad ; \quad \dot{K} > 0 \qquad 1.41$$

$$\sigma_\theta - \sigma_r = -k \quad ; \quad \dot{K} < 0 . \qquad 1.42$$

The first equation 1.41 holds, as can be seen from 1.15, when the tube is expanding plastically. Conversely, 1.42 is valid when the plastic flow is radially inward. When $\dot{K}$ equals zero, the condition that $\mu > 0$ is violated. Therefore, plastic flow ceases when the radial velocity vanishes. The cessation of plastic flow does not, in general, coincide with the reduction in magnitude of the applied pressure.

(2) Equations of Motion

The equations of motion, with no body force,

$$\sigma^{ij}_{\ ;j} = \rho a^i \qquad 1.43$$

where ρ is the mass density of the material, are satisfied identically when i = 2 and i = 3. For i = 1, equation 1.43 in terms of physical components reduces to

$$\frac{\partial \sigma_r}{\partial r} + \frac{\sigma_r - \sigma_\theta}{r} = \rho\left[\frac{\ddot{K}}{r} - \frac{\dot{K}^2}{r^3}\right] \qquad 1.44$$

when 1.33 and 1.9 are used. Integration of 1.44 with respect to r yields

$$\sigma_r = \rho \dot{K} \log r/b + \rho\frac{\dot{K}^2}{2}\left(\frac{1}{r^2} - \frac{1}{b^2}\right) - \int_r^b \frac{\sigma_\theta - \sigma_r}{\bar{r}}\, d\bar{r} \qquad 1.45$$

when the boundary condition that σ_r is zero at the outer radius r = b is applied. At r = a, $-\sigma_r$ is equal to the applied pressure. Therefore, 1.45 becomes

$$-p_o e^{-\alpha t} = \rho \ddot{K} \log a/b + \rho\frac{\dot{K}^2}{2}\left(\frac{1}{a^2} - \frac{1}{b^2}\right) - \int_a^b \frac{\sigma_\theta - \sigma_r}{\bar{r}}\, d\bar{r} \qquad 1.46$$

when it is evaluated at the bore and 1.1 is used. When $\sigma_\theta - \sigma_r$ is expressed in terms of K or its derivatives, equation 1.46 can be integrated to determine K as a function of time.

2. Total Plastic Flow

It has been assumed that p_o is sufficiently large to produce yielding throughout the wall of the tube. Since the tube is expanding, the yield condition 1.41 is appropriate. The substitution of 1.41 into 1.46 yields, after integration,

$$\ddot{K} = \frac{1}{\rho \log b/a}\left[p_o e^{-\alpha t} - k \log b/a + \frac{1}{2}\rho \dot{K}^2\left(\frac{1}{\epsilon^2} - \frac{1}{b^2}\right)\right]. \qquad 2.1$$

Equation 2.1 is a generalized Riccati's equation in $\dot{K}$ and is normally solved by numerical integration. The inner radius, a, and outer radius, b, are functions of time. However, the radial expansion in autofrettage is generally limited to one or two percent at the bore and therefore, a and b can be treated as constants. The equation describes behavior of the tube until plastic flow ceases, i.e., until some time, t_1, when the radial velocity and hence $\dot{K}(t_1)$ are zero. Evaluating 2.1 at t_1 we obtain

$$\ddot{K}_1 = \frac{1}{\rho \log b/a}\left[p_1 - k \log b/a\right] \qquad 2.2$$

where $p_1 = p_o e^{-\alpha t_1}$ and $K_1 = K(t_1)$. By using 2.2 and 1.41 in 1.45, the radial stress σ_{r1} at $t = t_1$ is found to be

$$\sigma_{r1} = \frac{p_1}{\log b/a} \log b/r \ . \qquad 2.3$$

The hoop stress at this time is

$$\sigma_{\theta 1} = k - \frac{p_1}{\log b/a} \log b/r \qquad 2.4$$

as can be seen by using 2.3 in 1.41. Equations 2.2, 2.3, and 2.4 together with 1.7, 1.11, and

$$\dot{K}_1 = 0 \qquad 2.5$$

show that the state of stress, velocity, and rate of deformation at the end of total plastic flow depend only on the pressure acting at that time.

The pressure, p_s, necessary to produce total plastic flow statically, i.e., with zero acceleration and negligible velocity is

$$p_s = k \log b/a. \qquad 2.6$$

This result is obtained by setting the acceleration to zero in 1.44, integrating with respect to r after using 1.41, applying the boundary condition at r = b, and equating the resulting radial stress to $-p_s$ at r = a.

The dependency of p_1 on p_o, α, and tube geometry is found by integrating 2.1 for different values of these parameters. For the particular tube under consideration, i.e., a = 2.825, b = 4.963, the term containing $\dot{K}^2$ is small when the expansion is limited to a few percent and numerical results for different values of α are nearly identical. Under these conditions, an approximate closed form solution to 2.1 is obtained when $\dot{K}^2$ in 2.1 is neglected. Integration yields

$$\dot{K} = \frac{1}{\rho \log b/a} \left[\frac{p_o}{\alpha} (1 - e^{-\alpha t}) - p_s t \right] \qquad 2.7$$

when 2.6 and the condition that $\dot{K}$ vanishes at t = 0 are used. Evaluating 2.7 at t_1 gives

$$e^{-\alpha t_1} = 1 - \frac{p_s}{p_o} \alpha t_1 \qquad 2.8$$

which can be solved for (αt_1) as a function of p_s/p_o. Therefore, for the case we are considering, $p_1/p_o = e^{-\alpha t_1}$ depends only on p_s/p_o and is independent of the decay rate.

Figure 3, which is a plot of p_o/p_s versus p_1/p_s, shows that the greater the peak cavity pressure, the lower the pressure at the cessation of total plastic flow.

The expansion of the bore during total plastic flow can be found by noting that the time rate of change of the inner radius is just the first equation of 1.15 evaluated at r = a, i.e.,

$$\frac{da}{dt} = \frac{\dot{K}}{a} . \qquad 2.9$$

Integration of 2.9 yields

$$a^2(t_1) = a_o^2 + 2 \int_o^{t_1} \dot{K}(t)\, dt \qquad 2.10$$

where a_o is the initial bore radius. An approximate solution to 2.10 can be obtained by using 2.7 together with 2.8. The result is

$$a^2(t_1) = a_o^2 + \frac{p_o - p_1}{p_s} \frac{(p_o + p_1 - 2 p_s)}{\alpha^2 \rho \log b/a} \qquad 2.11$$

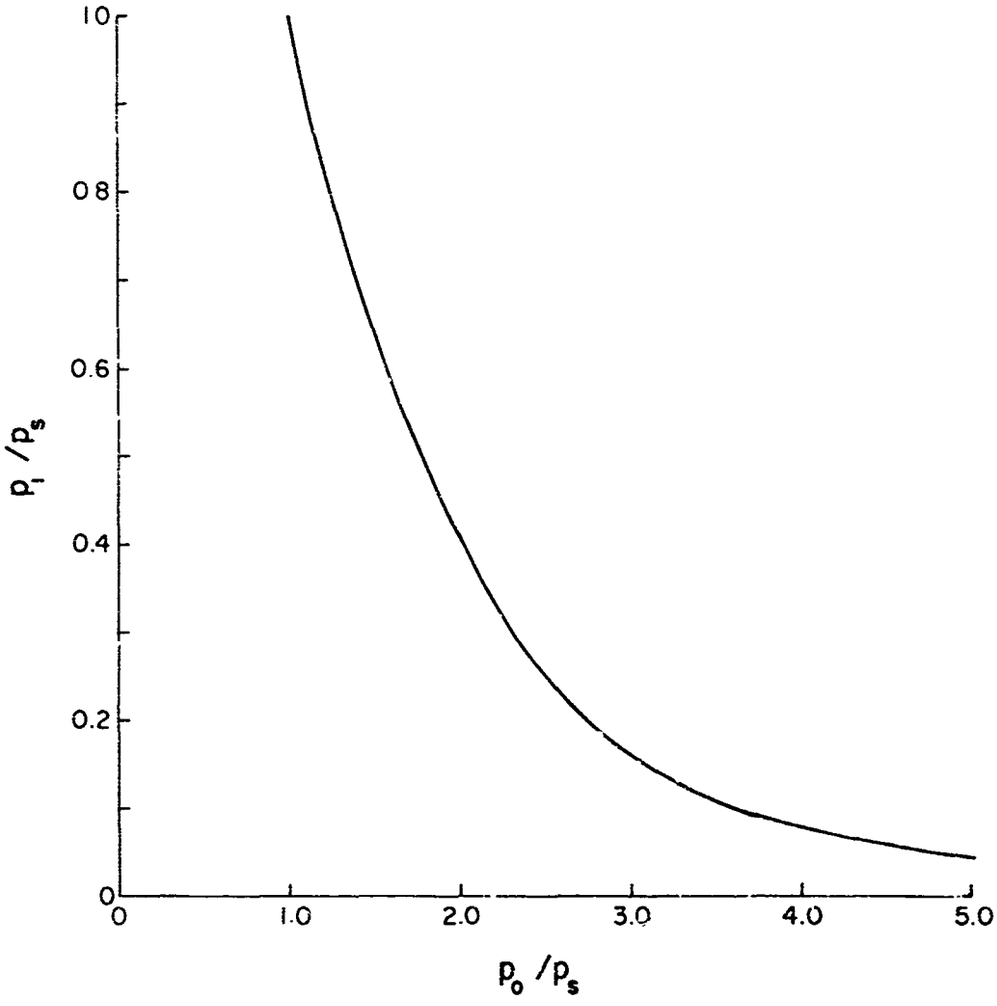

Figure 3 Peak Cavity Pressure vs. Pressure at Cessation of Total Plastic Flow

Although p_1 is independent of the decay rate, 2.11 shows the bore expansion, as expected, to be sensitive to changes in α.

3. Initial Elastic Unloading

At the cessation of plastic flow the tube is at rest, but not in equilibrium since $p_1 < p_s$. The tube begins to accelerate radially inwards (See 2.2 and 2.6) and elastic unloading begins. All changes in the stress and deformation from the initial state defined by 2.2 through 2.5 are governed by the elasticity equations. Thus, for $t \geq t_1$, the stresses are

$$\sigma_{ij} = (\sigma_{ij})_1 + \Delta\sigma_{ij} \tag{3.1}$$

where the deviatoric components of the change in stress are related to the change in strains by the incompressible elasticity equations 1.19.

The elastic displacement, velocity, and acceleration are given by 1.14 and 1.15 and the elastic change in $\sigma_\theta - \sigma_r$ by 1.24. By using 1.24, together with 3.1, 2.3, and 2.4, it is found that during elastic unloading

$$\sigma_\theta - \sigma_r = k + \frac{4G}{r^2} K. \tag{3.2}$$

It should be noted that K is proportional to the displacement measured from the deformed state at $t = t_1$. Therefore, the initial value of K is

$$K(t_1) = K_1 = 0 . \tag{3.3}$$

The differential equation for K(t)

$$\ddot{K} + \omega^2 K = \frac{p_1}{\rho \log b/a} e^{-\alpha(t - t_1)} \tag{3.4}$$

where

$$\omega^2 = \frac{2G}{\rho \log b/a} \left(\frac{1}{a^2} - \frac{1}{b^2}\right) \tag{3.5}$$

is obtained by using 3.2 in 1.46 and neglecting the convective term $\dot{K}^2$.

Equation 3.4 is the equation for the forced response of a linear oscillator whose natural frequency is ω. Therefore, ω represents the

breathing mode frequency of a thick-walled incompressible elastic tube. The solution to 3.4 is

$$K = \beta_1 \operatorname{Sin} \omega(t - t_1) + \beta_2 \operatorname{Cos} \omega(t - t_1) + \beta_3 e^{-\alpha(t - t_1)} + \beta_4 \qquad 3.6$$

where the constants β_1, β_2, β_3, and β_4 are found by substituting 3.6 into 3.4 and applying the initial conditions $K_1 = \dot{K}_1 = 0$. The result is

$$\beta_1 = \beta_3 \alpha/\omega$$

$$\beta_2 = -\beta_3 - \beta_4$$

$$\beta_3 = \frac{P_1}{\rho \log b/a} \quad \frac{1}{\alpha^2 + \omega^2} \qquad 3.7$$

$$\beta_4 = -k/\omega^2\rho$$

The response of the tube during elastic unloading, 3.6, is a linear combination of simple harmonic motion and exponential decay.

When 3.7 is used in 3.6, together with 2.6, we obtain

$$K = \frac{k}{\omega^2\rho}\left\{ \frac{\gamma\ \eta}{1+\gamma^2} \operatorname{Sin} \omega(t - t_1) + \left[1 - \frac{\eta}{1+\gamma^2}\right] \operatorname{Cos} \omega(t - t_1) + \frac{\eta}{1+\gamma^2} e^{-\alpha(t - t_1)} - 1 \right\} \qquad 3.8$$

where γ is the ratio of the decay constant α to the fundamental breathing mode frequency ω and η is the ratio of the pressure, p_1, at the initiation of elastic unloading to the static equilibrium pressure, p_s, i.e.,

$$\gamma = \frac{\alpha}{\omega} \qquad 3.9$$

$$\eta = \frac{P_1}{P_s} \qquad 3.10$$

The amplitude of the first, second, and fourth term in 3.8 is constant for given values of γ and η, while the amplitude of the exponential term decreases monotonically in time. Therefore stationary values of K decrease with time and since $K_1 = 0$ is a stationary value ($\dot{K} = 0$), it follows that K is non-positive, i.e., that

$$K \leq 0 \tag{3.11}$$

for all $t \geq t_1$. Furthermore, the minimum value of K, K_m corresponding to the largest amplitude of displacement, occurs at $t \to \infty$. The determination of K_m is straightforward. First, 3.8 is differentiated with respect to time and equated to zero. The resulting equation is

$$\text{Cos } \omega (t_m - t_1) = \frac{1 + \gamma^2 - \eta}{\eta \gamma} \text{ Sin } \omega (t_m - t_1) \tag{3.12}$$

when $t \to \infty$ and where t_m is one of the infinity of times at which 3.12 is satisfied. The identity $\text{Sin}^2 x + \text{Cos}^2 x = 1$ is used to eliminate the Cos term from 3.12, giving

$$\text{Sin}^2 \omega (t_m - t_1) = \frac{\gamma^2 \eta^2}{(1 + \gamma^2)\left[(1 - \eta)^2 + \gamma^2\right]}. \tag{3.13}$$

In solving for the Sin $\omega (t_m - t_1)$, the negative sign is chosen before the square root in order to minimize K. Thus,

$$\text{Sin } \omega (t_m - t_1) = \frac{-\gamma \eta}{\sqrt{(1 + \gamma^2)\left[(1 - \eta)^2 + \gamma^2\right]}}. \tag{3.14}$$

When 3.14 is used in 3.12 and the resulting expression for Cos $\omega (t_m - t_1)$ along with 3.14 is substituted into 3.8 and evaluated at $t = \infty$ we obtain

$$K_m = -\frac{k}{\omega^2 \rho}\left[1 + \sqrt{\frac{(1 - \eta)^2 + \gamma^2}{1 + \gamma^2}}\right] \tag{3.15}$$

after some simplification. We note from 3.15 that the maximum amplitude of displacement which occurs during elastic unloading for a given tube (fixed k, ρ, and ω) depends only on the parameters η and γ. It follows

from the definitions of η and γ, 3.9 and 3.10, and the discussion concerning p_1 in section 2 that $0 \leq \eta \leq 1$ and $0 \leq \gamma \leq \infty$. Therefore, K_m in 3.15 is bounded by

$$-\frac{2k}{\omega^2 \rho} \leq K_m \leq -\frac{k}{\omega^2 \rho} . \qquad 3.16$$

The value of the left hand side of the inequality occurs when $\eta = 0$ or $\gamma = \infty$. In either case, the initial pressure $p_1 = 0$, a circumstance which produces the maximum amplitude of initial acceleration. The right hand side of 3.16, which is the lower bound for the amplitude of elastic displacement, is obtained when $\eta = 1$ and $\gamma = 0$, corresponding to the static autofrettage process.

According to our model, elastic unloading is simply a constant amplitude oscillation about an equilibrium position which moves radially inward in time. Actually, the amplitude decreases with time due to the dissipative forces which eventually bring the tube to rest. However, the equations developed in this section for the description of tube behavior for $t \geq t_1$ will be considered to be valid for finite times if the tube remains elastic.

4. Initial Reyielding

A. The Condition for Initial Reyielding

Elastic behavior terminates when the stresses vary in such a way as to satisfy the yield condition 1.41 and 1.42, at one or more points in the tube wall. The difference between the hoop and radial stresses during initial elastic unloading is given by 3.2. We have shown that during this period, K is non-positive. When K is equal to zero, K has a relative maximum, so that $\dot{K}$ is also zero and $\ddot{K}$ is negative. Thus, according to 3.2, $\sigma_\theta - \sigma_r < k$ during initial elastic unloading (except when K is zero) and the yield condition 1.41 cannot be satisfied. If reyielding occurs, it does so when the tube is moving radially inward. The yield condition for $K < 0$ can be written in terms of K by substituting 3.2 into 1.42. The result is

$$-K = \frac{k\, r^2}{2G} . \qquad 4.1$$

Since the right hand side of 4.1 is minimized at the inner wall of the tube, reyielding begins at r = a, when

$$-K = \frac{k\, a^2}{2\, G} . \qquad 4.2$$

Thus, reyielding depends only on the amplitude of displacement during elastic unloading. Clearly, if the maximum amplitude of elastic displacement $-K_m$, exceeds the right hand side of 4.2, the tube will reyield. Therefore, using 3.15, 4.2, and 3.5 we obtain

$$1 + \sqrt{\frac{(1 - \eta)^2 + \gamma^2}{1 + \gamma^2}} \geq \frac{(1 - a^2/b^2)}{\log b/a} \qquad 4.3$$

as the condition for reyielding.

The right hand side of 4.3, which we shall call F(b/a) depends only on the tube geometry. It is plotted in Figure 4. Since $0 \leq \eta \leq 1$ and $0 \leq \gamma$, the left hand side of 4.3 is never greater than 2 or less than 1. It follows from 4.3 and Figure 4 that reyielding always occurs when $b/a \geq 2.2$. For values of b/a between 1 and 2.2, reyielding depends on the magnitude of the parameters η and γ. The left hand side of 4.3, denoted by $G(\gamma, \eta)$, is plotted in Figure 5. The values of γ and η for which the equality holds are plotted in Figure 6 for different values of b/a. Given specific values of γ, η, and b/a, the tube reyields when the coordinate point (η, γ) in Figure 6 lies below the particular b/a curve. Points above the curve indicate no reyielding.

B. Behavior Under Initial Reyielding

When the inequality 4.3 is satisfied, the tube begins to reyield initially at r = a at some time $t = t_2$. All quantities which are evaluated at this time will have the subscript 2.

The elastic displacement at t_2 is negative with the value given by 4.2. The radial velocity K_2 is also negative since reyielding begins before K reaches its maximum amplitude of negative displacement. $\dot{K}_2$ is found by differentiating 3.8 with respect to t and substituting for $e^{-\alpha(t_2 - t_1)}$ from 3.8 evaluated at t_2. This gives

$$\dot{K}_2 = \frac{k}{\omega^2 \rho}\left\{\frac{\eta - 1}{\gamma}\sin\omega(t_2 - t_1) + \cos\omega(t_2 - t_1) + \frac{a^2\omega^2\rho}{2G} - 1\right\} \qquad 4.4$$

when 4.2 is used. From 3.2 and 4.2, the difference in the radial and hoop stress at t_2 is

$$\sigma_{r2} - \sigma_{\theta 2} = k\left(2\frac{a^2}{r^2} - 1\right) \qquad 4.5$$

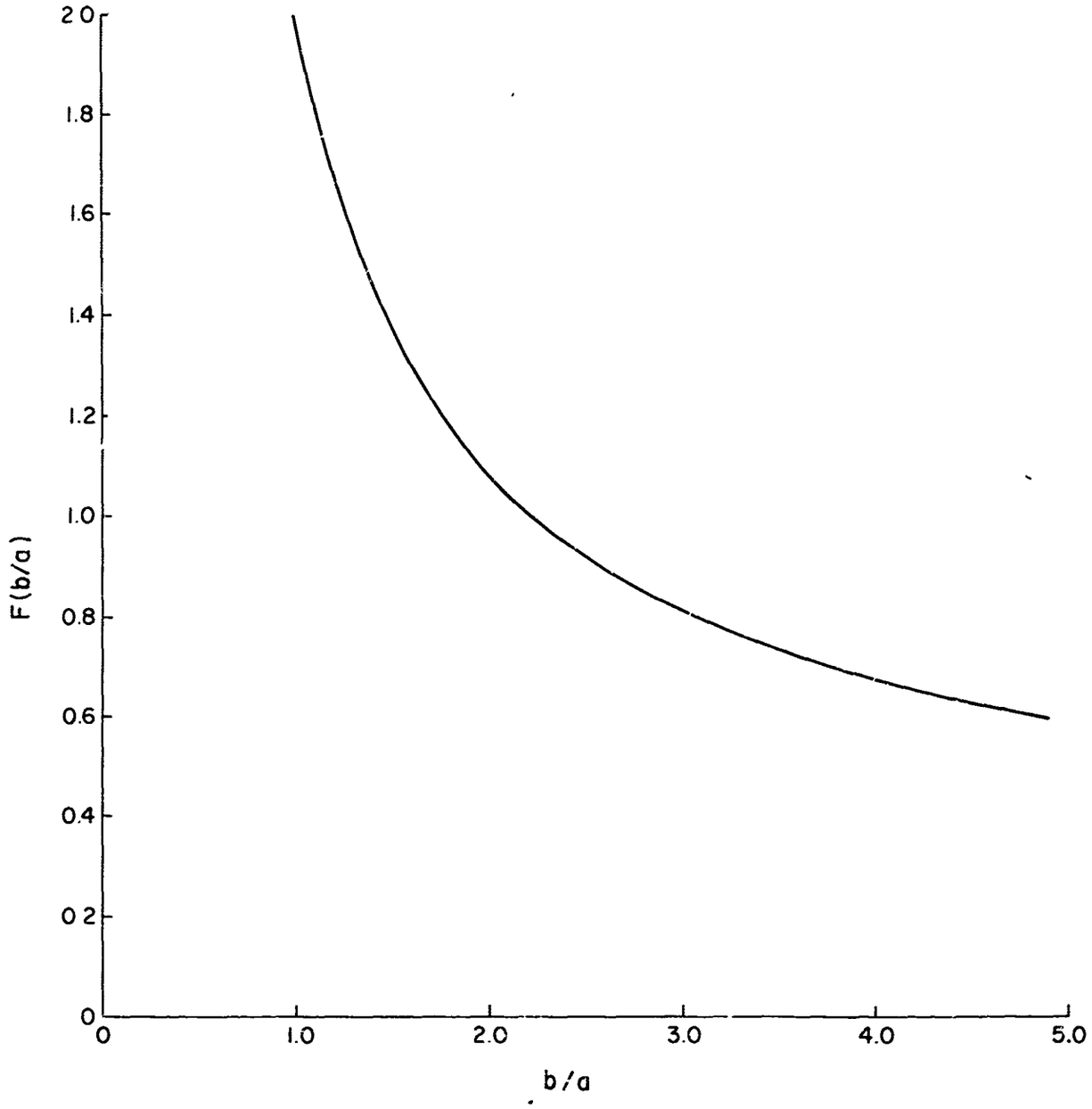

Figure 4 Reyield Functions, F, vs. Diametric Ratios

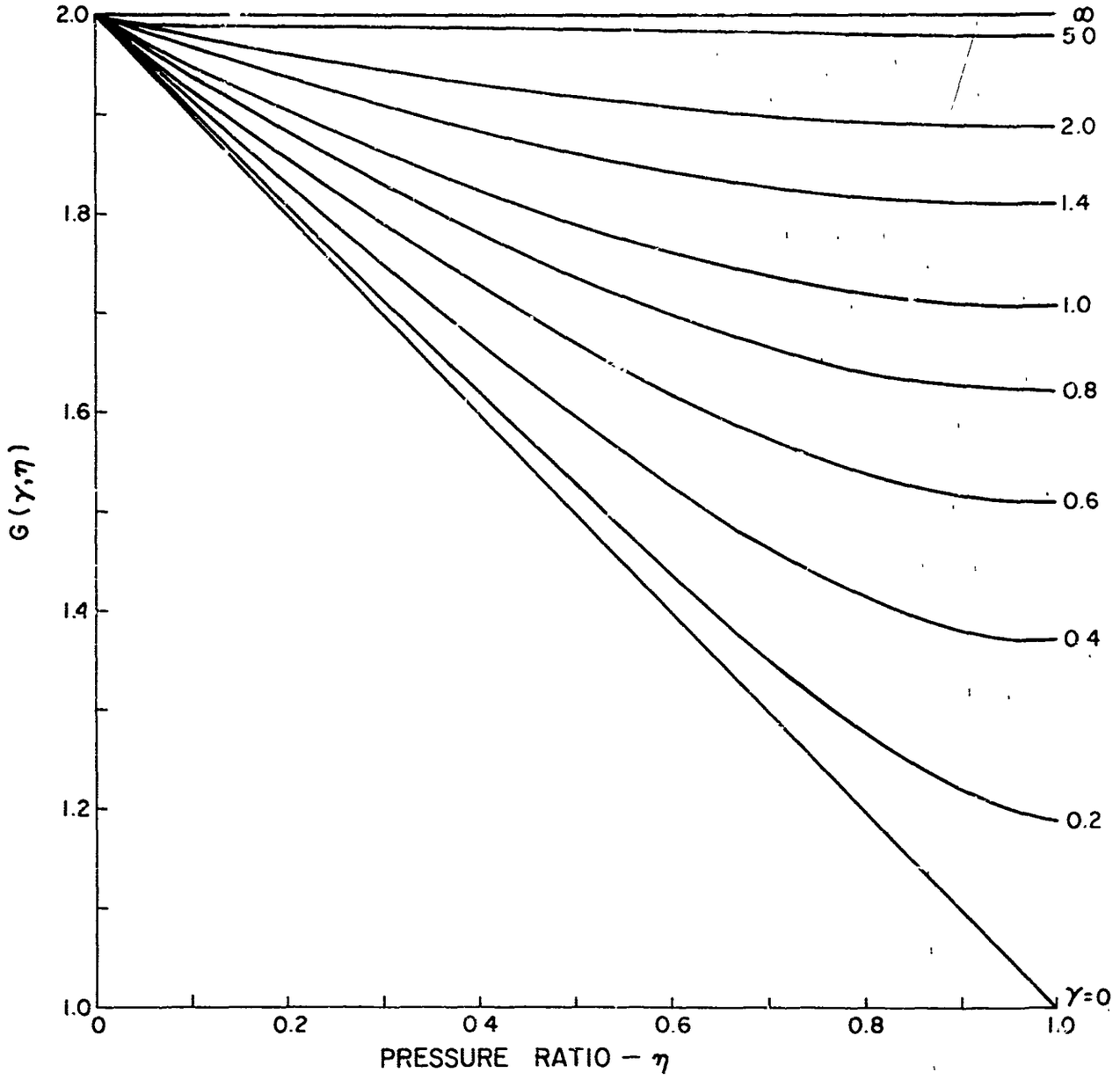

Figure 5 Reyield Function, G, As Function of γ, η

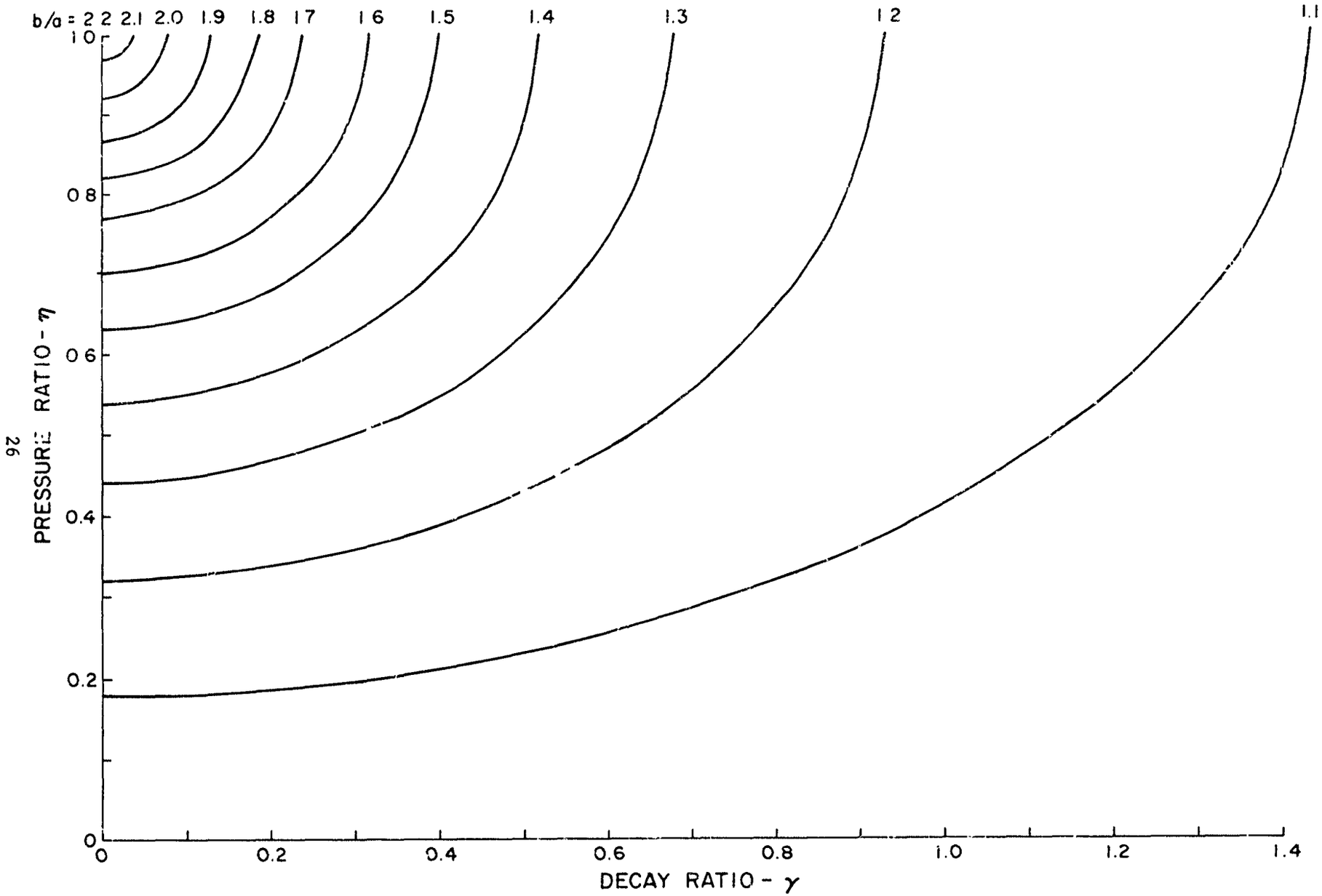

Figure 6 Pressure Ratio vs. Decay Ratio for Equality Between the Functions G and F

The initiation of reyielding is followed by the radial growth of the plastic region. At some time $t > t_2$ the plastic region is bounded by the elastic-plastic interface $r = \lambda$ as shown in Figure 7. The region $\lambda \leq r \leq b$ is continuing to respond elastically at this time.

Since plastic flow is confined, the change in strains is small and the convective terms in the material derivatives of displacement and velocity can be neglected. The change in displacement and the velocity and acceleration are therefore given by 1.14 and 1.15 respectively. In view of the continuity of the displacement across the elastic-plastic interface K(t) must be the same function of time in both regions. The stress field in each region will now be determined in terms of K(t) and $\lambda(t)$.

(1) Plastic Region: $a \leq r \leq \lambda$

The stresses σ_{ij}^{p} in the plastic region satisfy the yield condition 1.42 since the tube is moving radially inward. Thus, the equation of equilibrium 1.44 can be written

$$\frac{\partial \sigma_r^p}{\partial r} = \frac{\rho}{r} \ddot{K} - \frac{k}{r} \tag{4.6}$$

when the convective term in the acceleration is neglected. Integrating with respect to r and applying the boundary condition at r = a, gives

$$\sigma_r^p = \rho \ddot{K} \log r/a - k \log r/a - p_2 e^{-\alpha (t - t_2)} \tag{4.7}$$

where $p_2 = p_o e^{-\alpha t_2}$. From 4.7, together with 1.42, we obtain

$$\sigma_\theta p = \rho \ddot{K} \log r/a - k(1 + \log r/a) - p_2 e^{-\alpha (t - t_2)} \tag{4.8}$$

(2) Elastic Region: $\lambda \leq r \leq b$

The stresses σ_{ij}^{e} in the elastic region are given by

$$\sigma_{ij}^{e} = (\sigma_{ij})_2 + \Delta \sigma_{ij} \tag{4.9}$$

where $\Delta \sigma_{ij}$ represents the elastic changes in stress from the stress state $(\sigma_{ij})_2$ at t_2. When 1.24 is used in conjunction with 4.9 and 4.5, we obtain

$$\sigma_r^e - \sigma_\theta^e = k \left(2 \frac{a^2}{r^2} - 1\right) - \frac{4G}{r^2} K . \tag{4.10}$$

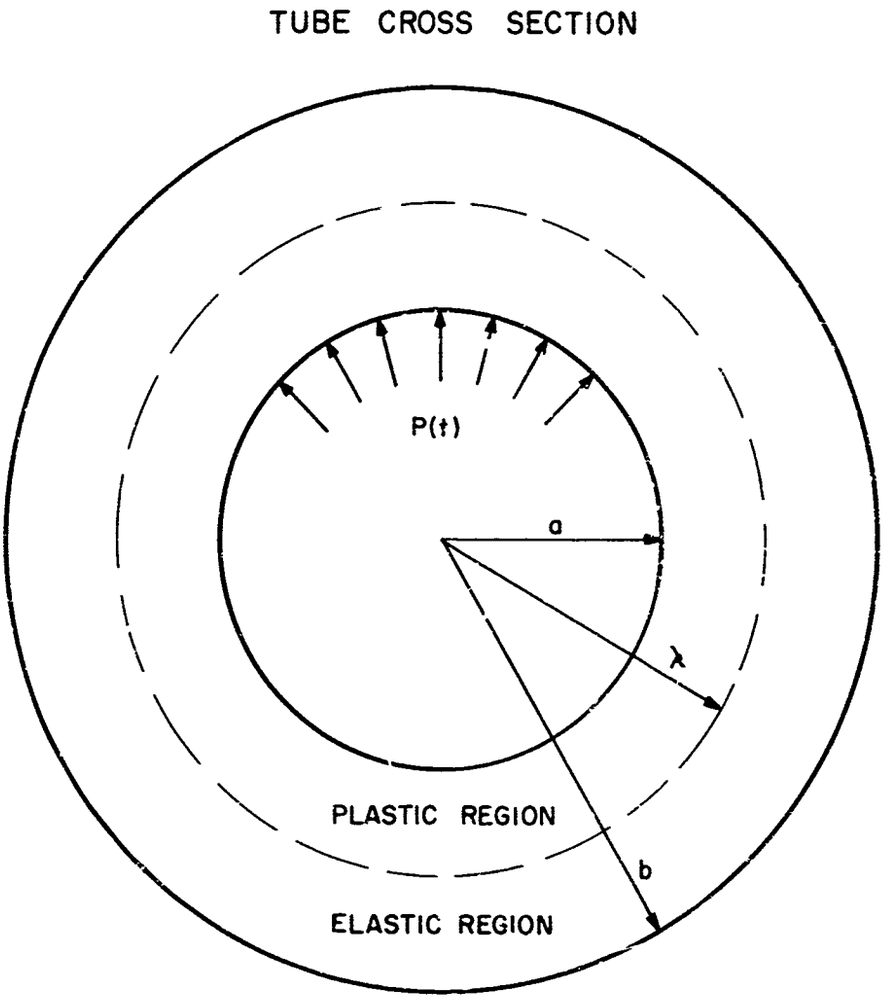

Figure 7 Tube Cross Section

The radial stress is written in terms of K(t) by substituting 4.10 into 1.44 (with $\dot{K}^2$ term neglected), integrating with respect to r and applying the boundary condition $\sigma_r = 0$ at r = b. The result is

$$\sigma_r^e = \log r/b\ (\rho \ddot{K} + k) + \left(\frac{1}{r^2} - \frac{1}{b^2}\right)(k a^2 - 2GK). \qquad 4.11$$

The radial and hoop stresses are continuous across the elastic-plastic interface. Equating 4.7 and 4.11 at r = λ we obtain

$$\rho \log b/a\ \ddot{K} + (2GK - ka^2)\left(\frac{1}{\eta^2} - \frac{1}{b^2}\right) - k \log \eta^2/ab = p_2 e^{-\alpha(t - t_2)} \qquad 4.12$$

Similarly, equating 1.42 and 4.10 at r = λ gives

$$\lambda^2 = a^2 - \frac{2G}{k} K . \qquad 4.13$$

when 4.13 is used, 4.12 reduces to

$$\rho \log b/a\ \ddot{K} - \frac{2G}{b^2} K - k \log\left(1 - \frac{2GK}{a^2 k}\right) = p_2\ e^{-\alpha(t - t_2)} + k\left[1 - \frac{a^2}{b^2} - \log b/a\right] \qquad 4.14$$

which is a non-linear differential equation in K(t) to be solved with zero initial displacement and the initial value of $\dot{K}$ given by 4.4. Approximate closed form solutions to 4.14 can be obtained under certain conditions. For the general case, the solution is obtained by numerical integration on a high speed digital computer. The position of the elastic-plastic interface is then determined from 4.13 and the stress field through the wall is obtained by using 4.7 and 4.8 for $r < \lambda$ and 4.10 and 4.11 for $r > \lambda$.

The initial reyield phase continues until the radial velocity goes to zero. When this occurs, the conditions for plastic flow are no longer satisfied and the material again behaves as an elastic solid.

The development in this section would have to be modified if the plastic region spread through the tube wall during reyielding. We shall now prove that this situation never arises.

At the initiation of reyielding, the tube is moving inwards with a radial velocity $\dot{K}_2/r$. The cavity pressure, p_2, is acting to decelerate the tube and bring it to rest. The tube's displacement during reyielding is therefore maximized by maximizing $\dot{K}_2$ and minimizing p_2. The case where $p_1 = 0$. obtained either by setting $\eta = 0$ or letting $\gamma \longrightarrow \infty$, satisfies both conditions and renders the absolute value of K a maximum. Since K is negative during initial reyielding, it follows from 4.13 that the extent of the plastic region is also maximized in this case. Thus, if the plastic region does not spread to r = b when $p_i = 0$, it will not do so for any pressure time history of the type we are considering.

When $\eta = 0$ or $\gamma \longrightarrow \infty$, it is found by using 3.8 and 4.1 that

$$\text{Cos } \omega (t_2 - t_1) = 1 - \frac{\omega^2 \rho a^2}{2G} \quad . \tag{4.15}$$

Differentiating 3.8, setting $\eta = 0$, and evaluating at t_2 gives

$$\dot{K}_2 = - \frac{k}{\omega \rho} \text{ Sin } \omega (t_2 - t_1) \quad . \tag{4.16}$$

By squaring both sides of 4.16 and using the square of 4.15 together with $\sin^2 + \cos^2 = 1$ and 3.5, $\dot{K}_2^2$ can be written independently of t_2 as

$$\dot{K}_2^2 = \frac{k^2 a^2}{\rho G} \left[1 - \frac{1 - a^2/b^2}{2 \log b/a} \right] \tag{4.17}$$

Equation 4.14, which describes the behavior of K during reyielding, is rewritten

$$\rho \log b/a \ddot{K} - \frac{2G}{b^2} K - k \log \left(1 - \frac{2GK}{a^2 k} \right) = k \left[1 - \frac{a^2}{b^2} - \log b/a \right] \tag{4.18}$$

since $p_2 = 0$. We shall now consider $\dot{K}$ to be a function of K, i.e.,

$$\dot{K} = f(K). \tag{4.19}$$

Then

$$\ddot{K} = \frac{df}{dK} \dot{K} = f \frac{df}{dK} \quad , \tag{4.20}$$

and 4.18 becomes

$$\rho \log b/a \; f \frac{df}{dK} = \frac{2G}{b^2} K + k \log\left(1 - \frac{2GK}{a^2 k}\right) + k \left(1 - \frac{a^2}{b^2} - \log b/a\right) \qquad 4.21$$

Integration of 4.21 and application of the condition that $\dot{K}$ is equal to $\dot{K}_2$ when K is zero yields

$$\rho \log b/a \; \dot{K}^2 = \frac{2G}{b^2} K^2 + 2k \left(1 - \frac{a^2}{b^2} - \log b/a\right) K - 2k K$$

$$- \frac{a^2 k^2}{G}\left(1 - \frac{2GK}{a^2 k}\right) \log\left(1 - \frac{2GK}{a^2 k}\right) + \rho \log b/a \; \dot{K}_2^2 \qquad 4.22$$

We shall now assume that the plastic region has extended through the tube and then show that this assumption is false by demonstrating that 4.22 cannot be satisfied under this condition. When $\lambda = b$, 4.13 gives

$$K = - \frac{k}{2G} (b^2 - a^2) \; . \qquad 4.23$$

Equation 4.22 reduces to

$$\dot{K}^2 = \frac{k^2 (b^2 - a^2)}{\rho G (\log b/a)^2} \left[-1 + \frac{1}{2} F (b/a)\right] \qquad 4.24$$

when 4.23 and 4.17 are used. For $b/a \neq 1$ the right hand side of 4.24 (see Figure 4) is always negative while the left hand side is non-negative. Thus, except for the limiting case of $b/a = 1$, our assumption that $\lambda = b$ is incorrect, and plastic flow during initial reyielding remains constrained. The actual position of elastic-plastic interface at the cessation of reyielding can be determined by solving 4.22 for K when $\dot{K}$ is zero and using the result to determine λ in 4.13.

5. General Elastic Unloading

A description of tube behavior following total plastic flow can now be given. The tube will oscillate about an equilibrium position which is moving radially inward as the pressure decays. If the displacement amplitude is sufficiently small, the oscillation is entirely elastic. With larger displacement amplitude the tube reyields one or more times. Each reyielding dissipates kinetic energy, so that the displacement and velocity of the tube

tend to decrease in time. Depending on the tube geometry, the tube may either continue reyielding until it is brought to rest, or cease reyielding when the amplitude of displacement becomes sufficiently small and then oscillate elastically until being brought to rest by internal damping. A typical reyield cycle begins with an elastic phase with the tube moving radially inward. The tube reyields while the radial velocity is still negative. The plastic region increases in size until the radial velocity vanishes. The tube then expands, first elastically and then elastically-plastically until the velocity again goes to zero. At this time, another cycle begins. Elastic unloading, in general, proceeds from a stress state in the tube wall, which is partially plastic and partially elastic. This stress state is unknown, since it depends on the stresses at the initiation of the previous reyielding and the position of the elastic-plastic interface when reyielding ceases. Therefore, we shall formulate general elastic unloading in terms of an arbitrary initial stress state.

Consider the elastic unloading phase which initiates at some time $t = t_n$ when the radial velocity is zero.* The stress state at this time consists of the radial stress $\sigma_{rn}(r)$ and the hoop stress $\sigma_{\theta\, n}(r)$. The subscript n implies the evaluation of these quantities at $t = t_n$.

The development of the governing equations for general elastic unloading parallels the development in section 3, the only difference being in the initial stress state. Therefore, only the pertinent results will be given. The difference between the hoop and radial stress for $t > t_n$ is

$$\sigma_\theta - \sigma_r = \sigma_{\theta n} - \sigma_{rn} + \frac{4G}{r^2} K \qquad 5.1$$

where

$$K = \frac{k}{\omega^2 \rho}\left\{\frac{\eta_n}{1+\gamma^2}\left[\gamma \operatorname{Sin}\omega\,(t - t_n) + e^{-\alpha(t - t_n)}\right]\right.$$
$$\left. -\left(\frac{n}{1+\gamma^2} - \frac{I_n}{p_s}\right)\operatorname{Cos}\omega\,(t - t_n) - \frac{I_n}{p_s}\right. \qquad 5.2$$

In the above equation p_s is defined by 2.6,

$$\eta_n = \frac{p_n}{p_s} \qquad 5.3$$

*For elastic unloading, n is an odd integer, i.e., 1, 3, 5, . . .
The even integers will be used to designate the initiation of reyielding.

where $p_n = p_o e^{-\alpha t_n}$ and

$$I_n = \int_a^b \frac{1}{r} (\sigma_{\theta n} - \sigma_{rn})\, dr \,. \qquad 5.4$$

To test if the tube reyields, it is only necessary to evaluate 5.1 at the extreme negative and positive values of K. There are two cases to consider. In the first case, when $\sigma_{\theta n} - \sigma_{rn}$ is equal to k through some portion of the tube wall, the tube initially contracts. It can be argued as in section 3, that K is non-positive while the tube remains elastic. It follows from 5.1 and the yield condition 1.41 that reyielding cannot initiate when the radial velocity is positive. The maximum negative displacement K_m, attained when $e^{-\alpha (t - t_n)} \longrightarrow 0$, is

$$K_m = -\frac{k}{\omega^2 \rho} \left[\frac{I_n}{p_s} + \frac{1}{1+\gamma^2} \sqrt{\gamma^2 \eta_n^2 + \left[\frac{I_n}{p_s} (1+\gamma^2) - \eta_n \right]^2} \right] . \qquad 5.5$$

The above equation is similar to 4.3 and was obtained by using the same procedure. By using 5.5 in 5.1, together with 1.42, the condition for reyielding during negative radial velocity is found to be

$$-\frac{4G}{r^2} K_m \geq k + \sigma_{\theta n} - \sigma_{rn} \qquad 5.6$$

for some $a \leq r \leq b$.

In the second case, the tube expands during the first half cycle of elastic unloading. The maximum positive value of K occurs at the end of the first half cycle when the radial velocity vanishes. The tube may or may not have reyielded at this time. If it does not, it will reyield during the second half cycle when the tube's velocity is negative. This follows when we note that $\sigma_{rn} - \sigma_{\theta n} = k$ over some portion of the tube wall and that $\sigma_r - \sigma_\theta$ from 5.1, will be greater than k if, at any time, K becomes negative. But K, from 5.2, is always negative at $\omega (t - t_n) = 2\pi$.

The previous discussion shows that reyielding, once begun, may occur indefinitely. Although reyielding continues, the energy dissipated through plastic flow becomes negligible when $p_n/p_1 << 1$. The velocity at the beginning of reyielding is small and the stresses do not noticeably change from cycle to cycle. Tube behavior is essentially elastic beyond this point. We shall assume, therefore, that reyielding ceases when $p_n/p_1 << 1$ and the velocity $\dot{K}_{n+1}$ at the beginning of reyielding is small compared to the maximum velocity during the cycle. This assumption is in agreement

with the physical behavior of the tube, since internal dissipative mechanisms reduce the oscillation amplitude and prevent the occurrence of reyielding after a finite number of cycles.

6. General Reyielding

Conditions at time t_{n+1} at which reyielding begins following the elastic unloading described in section 5, depend on the distribution of $\sigma_{\theta n} - \sigma_{rn}$, which in turn depends on the initial total plastic state of stress (n = 1) and the number and extent of previous reyielding phases. These constraints on $\sigma_{\theta n} - \sigma_{rn}$ apparently limit the region of reyielding to $a \leq r \leq \lambda$ and the extent of reyielding so that $\lambda \leq b$. In the examples we have investigated (reported in section 8), the plastic region has always extented outwards from the inner wall and plastic flow has remained constrained. We shall therefore restrict our formulation of general reyielding to the case where plastic flow is limited to the region $a \leq r \leq \lambda \leq b$ and at time t_{n+1} when reyielding begins, the plastic region includes the point r = a.* If, in a specific case, reyielding does not satisfy these conditions, then the analyses may be readily extended.

The non-vanishing components of stress at time t_{n+1} are $\sigma_{r(n+1)}(r)$ and $\sigma_{\theta(n+1)}(r)$. The difference in these two components is obtained by evaluating 4.1 at $t = t_{n+1}$. The development parallels that of section 4 and will therefore be quite brief. In the elastic region $\lambda \leq r \leq b$, the radial stress is

$$\sigma_r^e = \rho \log r/b \, \ddot{K} - 2GK \left(\frac{1}{r^2} - \frac{1}{b^2} \right) + h(r) - h(b) \qquad 6.1$$

where

$$h(r) = \int_b^r \frac{1}{\bar{r}} \left(\sigma_{\theta(n+1)} - \sigma_{r(n+1)} \right) d\bar{r} \qquad 6.2$$

The difference between the radial and hoop stress is

$$\sigma_\theta^e - \sigma_r^e = \sigma_{\theta(n+1)} - \sigma_{r(n+1)} + \frac{4G}{r^2} K \qquad 6.3$$

The stress field in the plastic region a r depends on the sign of the radial velocity. When the radial velocity is positive, then

$$\sigma_r^p = \rho \log r/a \, \ddot{K} + k \log r/a - p_{n+1} e^{-\alpha(t - t_{n+1})} \qquad 6.4$$

*The plastic region at the initiation of reyielding is not always confined to the point r = a. When reyielding occurs only during contraction of the tube, the plastic region at t_{n+1} extends from r = a to $r = \lambda_{n-1}$, where λ_{n-1} is the position of elastic-plastic interface at the end of the previous reyield phase. This follows when 5.1 is examined with K = 0.

and

$$\sigma_\theta^p - \sigma_r^p = k$$

where p_{n+1} is the pressure on the inner wall at time t_{n+1}. When the radial velocity is negative

$$\sigma_r^p = \rho \log r/a \ddot{K} - k \log r/a - p_{n+1} e^{-\alpha(t - t_{n+1})}$$

and 6.5

$$\sigma_\theta^p - \sigma_r^p = -k.$$

The condition of continuity of stress components across the elastic-plastic interface leads to the following two equations in K(t) and $\lambda(t)$,

$$K = \frac{\lambda^2}{4G} \left[\sigma_{r(n+1)}(\lambda) - \sigma_{\theta(n+1)}(\lambda) \pm k \right] \qquad 6.6$$

and

$$\rho \log b/a \ddot{K} + 2G\left(\frac{1}{\lambda^2} - \frac{1}{b^2}\right) K \pm k \log \lambda/a = p_{n+1} e^{-\alpha(t - t_{n+1})} + h(\lambda) - h(b). \qquad 6.7$$

The sign of k in these equations corresponds to the sign of the radial velocity, e.g., the + sign is used when the radial velocity is positive. Equation 6.6 is an algebraic relationship between K and λ which may be numerically inverted to give

$$\lambda = F(K) \qquad 6.8$$

or

$$\lambda = G(K) \qquad 6.9$$

depending on the sign of the velocity. When either 6.8 or 6.9 is substituted in 6.7, the resulting equation is a non-linear second order differential equation in K(t). For example, when $\dot{K} > 0$, 6.7 becomes

$$\rho \log b/a \ddot{K} + 2G\left\{\frac{1}{F(K)} - \frac{1}{b^2}\right\} + k \log F(k)/a =$$

$$p_{n+1} e^{-\alpha(t - t_{n+1})} + h\left[F(K)\right] - h(b). \qquad 6.10$$

The solution to 6.10 is obtained by numerical integration. The governing equation for K is valid until $\dot{K} = 0$ at t_{n+1}. At this time, elastic unloading begins again with $\sigma_{r(n+2)} - \sigma_{\theta(n+2)}$ obtained by evaluating 6.3 and the second equation of either 6.4 or 6.5 at t_{n+1}.

7. Residual Stress

The previous development showed that, following total plastic flow, reyielding may or may not occur. We will now determine the residual stress for both of these cases.

A. No Reyielding

In this case, the tube oscillates elastically following total plastic flow until internal dissipation brings the tube to rest. The value of K_∞, i.e., $\lim_{t \to \infty} K(t)$, is found from 3.8 by noting that the harmonic oscillation is damped out at $t = \infty$. Therefore

$$K_\infty = -\frac{k}{\omega^2 \rho} \qquad 7.1$$

The difference between the residual hoop stress $\sigma_{\theta\infty}$ and the residual radial stress $\sigma_{r\infty}$ is found to be

$$\sigma_{\theta\infty} - \sigma_{r\infty} = k\left[1 - \frac{2 \log b/a}{r^2(\frac{1}{a^2} - \frac{1}{b^2})}\right] \qquad 7.2$$

when 7.1 and 3.5 are used in 3.2. The residual radial stress is obtained by using 7.2 and 1.45 and setting $K = \dot{K} = 0$. The result is

$$\sigma_{r\infty} = -k \log b/r + k \log b/a \left[\frac{\frac{1}{r^2} - \frac{1}{b^2}}{\frac{1}{a^2} - \frac{1}{b^2}}\right] \qquad 7.3$$

The use of 7.3 in 7.2 gives the residual hoop stress as

$$\sigma_{\theta\infty} = k\left[1 - \log b/r - \log b/a\left[\frac{\frac{1}{r^2} + \frac{1}{b^2}}{\frac{1}{a^2} - \frac{1}{b^2}}\right]\right] \qquad 7.4$$

Evaluating 7.4 at r = a, we find the residual hoop stress at the bore to be

$$\sigma_{\theta\infty}(a) = k\left[1 - \frac{2 \log b/a}{1 - \frac{a^2}{b^2}}\right] \qquad 7.5$$

The residual stresses 7.3 and 7.4 are identical with those obtained statically for a fully plasticized imcompressible tube when $b/a < 2.2$. As noted previously, when $b/a > 2.2$ static reyielding occurs. Thus, the static and dynamic autofrettage processes produce the same residual stresses when there is no reyielding.

B. Reyielding Followed by Elastic Oscillation

In this case, the tube, after reyielding a sufficient number of times is assumed to oscillate elastically until coming to rest. If $t = t_j$ at the end of reyielding, then behavior for $t - t_j$ is governed by the equations of section 5 with n replaced by j. Using the same procedure as was followed in part (A) of this section, we find that the residual stresses are

$$\sigma_{r\infty} = g(r) - g(b)\frac{\left(\frac{1}{a^2} - \frac{1}{r^2}\right)}{\left(\frac{1}{a^2} - \frac{1}{b^2}\right)} \qquad 7.6$$

and

$$\sigma_{\theta\infty} = \sigma_{\theta j} - \sigma_{rj} + g(r) - g(b)\frac{\left(\frac{1}{a^2} + \frac{1}{r^2}\right)}{\left(\frac{1}{a^2} - \frac{1}{b^2}\right)} \qquad 7.7$$

where

$$g(r) = \int_a^r \frac{1}{r}\left(\sigma_{\theta j} - \sigma_{rj}\right) d r \,. \qquad 7.8$$

When there is no reyielding, $\sigma_{\theta j} - \sigma_{rj} = k$, $g(r) = k \log r/a$ and 7.6 and 7.7 reduce to 7.3 and 7.4 respectively. The residual hoop stress at the bore is found to be

$$\sigma_{\theta\infty}(a) = \sigma_{\theta j}(a) - \sigma_{rj}(a) - \frac{2\, g(b)}{\left(1 - \frac{a^2}{b^2}\right)} \qquad 7.8$$

When 7.7 is evaluated at r = a and it is noted from 7.8 that g(a) is zero. The difference between the hoop and radial stress at the bore at time t_j is either + k depending on the position of the tube. Consider the case where $\sigma_{\theta j}(a) - \sigma_{rj}(a) = k$. Since the tube is not fully plastic, $\sigma_{\theta j} - \sigma_{rj} < k$ over some portion of the tube wall. It follows from 7.8 that $g(b) < k \log b/a$ and that the right hand side of 7.9 is greater than the right side of 7.5. We cannot demonstrate the same result analytically when $\sigma_{\theta j} - \sigma_{rj} = -k$ at r = a. However, numerical results (section 8) indicate that the result is also valid for this case. Therefore, reyielding followed by elastic unloading results in a loss of residual compressive hoop stress at the bore.

8. Numerical Results

The results presented in this section were obtained with the use of a computer program which determines residual stress as a function of tube geometry, the decay rate α, and the pressure p_1 at the cessation of total plastic flow. The program follows the tube through successive cycles of reyielding and elastic unloading. If, at some time t_j, following reyielding, $(\lambda_j - \lambda_{j-2})/(b-a)$ and p_j/r_s are sufficiently small, the program assumes no further reyielding and computes residual stresses from the stress state at t_j using the equations given in (2) section 1. The program is not used for values of η and γ which do not produce reyielding since in this case the residual stress is determined directly from 7.3 and 7.4.

In Figure 8, the ratio of the dynamic residual hoop stress $\sigma_{\theta\infty}(a)$ to the static residual hoop stress at the bore $\sigma_{\theta\infty s}(a)$ is plotted versus γ for different values of η for b/a = 1.75 and a = 2.825. Values of $\sigma_{\theta\infty}(a)/\sigma_{\theta\infty s}(a) = 1$ indicate no loss in residual stress in the dynamic process. As γ is increased for a fixed value of η the residual stress drops rapidly until it becomes essentially zero. Even in the case of static loading ($\eta = 1$) the tube will experience a loss in residual stress when the decay rate is sufficiently large. As η decreases the tube reyields at lower values of γ and there is a corresponding decrease in residual hoop stress at the bore.

The distribution of residual hoop stress $\sigma_{\theta\infty}(r)$, divided by $\sigma_{\theta\infty s}(a)$, is shown in Figure 9 for the same tube where $\eta = 1$. The solid curve is

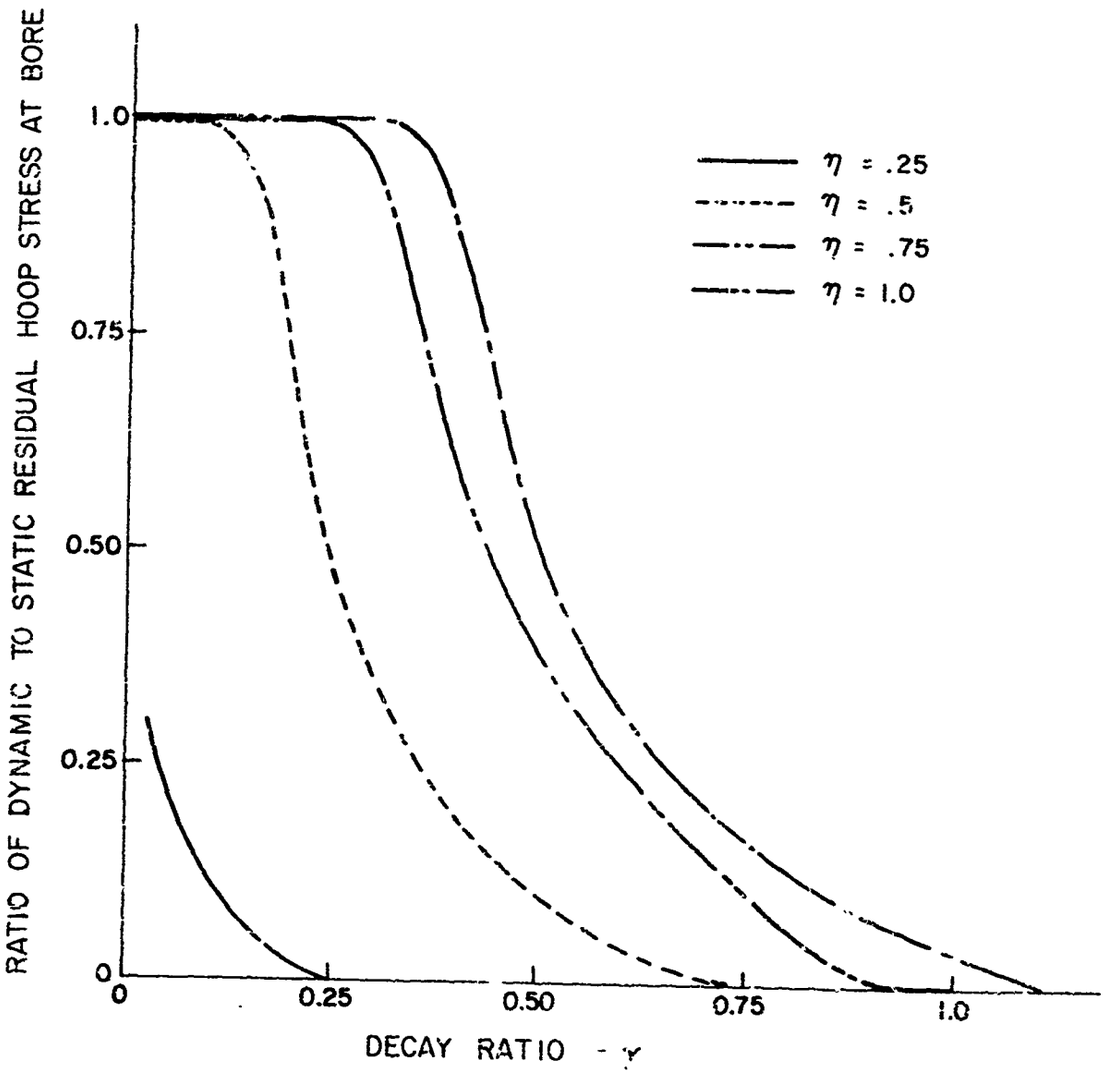

Figure 8 Stress Ratio Variations Due To Changes in Decay Ratio and Overpressure Ratio

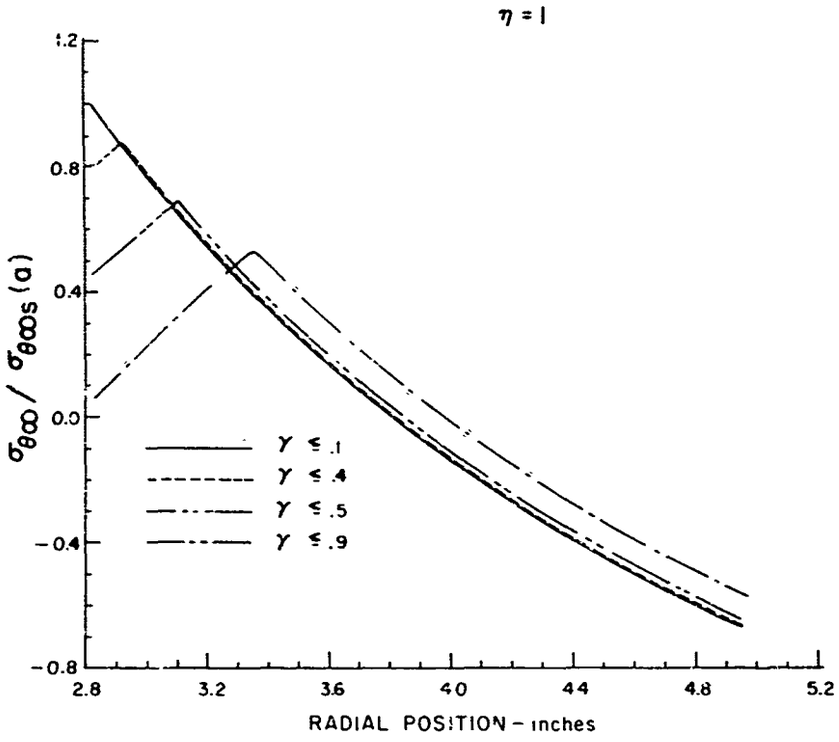

Figure 9 Residual Hoop Stress Distribution

distribution obtained in static autofrettage. The major change from the static residual stress pattern is continued to the region of plastic flow during reyielding.

Experimental evidence supporting these results is primarily qualitative since the actual pressure time history has not yet been determined. With the configuration shown in Figure 1, the decay rate is high. Quenching of the explosive products by the water quickly brings the cavity pressure to some low equilibrium value. If the difference between the peak pressure and p_s were small, there would therefore be no noticeable plastic deformation. In actual tests, however, the permanent deformation at the bore was generally between 1/2% and 8%. Thus, the initial peak pressure was also high, and following our discussion in section 2 we may conclude that p_1/p_s is fairly small. The combination of high γ and low η should produce a substantial loss in residual stress. In experiments where the radial piston was not used, the residual hoop stress at the bore was found to be only 25-35% of the static value.

The magnitude of residual hoop stress is considerably increased when the radial piston configuration (Figure 2) is used. This configuration acts to reduce the initial peak pressure (increasing η) and to prolong the pressure pulse (decreasing γ). The resulting hoop stresses at the bore obtained experimentally vary depending on the details of the particular test. In general, however, they range from 75-100% of the static value.

IV. EXPERIMENTAL METHODS

This section details the work accomplished both in the laboratory and analytically which has not been detailed in Section III, Mathematical Analysis.

1. Specifications

The Watervliet Arsenal was visited by John Weese and Richard Fay of the University of Denver accompanied by Jimmy D. Mote of the Martin Marietta Corporation. Meetings were held with Harold Goodheim, David Kendal, and others concerning the specifications and procedures under which the gun barrels are currently being autofrettaged. A tour of the facilities was made and technical material was obtained. The technical material consisted of reports covering both theoretical and practical aspects of the process and drawings of the M81, 152 mm gun barrel before and after autofrettage.

The specifications which are being used by Watervliet give the barrel expansion required to produce the desired residual stresses in the barrel after the final machining. The important dimensions of the barrel prior to autofrettage and the allowed expansions are shown in Figure 10. The table in this figure gives the allowable expansions as a function of the yield strength of the barrel. The yield strength of each barrel is

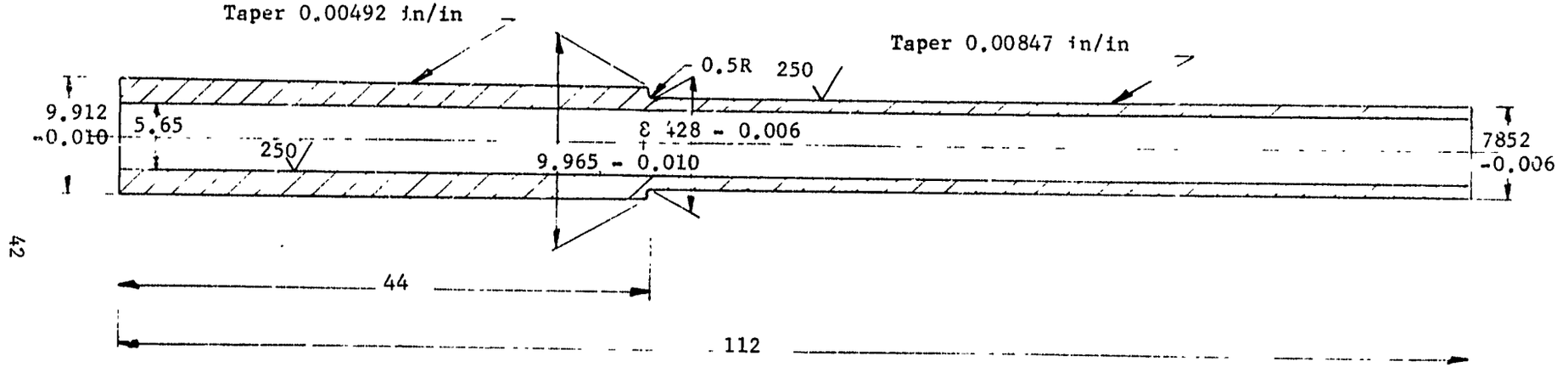

REQUIRED BORE ENLARGEMENTS

DISTANCE FROM BREECH END OF AUTOFRETTAGE TUBE	YIELD STRENGTH (PSI) PRIOR TO AUTOFRETTAGE		
	160,000	170,000	180,000
8.5"	.034 MIN .113 MAX	.016 MIN	.011 MIN
16.0	.036 MIN .113 MAX	.017 MIN	.011 MIN
42.5	.043 MIN .113 MAX	.018 MIN	.012 MIN
109	.009 MIN .113 MAX	.004 MIN	.003 MIN

Figure 10 M-81, 152 mm Gun Tube Prior to Autofrettage

determined by pulling a tensile specimen taken from each end. In the autofrettage of the M81, 152 mm barrel an external die is used to control the expansion which is produced by the application of 120,000 psi hydraulic pressure in the bore of the barrel.

A new process is being used for the autofrettage of 175 mm gun barrels which does not require the external die. In this process the circumference of the barrel is measured very accurately during the expansion; the process proceeds until the desired expansion has been obtained.

A new swaging process is being used for the autofrettage of the M162, 152 mm barrel. In this process a tungsten carbide mandrel approximately 6 in. long is forced through the bore which has been plated with 0.001 in. of lead. The breech end of the barrel is held by a screwed fitting on the end of a hydraulic cylinder which supplies the 0.5×10^6 lb force required to start and the 0.25×10^6 lb force required to maintain the motion of the mandrel through the bore.

The quality control exercised in the three autofrettage processes described above consists of determining the yield strength of each barrel and then measuring the bore after autofrettage to assure that the proper expansion has been produced to give the desired residual stresses. Since the tensile specimens for the yield stress determination are taken from the ends of the barrels there is an area of uncertainty regarding the material properties of the center of the barrel.

The specifications given on Figure 10 for the expansion of the barrels as a function of the yield strength of the material were scaled down for use with the 1/5th scale barrels used in the experimental program. This information is given in terms of percent bore expansion and inches on Figure 11.

2. Charge Strength vs. Bore Expansion

For the purpose of determining the relationship between the strength of the explosive charge and the expansion of the barrels, five 1/5th scale barrels were made and expanded with charges of Detasheet having different weights per unit length. The 1/5th scale barrels referred to here are 1.130 ± 0.002" I.D. x 1.982 ± 0.002" O.D. x 10" long and are essentially a 1/5th scale of the breech section of the 152 mm barrel with the taper neglected. The barrels used in this series of shots were made by a local machine shop from annealed 4340 steel tubing and subsequently heat treated to a 34-36 Rockwell C hardness. The charges consisted of one or two wraps of Type C Detasheet on a wood dowel as shown in Figure 1. Also, as shown in Figure 1, the charges were centered in the tubes by wood end supports and initiated with No. 8 blasting caps. The explosive expansion process was conducted with the barrel submerged 18 in. in water in a 4 ft diameter by 4 ft deep cylindrical pool.

The maximum bore expansion for each barrel is shown plotted in Figure 12 as a function of the weight of the explosive charge. The series of five points fall in nearly a straight line. Figure 13 shows the curves of the bore expansion as a function of the distance from the ignition end of the barrel. The expansions are rather uniform over a large portion of the barrels; the exception of this is the lower curve (1.12 gm/in.) which indicates a poor charge performance over approximately half of the tube. This poor performance is believed to be a result of the presence of an air bubble inside the barrel at the time of charge initiation. Steps were taken in subsequent experiments to reduce the possibility of this occurrence. These steps include a redesign of the charge end supports to provide more vent area and the use of a wetting agent on the bore of the barrel and surface of the charge.

The barrels used in the experiments described above were made of 4340 steel which was to be heat treated to 34-36 Rockwell C. It was found from the results of hardness and tensile tests performed on pieces taken from one of these barrels that the hardness was 32 Rockwell C and the yield strength was 125,000 psi. It was also learned that the hardness which had been specified was not sufficient to give the desired 160,000 psi minimum yield. Two more tensile specimens were made from the same material; these were heat treated to 40 Rockwell C. The yield strength of these specimens was found to be 170,000 psi.

The remaining 10 in. long barrels which had not been tested were reheat treated to bring their hardness up to Rockwell C 40. One of these barrels was expanded using a Detasheet charge weighing 1.25 grams per inch and having the same configuration shown in Figure 14. The bore expansion obtained with this shot is shown plotted as a function of the distance from the initiation end in Figure 15. Also shown in this figure are the expansion limits which were scaled down from those required for the full size barrel. It can be seen on this plot that the entire length of the expanded barrel falls within the limits given for a barrel having a yield strength of 170,000 psi.

Several of the hardened barrels were expanded with charges of Detasheet, having the previously described configuration, and ranging from 1.05 to 2.4 gm/in. A plot of the maximum expansion vs. charge weight for these barrels is given in Figure 16.

3. Repeatability Study

For the purpose of determining the repeatability of the explosive expansion process, five 1/5th scale barrels having identical material properties were expanded with 1.26 + 0.01 gram per inch Detasheet charges. The bore expansions obtained in these shots are presented in Figure 17 plotted as a function of the distance from the end of the barrel at which the charge was initiated. The results shown in this figure indicate that the process is quite repeatable.

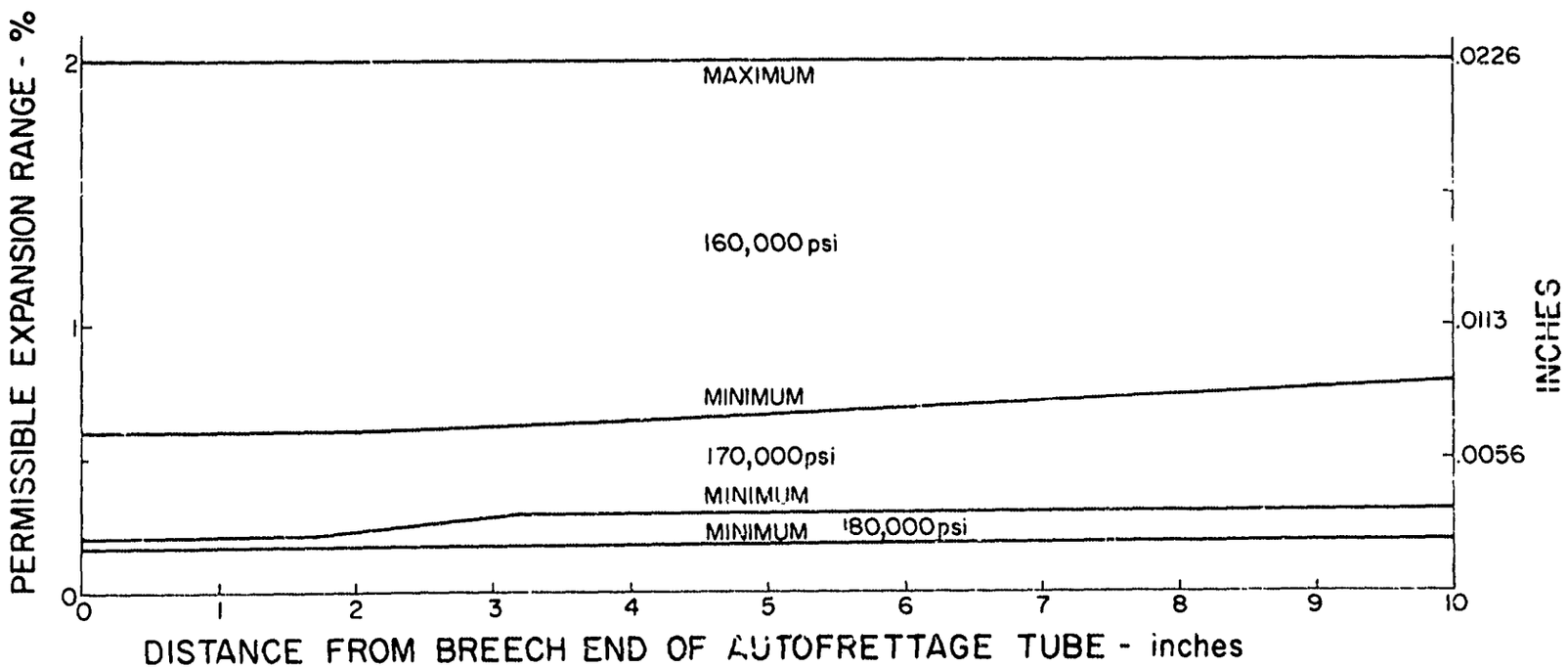

Figure 11 Required Range of Bore Enlargements for Various Yield Strengths Prior to Autofrettage
1/5 Scale Barrels

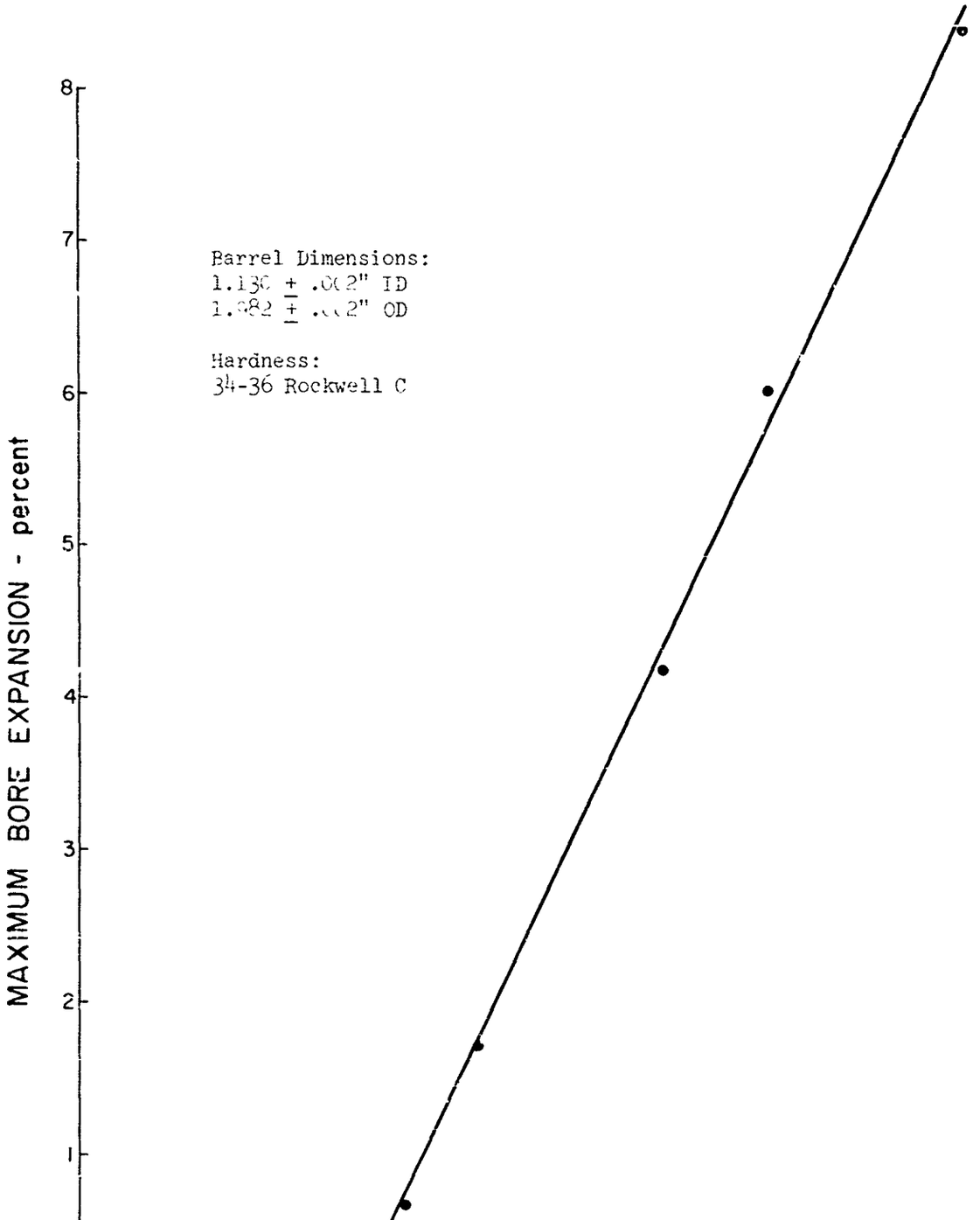

Figure 12 Maximum Bore Expansion As a Function of Detasheet Charge Weight for 1/5th Scale 4340 Steel Barrels 10" Long

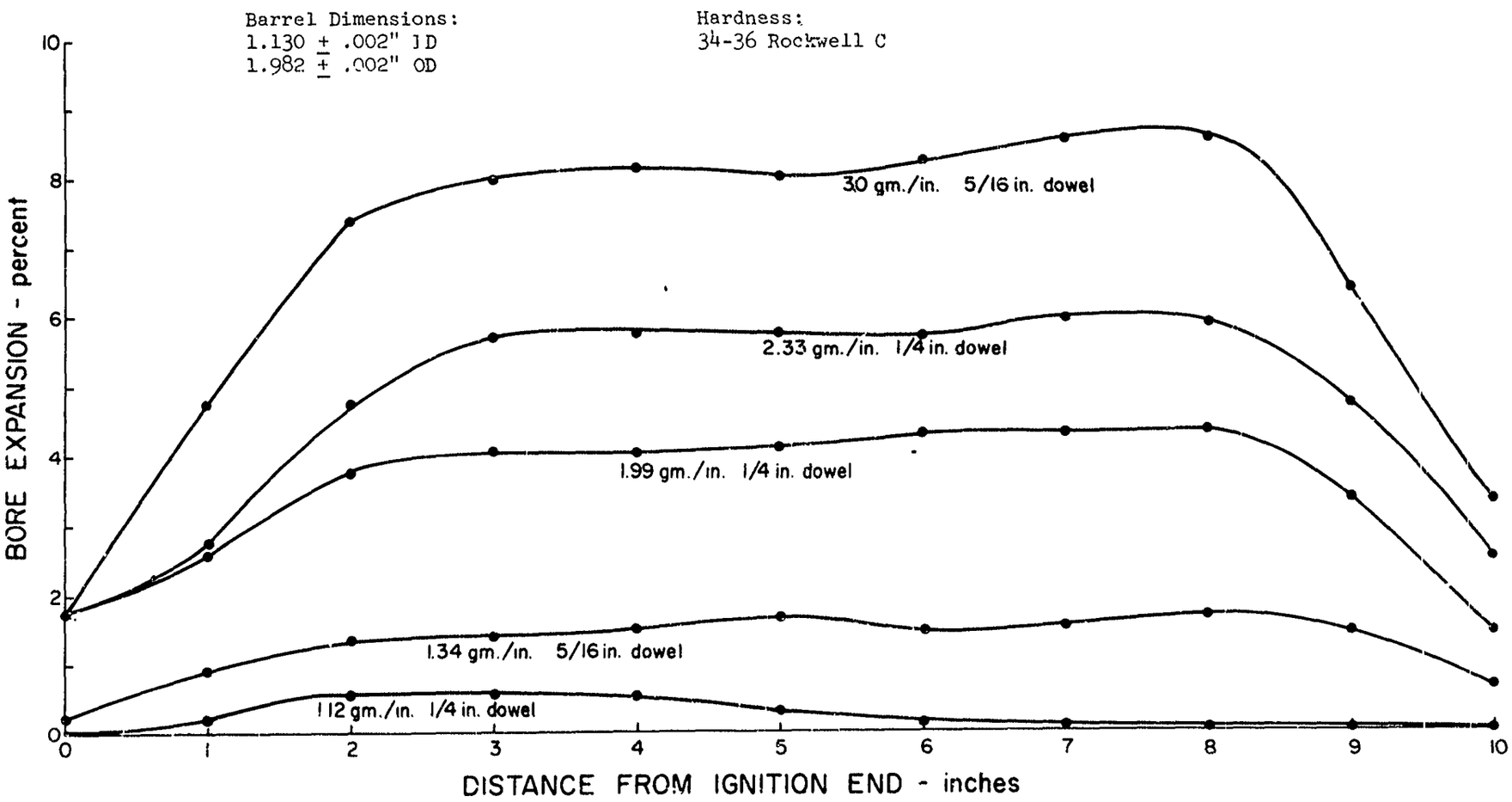

Figure 13 Percent Bore Expansion Along 10" Sections of 1/5th Scale 4340 Steel Barrels for Different Detasheet Charge Weights

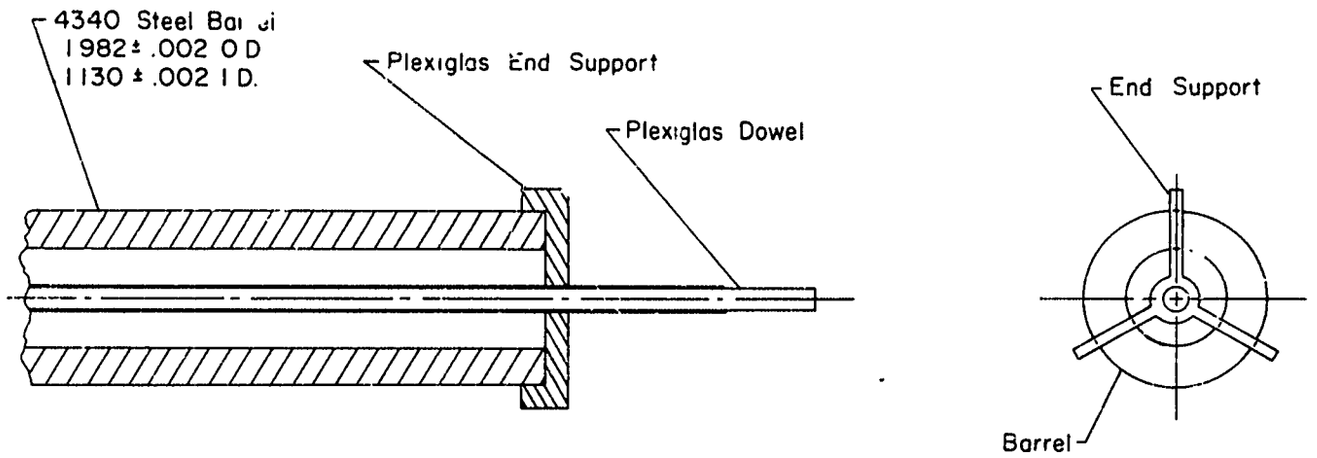

Figure 14 Sketch Showing Modification in End Supports for Improved Venting and End Expansion

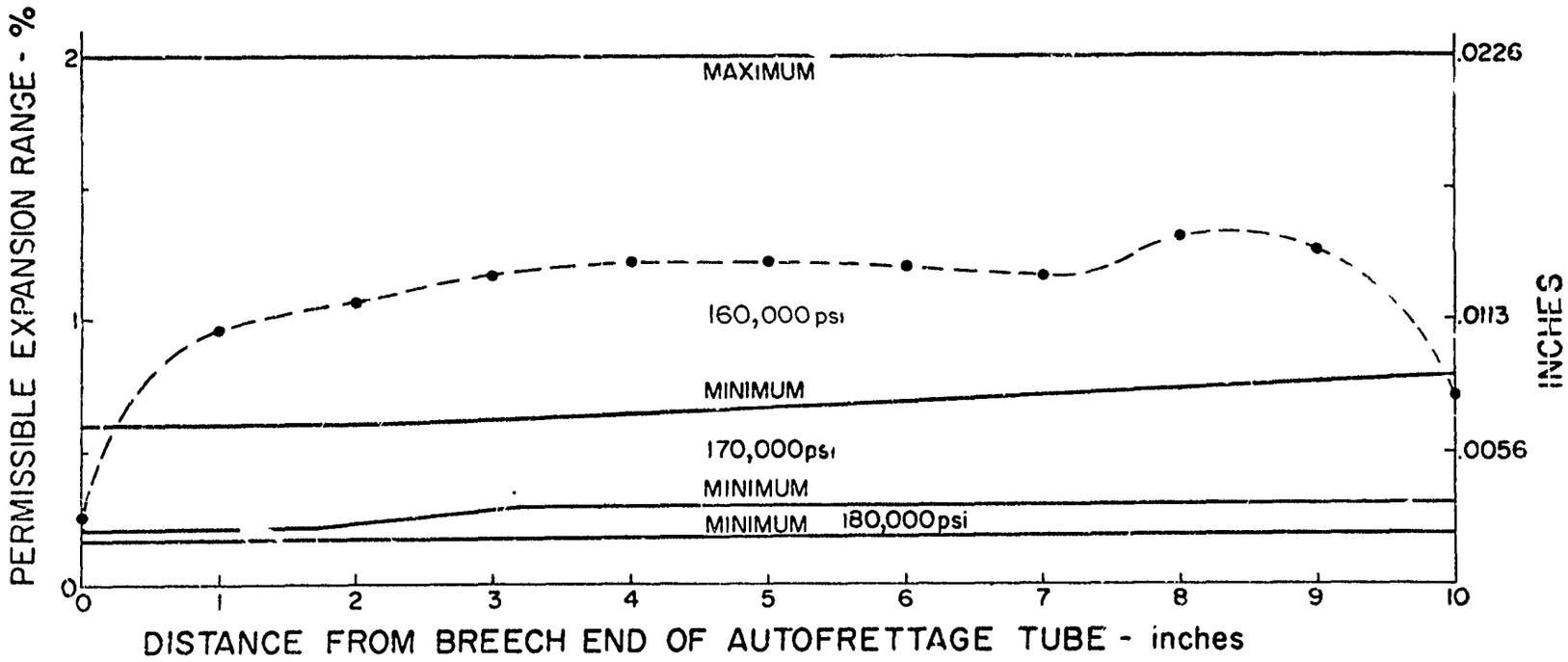

Figure 15 Required Range of Bore Enlargements for Various Yield Strengths Prior to Autofrettage, 1/5th Scale Barrels, Showing 170,000 psi Yield ..rel Superimposed

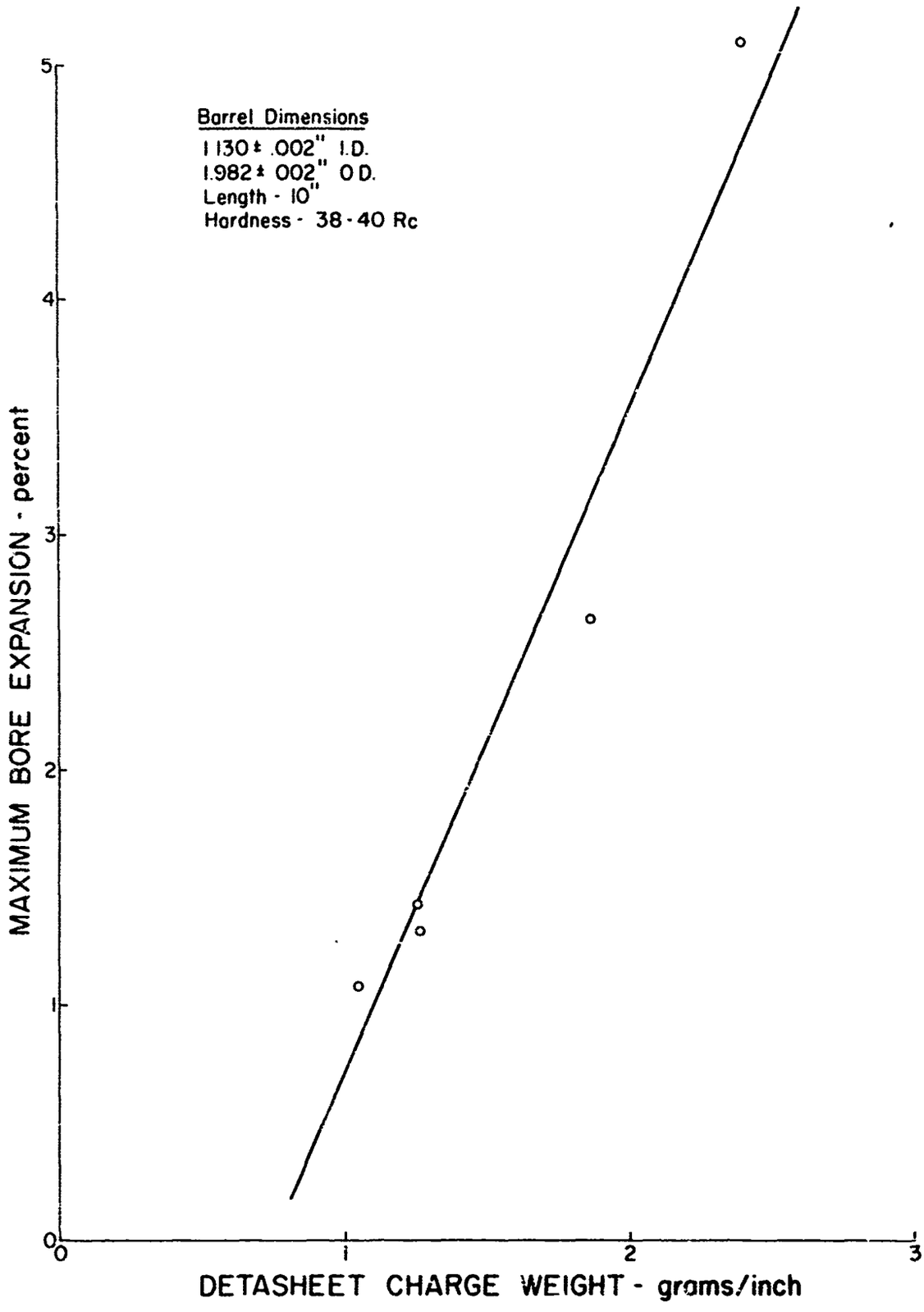

Figure 16 Maximum Bore Expansion As a Function of Detasheet Charge Weight for 1/5th Scale 4340 Steel Barrels 10" Long

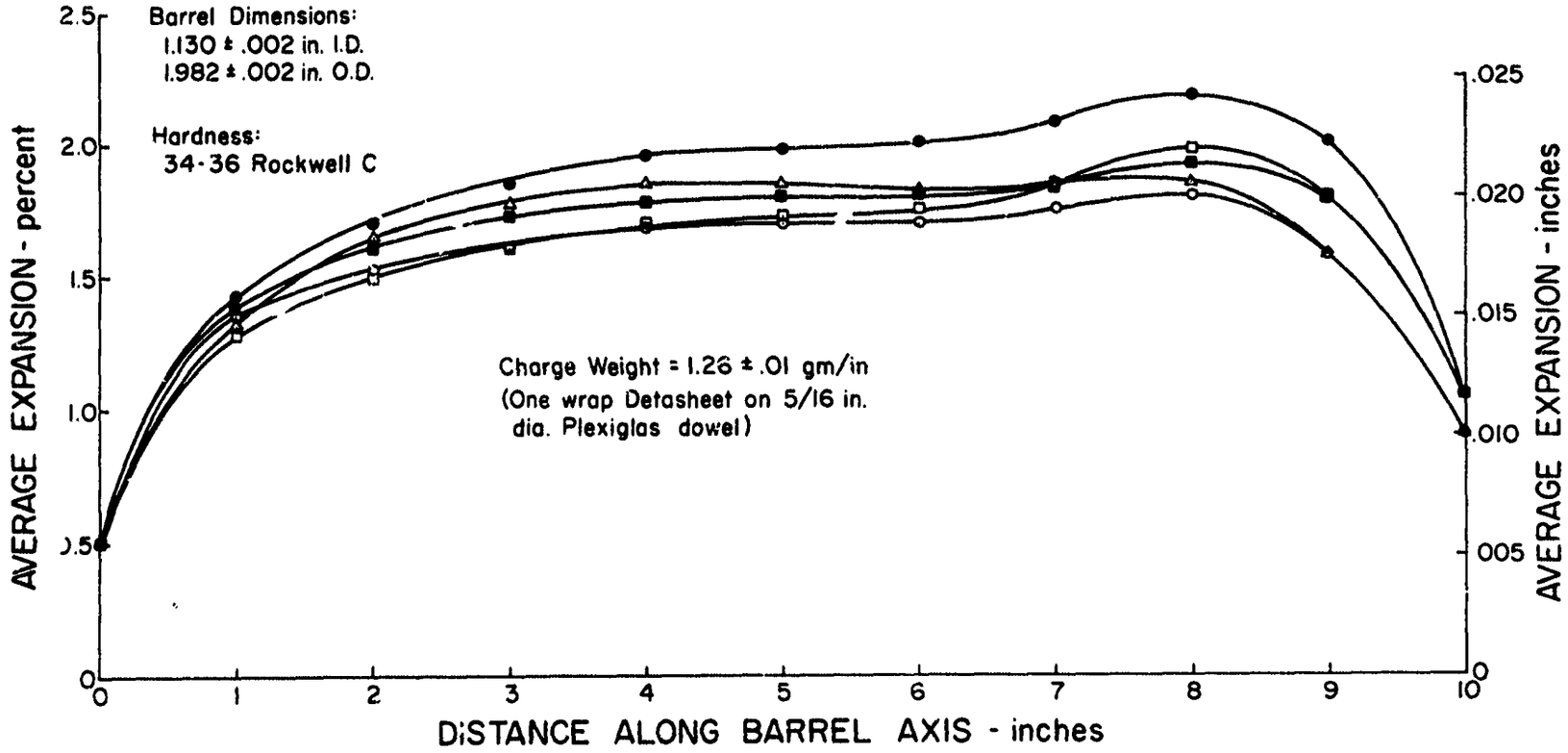

Figure 17 Bore Expansion of 1/5th Scale 4340 Steel Barrels (Repeatability Tests)

In preparation for the repeatability experiments, some minor modifications were made in the test set-up. Figure 14 shows the charge and the method of centering the charge which was used in the repeatability shots. In previous shots wooden end caps were used to center the charge; as shown in the figure, these were replaced with charge holders made of Plexiglas. Also, the wood dowel which was used previously as a core for the Detasheet was replaced with a Plexiglas dowel. The change to Plexiglas dowels was necessary to achieve the straightness and dimensional accuracy desired. Except for the changes indicated above, the test set-up was the same as shown in Figure 1.

4. Similitude Study and Scaling Laws for Autofrettage

A similitude study has been performed on the explosive autofrettage process for the purpose of developing the scaling laws. The following pages contain a presentation of the scaling law derivation.

Scaling Laws for Autofrettage

	Dependent Variable		Dimension
1.	W	charge per unit length	M/L
	Independent Variables		
2.	φ	specific energy of charge, i.e., energy/unit mass	L^2/T^2
3.	v	detonation velocity	L/T
4.	ρ_c	charge density	M/L^3
5.	d	outside diameter of charge	L
6.	D	initial inside diameter of barrel	L
7.	h	initial thickness of barrel	L
8.	L	length of barrel	L
9.	ϵ	permanent hoop strain at bore due to autofrettage	-
10.	λ	any typical dimension	L
11.	ρ_w	density of water (energy transfer medium)	M/L^3
12.	C_w	velocity of shock wave in water	L/T

	Independent Variables		Dimension
13.	E	modulus of elasticity of barrel	M/LT^2
14.	σ	yield stress of barrel	M/LT^2
15.	ρ_b	density of barrel material	M/L^3
16.	ρ_α	density of dowel material	M/L^3
17.	E_α	modulus of elasticity of dowel material	M/LT^2
18.	σ_α	crushing strength of dowel material	M/LT^2

There are 18 variables and 3 basic dimensions, i.e., mass, length and time. Hence, from Buckingham's π theorem, there will be 15 dimensionless variables as shown below:

$$\pi_1 = \frac{(W_e)}{(\sigma h^2 \epsilon)}$$

$$\pi_2 = e/v^2$$

$$\pi_3 = \rho_c/\rho_w$$

$$\pi_4 = d/D$$

$$\pi_5 = h/D$$

$$\pi_6 = \epsilon$$

$$\pi_7 = \lambda/D$$

$$\pi_8 = L/D$$

$$\pi_9 = v/C_w$$

$$\pi_{10} = \sigma/E$$

$$\pi_{11} = \rho_c/\rho_\alpha$$

$$\pi_{12} = \sigma_\alpha/\sigma$$

$$\pi_{13} = \sigma_\alpha/E_\alpha$$

$$\pi_{14} = C_w\sqrt{\rho/E}$$

$$\pi_{15} = E/E_\alpha$$

Using the subscripts p and m for prototype and model respectively, the scaling law will be given by:

$$\pi_{1p} = \pi_{1m},$$

if the similitude requirements given by the following relationships are satisfied:

$$\pi_{2p} = \pi_{2m}$$

$$\pi_{3p} = \pi_{3m}$$

$$\vdots \qquad \vdots$$

$$\pi_{15p} \qquad \pi_{15m}$$

Scale Factors

Since there are three basic dimension, three scale factors may be chosen arbitrarily. They are the following:

$$N_1 = D_p/D_m = 5$$

$$N_2 = \sigma_p/\sigma_m = 1$$

$$N_3 = \rho_{bp}/\rho_{bm} = 1$$

The scale factors for the remaining variables can then be deduced in terms of the arbitrary scale factors using the scaling law and prescribed similitude requirements.

From π_{10}, $E_p = E_m$, this will be satisfied if the gun barrel material is the same for model and prototype.

From π_3, $\rho_{wp} = \rho_{wm}$
From π_{14}, $C_{wp} = C_{wm}$
} Both scale factors for ρ_w and C_w will be satisfied

if water is used as the energy transfer medium for both model and full scale.

From π_9, $v_p = v_m$
From π_2, $e_p = e_m$
Both scale factors for v and e will be satisfied

if the same explosive is used for both model and full scale.

From π_4, $d_p = N_1 d_m = 5 d_m$

From π_5, $h_p = N_1 h_m = 5 h_m$

From π_8, $L_p = N_1 L_m = 5 L_m$

From π_7, $\lambda_p = N_1 \lambda_m = 5 \lambda_m$

From π_{11}, $\rho\alpha_p = \rho\alpha_m$

From π_{12}, $\sigma\alpha_p = \sigma\alpha_m$

From π_{13}, $E\alpha_p = E\alpha_m$

The scale factors for $\rho\alpha$, $\sigma\alpha$, and $E\alpha$ will be satisfied by using the same material for the dowel for both model and full scale.

From π_6, the permanent hoop strain imposed on the bore must be the same for model and full scale.

Finally, the scaling law for the explosive is given by

$$W_p = N_1^2 W_m = 25 W_m$$

5. End Effects Study

Several barrels were expanded with charges of different configurations to determine if it is possible to approach the ideal condition of equal expansion over the entire length of the barrel by using charges which have more explosive near the ends of the barrel. The charge configuration which has been designated as standard for the previous shots consists of a plexiglas rod wrapped with one layer of Detasheet explosive. The charge is detonated at one end with a blasting cap. These charges expanded the tube rather uniformly over approximately 8" of the length with the expansion tapering down to 25-70% of the central expansion on the ends. The reduced expansion on the ends of the tubes has been referred to as "end effects."

The first attempt to reduce the end effects was made using a charge consisting of the standard charge configuration with extra wraps of Detasheet 2 in. long placed so that they coincided with the ends of the barrel. The charge configuration drawing and a plot of the bore expansion which it produced are presented in Figure 18. A bore expansion curve from a shot with the standard charge configuration is also shown in the figure as a comparison. The end expansion produced by the modified charge is greater than desired; however, the results of this shot suggested that the end effects could be modified as desired by using a modified charge configuration.

After reviewing the results obtained with the extra wraps of Detasheet at the ends of the barrel, it was believed that while the size of the charge at the ends was sufficient, there was too much charge just inside the ends. For the next shot a mandrel was made which had tapered sections of increasing diameter coinciding with the ends of the barrel so that one wrap of Detasheet would give a charge weight which increased in a linear fashion at the ends of the barrel. The drawing of the mandrel and a plot of the bore expansion from this shot are shown in Figure 19. Again, the bore expansion produced by the standard charge configuration is presented for comparison. Practically no difference in the shape of the bore expansion curves can be seen in this figure. The difference in the amplitude is no more than might be expected between two expansion plots from shots which both used the standard charge configuration.

The explanation for the lack of additional expansion on the ends of the barrel may be that the additional energy in the charge was absorbed by

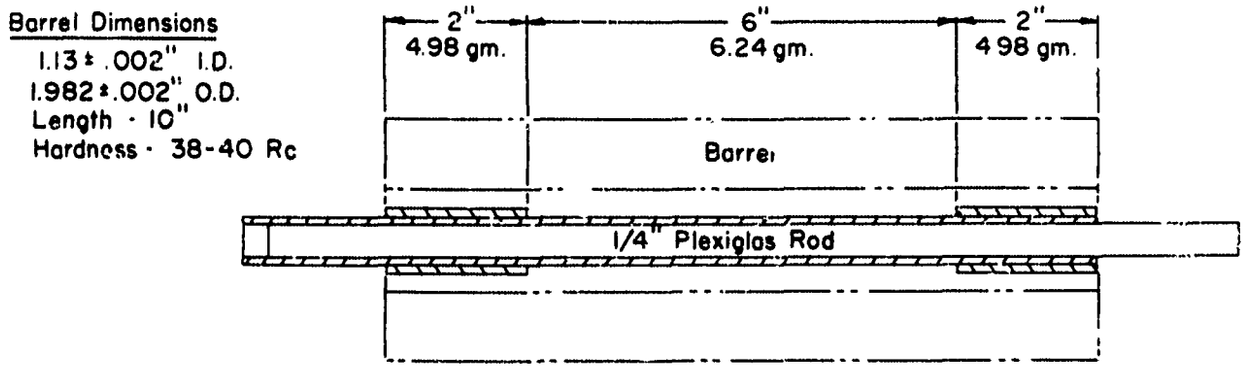

MODIFIED DETASHEET CHARGE CONFIGURATION

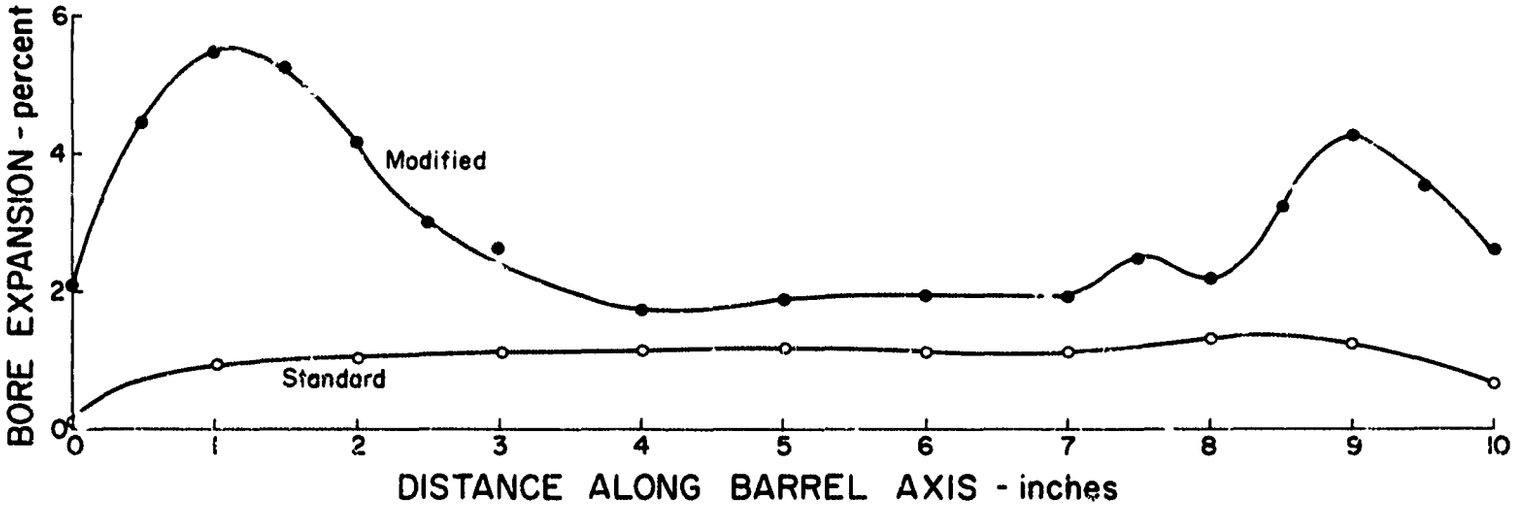

Figure 18 Bore Expansion of 1/5th Scale 4340 Steel Barrels with Modified Charge Configurations

Barrel Dimensions

1.13 ± .002" I.D.
1.982 ± .002" O.D.
Length - 10"
Hardness - 38-40 Rc

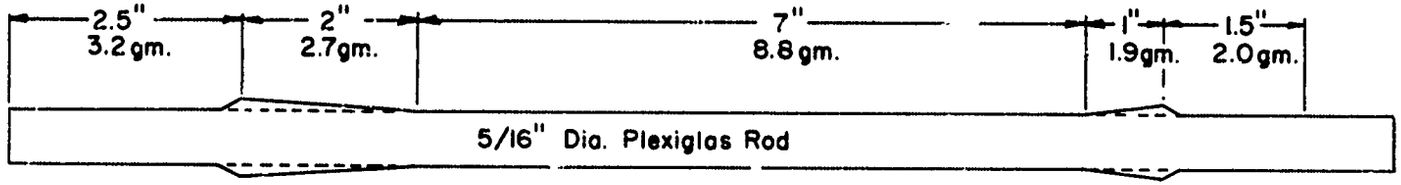

TAPERED MANDREL AND DETASHEET CHARGE CONFIGURATION

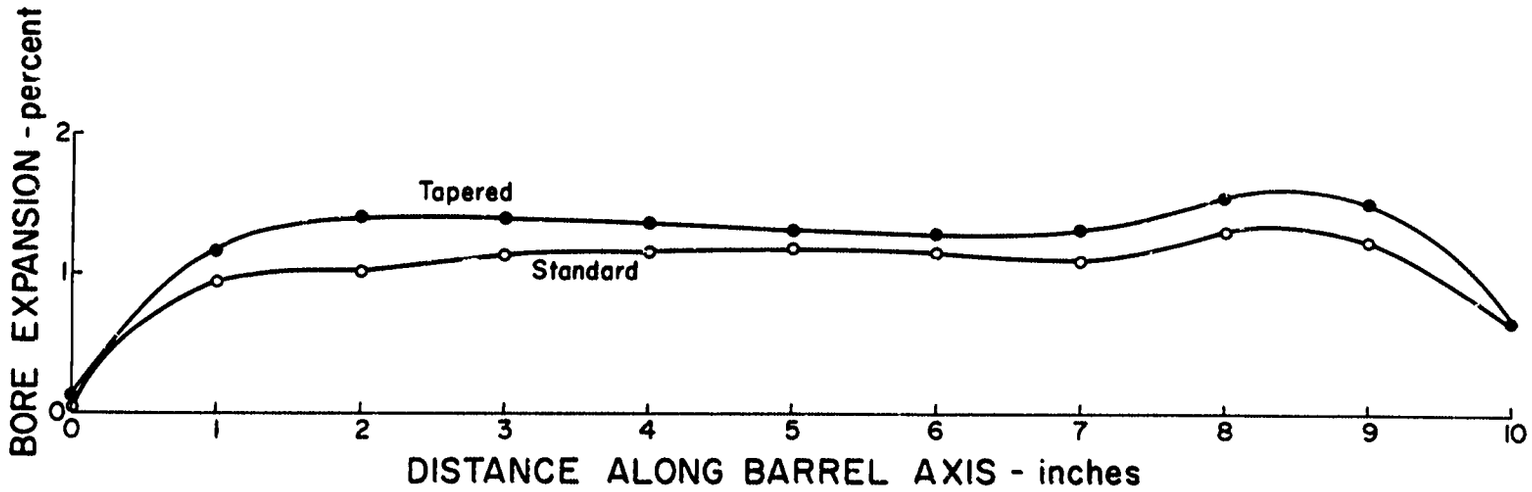

Figure 19 Bore Expansion of 1/5th Scale 4340 Steel Barrels with Modified Charge Configuration

the additional dowel material. Also, since shock waves are transmitted in both directions from the exploding Detasheet there may be a phase relationship between reflected waves which is important.

In the last two shots of the series, extra wraps of Detasheet were again used to provide more energy for expansion at the ends of the barrels. In the first of these tests the extra wrap on the ignition end of the charge was placed so that it was 1 in. on the inside and 1 in. on the outside of the barrel; the extra wrap on the other end of the charge was placed so that it was entirely on the outside of the tube with the edge of the wrap coinciding with the end of the barrel. A drawing of the charge configuration and a plot of the resulting bore expansion are presented in Figure 20. The expansion on the ignition end of the barrel was too great but the expansion on the other end came very close to the ideal. The charge configuration was made different on the two ends of the tube so that more could be learned from each shot.

In the last test which was made on the modification of end effects, the extra explosive on the ignition end of the tube consisted of two extra wraps, one 2" long and one 1" long, arranged so that their ends coincided with the end of the barrel. The extra explosive on the other end consisted of one extra wrap 2" long placed 1/4" inside the barrel and 1-3/4" on the outside. A drawing of the charge configuration and a plot of the resulting bore expansion are presented in Figure 21. The results of these tests indicate that the ideal expans[illegible] over the length of the barrel can be approached with an extra wrap o[illegible]asheet 2" long placed 1/4" inside the end of the barrel.

6. Dynamic Strain Measurements

The problem of obtaining dynamic strain data which was desired for use in the mathematical analysis has been attacked. Strain gages were attached to the outside of the barrels and oriented so that hoop and longitudinal strains could be measured. The gages were excited by constant current DC sources. A Tektronics Model 555 Oscilloscope is used for readout. A Polaroid equipped scope camera is used to make a record of the scope trace. A scope triggering circuit was built which provides a 12 volt pulse to the scope when a circuit is opened. The switch to open this circuit consists of a small wire which is positioned so that it is broken by the explosion of the blasting cap which initiates the explosive charge. It was concluded from the results of several tests with wires and blasting caps in the configuration required for the charge initiation that 28 gage magnet wire gave reliable results. Larger wires were found to separate too slowly to trigger the scope in time to measure the output from the gages. The strain gages were Bean Type BAE-06-187BB-120 and were mounted in the conventional manner using RTC cement and Gagekote Type A. The gages were waterproofed with silicone rubber. The strain gages were able to survive the event and remain well attached to the tube; however, the dynamic activity of the lead wires induced by the shock wave resulted in the destruction of the terminal strips and the separation of the wires from the gages.

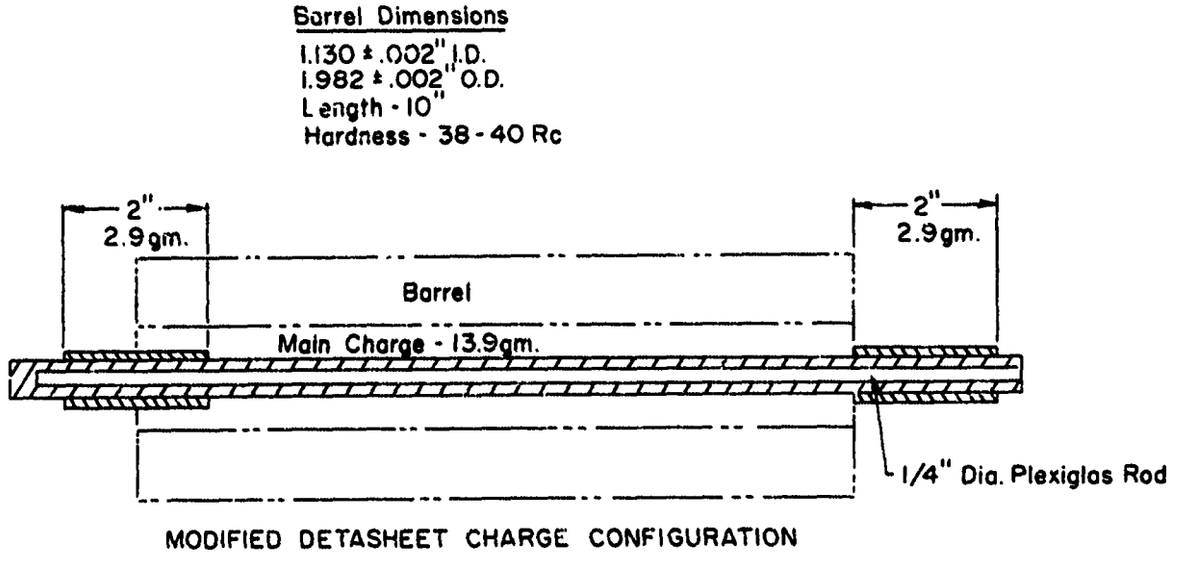

MODIFIED DETASHEET CHARGE CONFIGURATION

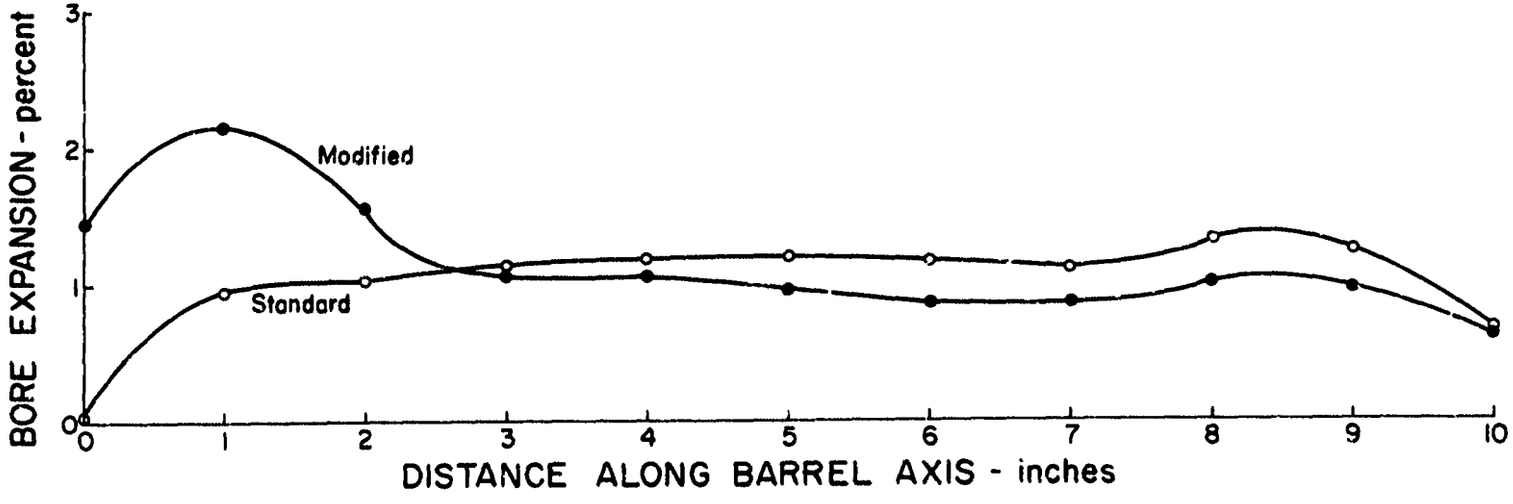

Figure 20 Bore Expansion of 1/5th Scale 4340 Steel Barrels with Modified Charge Configuration

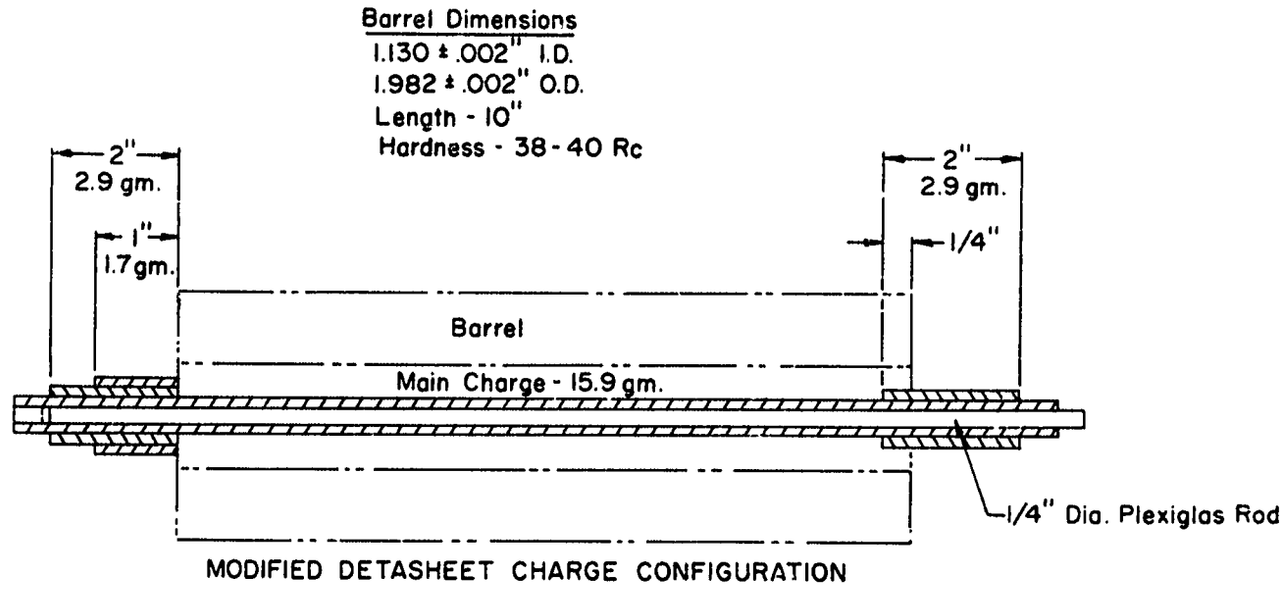

MODIFIED DETASHEET CHARGE CONFIGURATION

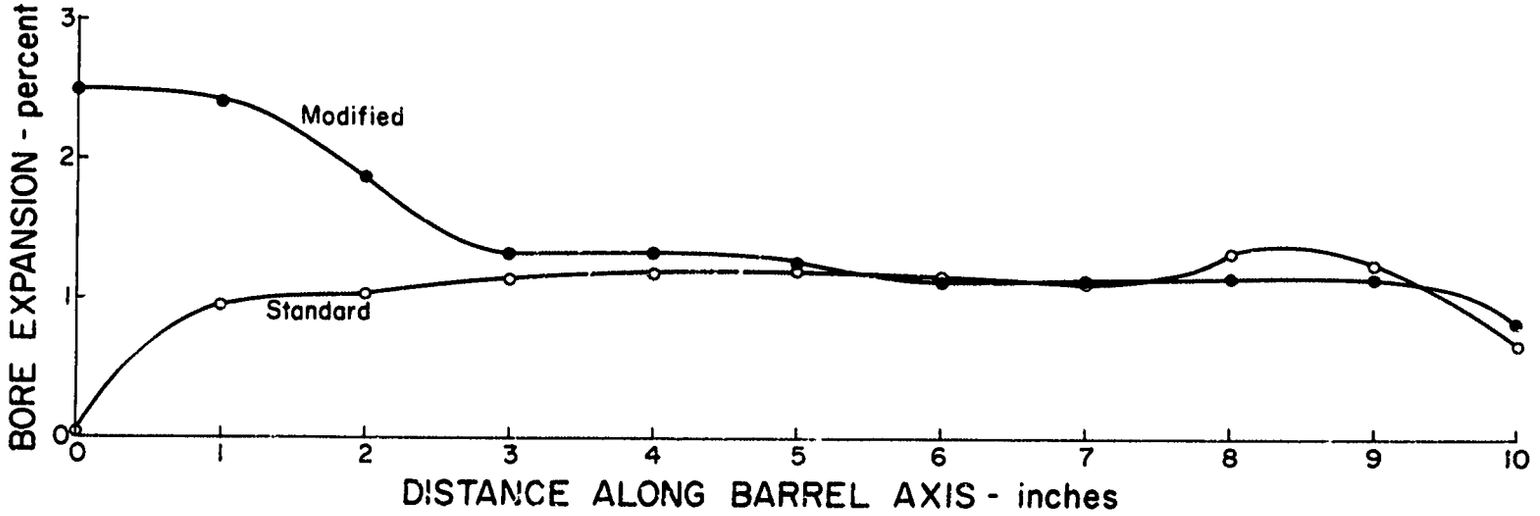

Figure 21 Bore Expansion of 1/5th Scale 4340 Steel Barrels with Modified Charge Configurations

This problem was solved by binding the lead wires to the barrel with fiber reinforced tape. Figure 22 shows a trace of the dynamic strain in the hoop direction. Due to the long set up time required to obtain the dynamic strains, this phase of the effort was held to a minimum.

7. Residual Stress Determination

A computer program was written which will compute the residual stresses in an autofrettaged tube from strain gage data obtained on the outside of the tube after successive enlargements are made in the bore with a boring tool. The method, described here, is known as the Sachs boring-out method.

A. Residual Stress Analysis

Consider a cylinder of inside radius, a, and outside radius, b, which is known to have a residual stress distribution which is axially symmetric, and a case of plane strain.

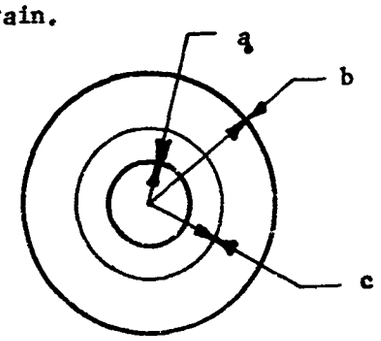

The distribution of stress must satisfy the equilibrium equation which in this case is

$$\frac{d}{dr}\ (r\,\sigma_{rr}) - \sigma_{\theta\theta} = 0 \qquad 7.1$$

but is otherwise unrestricted.

Let one (or more) strain gages be mounted on the exterior of the cylinder to measure changes in hoop strain at the outer surface, b. If the cylinder is carefully drilled out to an inside radius, c, and the cylinder is carefully brought to the same temperature as before drilling, the strain gage will indicate a change in reading due to removing an inner core of stressed material. The problem then is to relate the change in strain reading to the state of residual stress.

Before starting the analysis, let us recall some of the elementary formulas. Below are the constitutive equations for plane strain.

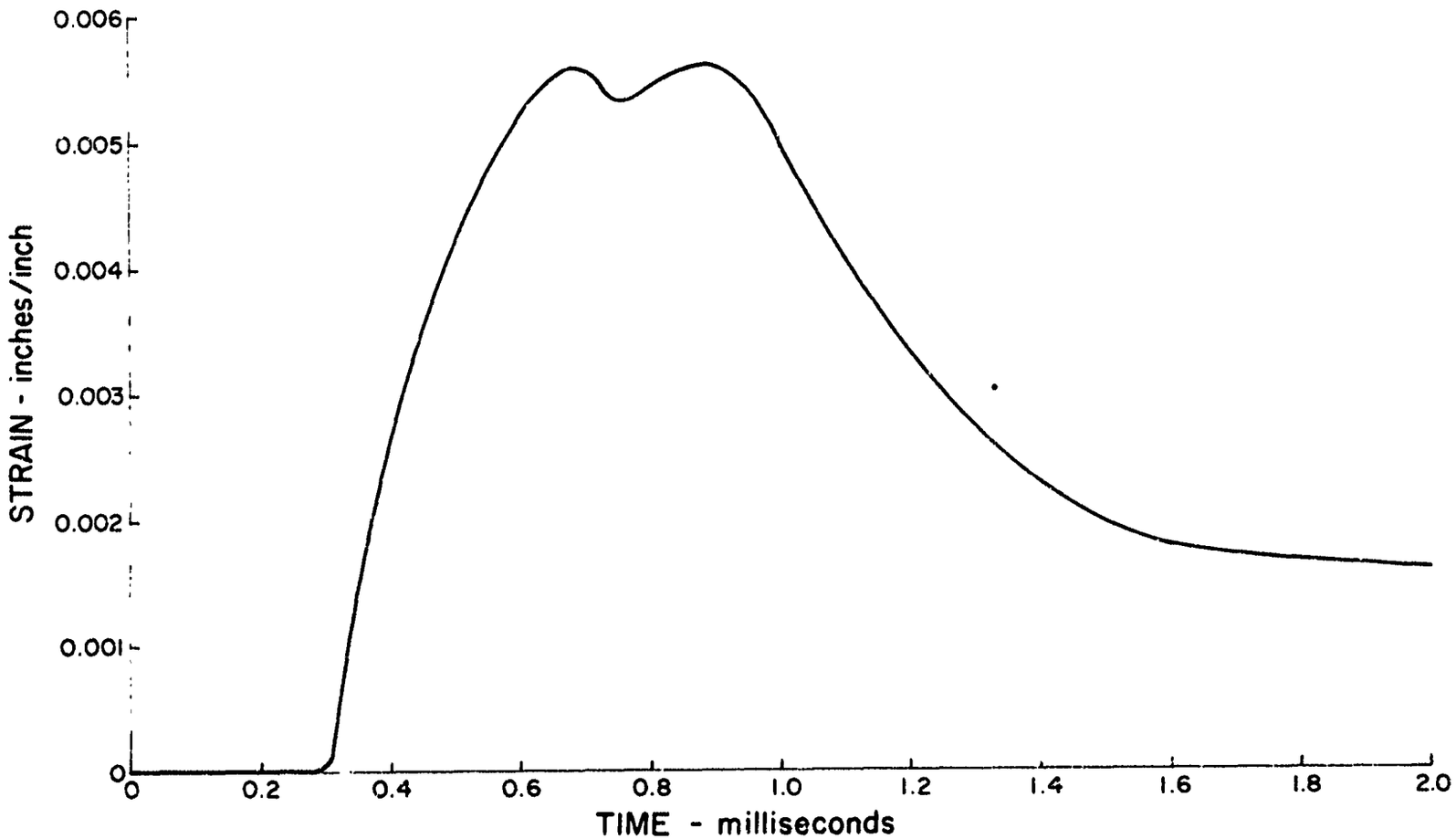

Figure 22 Dynamic Hoop Strain - 1/5th Scale Tube

$$Ee_{rr} = \sigma_{rr} - \nu(\sigma_{\theta\theta} + \sigma_{zz})$$
$$Ee_{\theta\theta} = \sigma_{\theta\theta} - \nu(\sigma_{rr} + \sigma_{zz}) \qquad 7.2$$
$$Ee_{zz} = \sigma_{zz} - \nu(\sigma_{rr} + \sigma_{\theta\theta}) = 0$$

$$\sigma_{rr} = \frac{E}{(1-2\nu)(1+\nu)}\left[(1-\nu)\, e_{rr} + \nu e_{\theta\theta}\right]$$

$$\sigma_{\theta\theta} = \frac{E}{(1-2\nu)(1+\nu)}\left[(1-\nu)e_{\theta\theta} + \nu\, e_{rr}\right] \qquad 7.3$$

Strain displacement equations for axisymmetric problems are

$$e_{rr} = \frac{du}{dr}\ ,\quad e_{\theta} = \frac{u}{r}\ .$$

The basic formulas for thick-walled cylinders are:

Internal pressure, P

$$\sigma_{rr} = \frac{P a^2}{b^2 - a^2}\left(1 - \frac{b^2}{r^2}\right) \qquad \sigma_{\theta\theta} = \frac{P a^2}{b^2 - a^2}\left(1 + \frac{b^2}{r^2}\right) \qquad 7.4$$
$$Ee_{\theta} = \frac{Eu}{r} = \frac{P a^2}{b^2 - a^2}(1+\nu)\left[(1-2\nu) + \frac{b^2}{r^2}\right]$$

External pressure, P

$$\sigma_{rr} = -\frac{P b^2}{b^2 - a^2}\left(1 - \frac{a^2}{r^2}\right) \qquad \sigma_{\theta\theta} = \frac{P b^2}{b^2 - a^2}\left(1 + \frac{a^2}{r^2}\right) \qquad 7.5$$
$$E\frac{u}{r} = -\frac{P b^2}{b^2 - a^2}(1+\nu)\left[(1-2\nu) + \frac{a^2}{r^2}\right]$$

Consider now what happens as the cylinder is bored out to an inside radius, c_o. In the original cylinder, there existed at the radius r = c, a residual radial stress, R_r, and a residual hoop stress, R_θ. Let us suppose the inner core is removed by making a cut of radius C and then sliding out

the inner core of $0 \leq r \leq c$.

Behavior of the outer cylinder:

Removing the inner core effectively releases the stress R_r at $r = c$. Upon setting $P = +R_r$ the change in strain at the outer surface is seen to be

$$E\,\delta e_{\theta\theta} = \frac{R_r\, c^2}{b^2 - c^2}(1+\nu)\left[1 - 2\nu + \frac{b^2}{b^2}\right] = \frac{2\,R_r\, c^2\,(1-\nu^2)}{b^2 - c^2}$$

Note that R_r has been assumed compressive, from which

$$R_r = \frac{b^2 - c^2}{2(1-\nu^2)c^2}\; E\,\delta e_{\theta\theta} \qquad 7.6$$

The changes in the residual stresses in the outer cylinder are

$$\delta\sigma_{rr} = \frac{R_r\, c^2}{b^2 - c^2}\left(1 - \frac{b^2}{r^2}\right) = \frac{E\,\delta e_{\theta\theta}}{2(1-\nu^2)}\left(1 - \frac{b^2}{r^2}\right)$$

$$\delta\sigma_{\theta\theta} = \frac{R_r\, c^2}{b^2 - c^2}\left(1 + \frac{b^2}{c^2}\right) = \frac{E\,\delta e_{\theta\theta}}{2(1-\nu^2)}\left(1 + \frac{b^2}{r^2}\right) \qquad 7.7$$

Behavior of the inner cylinder:

When the inner cylinder is withdrawn, the stress R_r is relaxed from the outer surface ($r = c$). Thus, the change in stress in the inner cylinder is

$$\delta\sigma_{rr} = -\frac{R_r\, c^2}{c^2 - a^2}\left(1 - \frac{a^2}{r^2}\right) = -\frac{b^2 - c^2}{c^2 - a^2}\,\frac{E\,\delta e_{\theta\theta}}{2(1-\nu^2)}\left(1 - \frac{a^2}{r^2}\right)$$

$$\delta\sigma_{\theta\theta} = -\frac{R_r\, c^2}{c^2 - a^2}\left(1 + \frac{a^2}{r^2}\right) = -\frac{b^2 - c^2}{c^2 - a^2}\,\frac{E\,\delta e_{\theta\theta}}{2(1-\nu^2)}\left(1 + \frac{a^2}{b^2}\right) \qquad 7.8$$

Note that when the inner cylinder is withdrawn the final state of stress is

$$\sigma_{rr1} = \sigma_{rro} + \delta\sigma_{rr} \qquad \sigma_{\theta\theta 1} = \sigma_{\theta\theta o} + \delta\sigma_{\theta\theta}$$

Hence, σ_{rr} is zero at r = a and r = c. If the inner cylinder is thin so that (c-a)/c<<1 it follows that σ_{rr1} cannot become very large if the variation of residual strain is not very large. Thus, if both σ_{rr1} and $\partial \sigma_{rr1}/\partial r$ are small, by the equilibrium equation $\sigma_{\theta\theta 1}$, is also small and

$$\sigma_{\theta\theta_o} \approx -\delta\sigma_{\theta\theta} = \frac{R_r c^2}{c^2 - a^2}\left(1 + \frac{a^2}{r^2}\right) = \frac{E\,\delta e_{\theta\theta}}{2(1-\nu^2)}\left(\frac{b^2 - c^2}{c^2 - a^2}\right)\left(1 + \frac{a^2}{r^2}\right)$$

$$\text{at } r = a \qquad \sigma_{\theta\theta_o} = \frac{E\,\delta e_{\theta\theta}}{1-\nu^2}\left(\frac{b^2 - c^2}{c^2 - a^2}\right) \qquad 7.9$$

Multiboring to Determine Distribution of Residual Stress

To determine the distribution of residual stress in the cylinder in a region $a \leq r \leq c_n$ let there be a series of borings to radii C_1, C_2, ... C_n with a corresponding number of strain measurements δe_1, δe_2, ... δe_n. The problem then is to develop the algorithm for calculating the residual stress in the original cylinder.

Let the distribution of residual stress in the original cylinder be σ_{ro}, $\sigma_{\theta o}$. The incremental residual radial stress found by the kth cut be R_k so that

$$R_k = \frac{b^2 - c_k^2}{c_k^2}\,\frac{E}{2(1-\nu^2)}\,\delta e_k \qquad 7.10$$

The change in residual stress at radius c_m, $k \leq m \leq n$, is from equation 7.7

$$\delta\sigma_{r_{km}} = \frac{R_k c_k^2}{(b^2 - c_k^2)}\left(1 - \frac{b^2}{r_m^2}\right) = \frac{E\,\delta e_k}{2(1-\nu^2)}\left(1 - \frac{b^2}{r_m^2}\right)$$

$$\delta\sigma_{\theta km} = \frac{R_k c_k^2}{b^2 - c_k^2}\left(1 + \frac{b^2}{r_m^2}\right) = \frac{E\,\delta e_k}{2(1-\nu^2)}\left(1 + \frac{b^2}{r_m^2}\right) \qquad 7.11$$

The change in residual stress at radius c_{k-1} is

$$\delta\sigma_{r_{k\,k-1}} = 0$$

$$\delta\sigma_{\theta_{k\,k-1}} = -\frac{2 R_k c_k^2}{c_k^2 - c_{k-1}^2} = -\frac{E\,\delta e_k}{1-\nu^2}\left(\frac{b^2 - c_k^2}{c_k^2 - c_{k-1}^2}\right) \qquad 7.12$$

The stresses at the outer surface of the cylinder can be calculated using Equations 1 and 4. From Equation 4, σ_{rr} is zero when r = b. From Equation 1,

$$\sigma_{\theta\theta} = \frac{\delta}{\delta r} (r\sigma_{rr}) \qquad 7.13$$

Using the equations previously developed, the radial stress distribution can be found. Once this is known, the righthand side of Equation 13 can be calculated for every radius. In order to determine the value of the quantity at the outer radius of the cylinder, a hyperbolic fit is used to extrapolate the right side of the equation to the outer radius. Once this is accomplished, the remaining stress, $\sigma_{\theta\theta}$, is specified.

B. Computer Program Listing

The computer program listing for calculating the residual stress is shown on the following pages.

C. Procedures for Obtaining Residual Strain

1. Strain Gage Mounting. Bean No. BAE-06-250BB-120TE

The gages were mounted on the tube according to the procedures received with the strain gages. Figure 23 is a sketch showing the location of the gages on the 3-inch long tube which was used in the tests. It is necessary to have a gage mounted on an unstrained steel bar having the same coefficient of expansion as the specimen. This piece of material, known as the "temperature compensating block" or "compensating block," should have two gages mounted on it according to the instructions referred to above. The lead wires to one of these gages should be marked "compensating" while the leads to the other should be marked "test".

2. Temperature Equilibrium

Before any boring out of the tube can be attempted it is necessary to establish that the tube is in thermal equilibrium between the outside surface, the center of the wall, and the inside surface. This may be done by resistance welding thermocouples (iron-constantan were used) to the inside and outside wall of the tube and by drilling a small hole longitudinally in the tube wall at the midpoint, and cementing a thermocouple into the hole. The specimen, along with the compensating block is placed in an insulated container with the lead wires arranged so that the thermocouples and strain gages can be read without disturbing the test piece or the compensating block. The insulated container is maintained at room temperature in any convenient thermostatically controlled room and will perform satisfactorily as long as the fluctuations in the room temperature are gradual.

3. Reading the Gages

After thermal equilibrium has been established as indicated by potentiometer readings of the thermocouples to $\pm$ 0.01 mv ($\pm$ 0.1°F), a series of strain gage readings should be taken to establish a zero reading for each gage. (An SR-4 Baldwin Strain Indicator was used in the tests

```
          BEGIN                                                          *  ERSC
COMMENT       J. A. WEESE UNIVERSITY OF DENVER.                          *  ERSC
          THIS PROGRAM CALCULATES THE RESIDUAL STRESSES IN A THICKWALLED  *  ERSC
          CIRCULAR CYLINDER FROM EXPERIMENTAL DATA OBTAINED BY BORING OUT *  ERSC
          THE INSIDE OF THE CYLINDER AND FOR EACH BORE DIAMETER MEASURING *  ERSC
          THE CHANGE IN HOOP STRAIN AT THE OUTER SURFACE.                 *  ERSC
            INPUT DATA                                                    *  ERSC
              FIRST CARD   OUTSIDE AND INSIDE DIAMETERS OF CYLINDER IN    *  ERSC
                           INCHES. USE F8.4 WITH DECIMAL POINTS IN        *  ERSC
                           COLUMNS 4 AND 14                               *  ERSC
              SECOND CARD  INSERT THE NAME OF THE MATERIAL IN THE FIRST 18 *  ERSC
                           COLUMNS  YOUNGS MODULUS AS AN E10.3 IN COLUMNS *  ERSC
                           21 THRU 30 AND POISSONS RATIO AS AN F6.3 IN    *  ERSC
                           COLUMNS 36 THRU 41. USE E IN PSI.              *  ERSC
              THIRD CARD   NUMBER OF PAIRS OF BORE DIAMETERS AND STRAIN   *  ERSC
                           READINGS AS AN I2 IN COLUMNS 1 AND 2.          *  ERSC
              REST OF CARDS PAIRS OF BORE DIAMETERS IN INCHES AND CHANGE  *  ERSC
                           IN STRAIN READINGS. USE F8.4 WITH DECIMAL IN   *  ERSC
                           COLUMN 4 FOR THE BORE AND AN F8.2 WITH DECIMAL *  ERSC
                           IN COLUMN 16 FOR THE INCREMENTAL STRAIN. THE   *  ERSC
                           LATTER IS TO BE INSERTED IN MICRO-INCHES PER   *  ERSC
                           INCH USING + FOR EXTENSION AND - FOR           *  ERSC
                           CONTRACTIONS OF THE OUTER SURFACE.             *  ERSC
  FILE OUT       LINE 18(2,15);                                          *  ERSC
  FILE IN        CARD (2,10);                                            *  ERSC
  FORMAT OUT     FO1("EXPERIMENTALLY DETERMINED RESIDUAL STRESSES IN A ",*  ERSC
                     "THICK WALLED CYLINDER"/// " OUTSIDE DIAMETER = ",  *  ERSC
                     F8.4," IN     INSIDE DIAMETER = ",F8.4," IN"//),    *  ERSC
                 FO2("MATERIAL IS ",3A6,X5,"E =",E10.3," PSI  NU = ",    *  ERSC
                     F6.3 /// "EXPERIMENTAL DATA" // " BORE DIAMETER",X7,*  ERSC
                     "INCREMENTAL STRAIN" / X5,"IN",X15,"MICRO-IN PER ", *  ERSC
                     "IN"),                                               *  ERSC
                 FO3(X3,F8.4,X15,F8.2),                                  *  ERSC
                 FO4(//"RESIDUAL STRESS DISTRIBUTION"/"DIAMETER",X13,    *  ERSC
                     "RESIDUAL STRESS IN KSI" / X3,"IN",X17,"HOOP",      *  ERSC
                     X9,"RADIAL",X10,"D(RSR)/DR"),                       *  ERSC
                 FO5(F8.4,X11,F10.3,X5,F10.3,X6,F10.3);                  *  ERSC
  FORMAT IN      FI1(2(F8.4,X2)), FI2(3A6,X2,E10.3,X5,F6.3),FI3(I2),     *  ERSC
                 FI4(F8.4,X2,F8.2);                                      *  ERSC
  REAL           A,B,E,NU,ENU,BR2,S1,S2,S3,S4,DO,D1,D2,D,X,X2,RX;        *  ERSC
  LABEL          REED,DUNN;                                              *  ERSC
  ALPHA          M1,M2,M3;                                               *  ERSC
  ARRAY          BD,DEBAR,BRP,BRM,SR,STD,RSR,ST[0:30],DSR,DST[0:30,0:30];*  ERSC
  INTEGER        N,I,K,M,J;                                              *  ERSC
  REED:          READ(CARD,FI1,B,A)[DUNN];                               *  ERSC
                 WRITE(LINE,FO1,B,A);                                    *  ERSC
                 READ(CARD,FI2,M1,M2,M3,E,NU);                           *  ERSC
                 WRITE(LINE,FO2,M1,M2,M3,E,NU);                          *  ERSC
```

```
     READ(CARD,FI3,N);                                          *  ERSC
     FOR I ← 1 STEP 1 UNTIL N DO                                *  ERSC
BEGIN                                                           *  ERSC
     READ(CARD,FI4,BD[I],DEBAR[I]);                             *  ERSC
     WRITE(LINE,FO3,BD[I],DEBAR[I]);                            *  ERSC
END;                                                            *  ERSC
     WRITE(LINE,FO4);                                           *  ERSC
     ENU ←(0,5 × E × @-09)/(1 - NU*2);                          *  ERSC
     BD[0] ← A; DEBAR[0] ← 0;                                   *  ERSC
     FOR I ← 0 STEP 1 UNTIL N DO                                *  ERSC
BEGIN                                                           *  ERSC
     BR2    ← (B/BD[I])*2;                                      *  ERSC
     BRP[I] ← 1 + BR2;                                          *  ERSC
     BRM[I] ← 1 - BR2;                                          *  ERSC
END;                                                            *  ERSC
     FOR K ← 1 STEP 1 UNTIL N DO                                *  ERSC
     FOR M ← K STEP 1 UNTIL N DO                                *  ERSC
BEGIN                                                           *  ERSC
     DSR[K,M] ← ENU×DEBAR[K]×BRM[M];                            *  ERSC
     DST[K,M] ← ENU×DEBAR[K]×BRP[M];                            *  ERSC
END;                                                            *  ERSC
     FOR K ← 1 STEP 1 UNTIL N DO                                *  ERSC
BEGIN                                                           *  ERSC
     DSR[K,K-1] ← 0;                                            *  ERSC
     DST[K,K-1] ←-2 × DEBAR[K] × (B*2 - BD[K]*2) × ENU /        *  ERSC
         (BD[K]*2 - BD[K-1]*2);                                 *  ERSC
END;                                                            *  ERSC
     DSR[0,0] ← DST[0,0] ← DST[N+1,N] ← 0;                      *  ERSC
     FOR I ← 0 STEP 1 UNTIL N DO SR[I] ← ST[I] ← 0;             *  ERSC
     FOR K ← 0 STEP 1 UNTIL N DO                                *  ERSC
BEGIN                                                           *  ERSC
     FOR J ← 1 STEP 1 UNTIL K DO                                *  ERSC
     SR[K] ← SR[K] - DSR[J,K];                                  *  ERSC
     FOR J ← 1 STEP 1 UNTIL K + 1 DO                            *  ERSC
     ST[K] ← ST[K] - DST[J,K];                                  *  ERSC
END;                                                            *  ERSC
     S1 ← S2 ← S3 ← S4 ← D0 ← D1 ← D2 ← 0;                      *  DIFF
     N ← N+1; SR[N] ← 0;                                        *  DIFF
     FOR I ← 0 STEP 1 UNTIL N DO RSR[I] ← BD[I]×SR[I]×0,5;      *  DIFF
     FOR I ← 1,2,3 DO                                           *  DIFF
BEGIN                                                           *  DIFF
     X ← (BD[I] - BD[0])×0,5;                                   *  DIFF
     S2 ← S2 + X*2; S3 ← S3 + X*3; S4 ← S4 + X*4;               *  DIFF
     D1 ← D1 + RSR[I]×X; D2 ← D2 + RSR[I]×X*2;                  *  DIFF
END;                                                            *  DIFF
     D ← S2×S4 - S3×S3;                                         *  DIFF
     STD[0] ← (D1×S4 - D2×S3)/D;                                *  DIFF
     STD[1] ← STD[0] + (BD[1]-BD[0])×(D2×S2-D1×S3)/D;           *  DIFF
     FOR I ← 2 STEP 1 UNTIL N-2 DO                              *  DIFF
BEGIN   S1←S2←S3←S4←D0←D1←D2←0;                                 *  DIFF
     FOR K ← -2 STEP 1 UNTIL 2 DO                               *  DIFF
BEGIN                                                           *  DIFF
     X ← 0,5×(BD[I+K]-BD[I]); X2 ← X*2; RX ← RSR[I+K]×X;        *  DIFF
     S1 ← S1+X; S2 ← S2+X2; S3 ← S3+X×X2; S4 ← S4 + X2*2;       *  DIFF
     D0 ← D0 + RSR[I+K]; D1 ← D1 + RX; D2 ← D2 + RX × X;        *  DIFF
```

```
            END;                                                                    *  DIFF
                D ← 5×(S2×S4-S3*2)-S1×(S1×S4-S2×S3)+S2×(S1×S3-S2*2);                *  DIFF
                STD[I] ← (-D0×(S1×S4-S2×S3)+D1×(5×S4-S2*2)                          *  DIFF
                        -D2×(5×S3-S1×S2))/D;                                        *  DIFF
            END;                                                                    *  DIFF
                S1 ← S2 ← S3 ← S4 ← D0 ← D1 ← D2 ← 0;                               *  DIFF
                FOR I ← 1,2,3 DO                                                    *  DIFF
            BEGIN                                                                   *  DIFF
                X ← (BD[N-I] - BD[N])×0.5; X2 ← X*2;                                *  DIFF
                S2 ← S2 + X2; S3 ← S3 + X×X2; S4 ← S4 + X2*2;                       *  DIFF
                D1 ← D1 + RSR[N-I]×X; D2 ← D2 + RSR[N-I]×X2;                        *  DIFF
            END;                                                                    *  DIFF
                D ← S2×S4 - S3*2;                                                   *  DIFF
                STD[N] ← (D1×S4 - D2×S3)/D;                                         *  DIFF
                STD[N-1] ← STD[N] + (BD[N-1]-BD[N])×(D2×S2-D1×S3)/D;                *  DIFF
                FOR I ← 0 STEP 1 UNTIL N DO                                         *  ERSC
                WRITE(LINE,F05,BD[I],ST[I],SR[I],STD[I]);                           *  ERSC
                WRITE(LINE[PAGE]);                                                  *  ERSC
                GO TO REED;                                                         *  ERSC
DUNN:       END.                                                                    *  ERSC
```

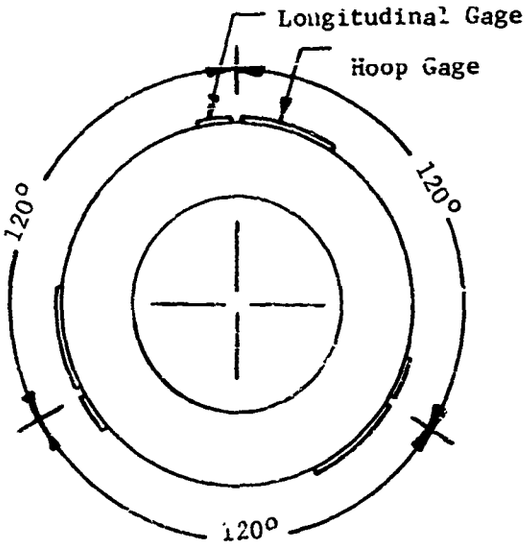

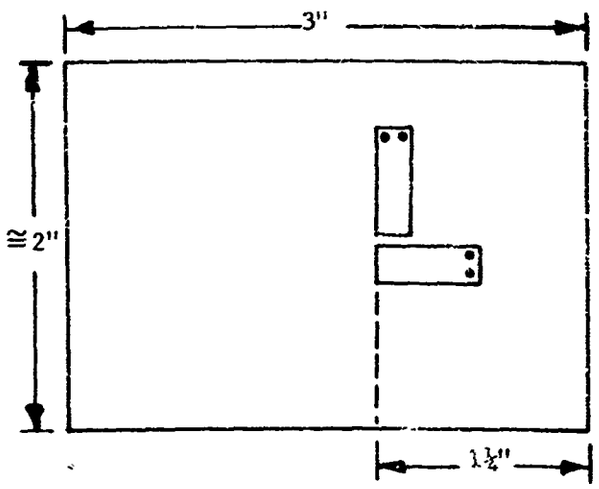

Figure 23 Barrel Specimen Showing Strain Gages in Place

made by DRI). It is advisable to allow all of the pieces to "soak" in the container at least several hours and monitor the temperature inside the container with a laboratory quality mercury thermometer to be certain that no rapid temperature changes occur. The compensating block and the actual test piece must be located very close together at the same level in the container to be certain that they are in the same environment. (In the DRI tests the thermocouples were iron-constantan with a reference junction temperature of 32°F. The reference junction was maintained at 32°F by using crushed ice and water and making certain that all cold junctions were in the center of the container with ice packed around them). In addition to the compensating gage, a second gage should be mounted on the compensating block. This gage can be used to check the performance of the strain indicator, i.e., the reading taken on this gage must be the same each day plus or minus a small error since the compensating block is never disturbed in any way.

The inside diameter of the tube may be measured at this time. At DRI this was done using a Scherr-Tumico Series 210, number 2105, bore gage. This gage consists of a tube about 12" long with a dial gage (calibrated in 1/1000 in.) mounted on one end and a bore measuring attachment at the other. When the bore measuring attachment is depressed, the dial gage indicates the change. The gage is used by setting the attachment to a predetermined value using micrometer. When the bore gage is inserted into the tube, the change from this setting is indicated by the dial gage and is either added to or subtracted from the initial setting (determined by noting whether the needle on the dial gage moves in the + or - direction).

4. Taking a Cut

After a complete set of readings (temperature, strain gages and inside diameter) have been recorded, the test specimen is removed from the container and "chucked up" in a lathe. The lathe chuck must be modified to clamp the test piece uniformly around its circumference. This was done by machining three 3034 aluminum bars, Figure 25, which were bolted to the jaws of a "Burnerd 3 Jaw Grip-Tru Chuck," making, in effect, a soft collet. The test piece, when mounted in the collet, is clamped securely. The chuck is then indexed into center $\pm$ .0005" by adjusting the chuck. (The Burnerd Grip-Tru Chuck is very convenient to use for this purpose since it can be adjusted to center after the jaws have been tightened). When the final adjustments have been made, a .020" cut is taken on the radius of the test piece using, in this case, a boring bar with a carbide tool.

After the tool has made one pass it is generally necessary to inspect the bore visually to determine if the cut is smooth enough to be satisfactory. Occasionally, due to hard spots, the tool will wear very quickly requiring that a new tool be installed and a clean up pass about .005" deep be made through the tube. A lathe operator skilled in machining hard steels using carbide tools should be employed. (Note that when mounting the tube in the lathe the lead wires from the strain gages and the thermocouples must be wound and taped to the chuck to prevent them from whipping around. Also, the thermocouple which was welded to the inside surface of the tube must be replaced after the cut is completed.) When the lathe work is done the piece is removed and placed back in the container where it is allowed to remain undisturbed until it reaches thermal equilibrium whereupon the whole operation is repeated. Thus, when listed in step-by-step form, the following procedures are recommended:

(a) Select the barrel specimen to be tested.

(b) Select the strain gages to be used.

(c) Mount the strain gages on the barrel specimen using the previously outlined technique and install lead wires.

(d) Make up a compensating block of the same material, and mount two of the same type strain gages used above and install lead wires.

(e) Mount thermocouples on test piece and on compensating block, using appropriate thermocouple mounting techniques. When measuring temperatures with thermocouples use appropriate cold junction temperatures and measuring equipment.

(f) Let both pieces "soak" several hours monitoring temperatures and gage readings in order to establish all of the initial readings accurately.

(g) Monitor the compensating block as often as possible to ensure that the strain indicator is consistent. Do not move or disturb the compensating block in any way once the testing is begun.

(h) Record the initial thermocouple and strain gage readings. Remove the test piece from the container and remove the thermocouple from the inside wall.

(i) Mount the test piece in the chuck (described previously) making sure that the wires are out of the way by wrapping them around the chuck and taping securely.

(j) Index the test piece to center using a dial gage, to a tolerance of $\pm$ .0005".

(k) Measure the ID of the bore using an appropriate bore gage. Measurement should be accurate to $\pm$ .0002"

(l) Take the desired depth of cut with the boring bar and the appropriate tool. If necessary take a clean up cut of about .005" to leave the inside of the bore as smooth as possible.

(m) Remove the test piece from the lathe and replace the thermocouple on the inside surface by resistance welding.

(n) Replace test piece in container and allow sufficient time for the test piece and the compensating piece to come to thermal equilibrium. This requires about two hours minimum.

(o) When thermal equilibrium has been established, repeat steps (h) through (n).

Figures 24 through 26 are photographs showing the test specimens in different steps of the process.

D. Results from Process

Figure 27 is a plot of the stress pattern calculated using the computer program developed to reduce the experimental data obtained in the boring out process. The compression hoop stress at the bore of the tube was found to be lower than expected in the first barrel tested. Other stress results will be listed in the sections describing the methods used to produce them.

8. Radial Piston Effects

It was decided to use a cylinder inside the bore of the tube to be autofrettaged which would contain the explosives and thus act as a piston in the fashion that a piston is sometimes used in shock tube experiments to prolong the time that flow takes place. A tube was autofrettaged using a 0.5 in. O.D. tube of 304 stainless steel to contain the explosive charge. The residual stress in this tube was found to be 47,000 psi which is about 50% higher than that obtained without the tube. Since the analysis indicates that the mass of the piston affects the duration of the pressure pulse on the inside of the tube, a lead tube was used as the piston in another experiment. A linear charge density of approximately 2 g. per inch was used and the residual deformation of the tube was found to be 8%. This value is almost three times the value to be expected with no piston used. The residual stress pattern in the tube expanded using the lead piston inside the bore and was determined to be about 42,000 psi which was lower than that found using the 1/2 in. diameter stainless steel piston.

In order to eliminate differences due to the diameter of the piston used, a tube was expanded using a 3/4 in. diameter stainless steel piston which matches the diameter of the lead tube used. The residual stress in this tube was found to be 46,000 psi. The difference in the residual stress was felt to be due to the lead piston giving when the shock wave from the inside of the tube was reflected back to the piston, while the stainless steel, being of much higher strength than the lead, was able to hold its position and thus maintain the pressure in the tube a little longer.

In order to check the effect of confining the ends of the tube to prevent the water from flowing out of the tube, a fixture was built as shown in Figure 28. The extra pieces at the ends of the tube were used to allow the shock wave to be more stable as it passed through the tube to be expanded and thus reduce end effects. Two tubes were expanded in this fixture using charges 14 inches long of 1.04 grams/inch of Detasheet, one with a 3/4 inch O.D. lead piston, the other with a 3/4 inch O.D. stainless steel piston. The residual stress found in these tubes was:

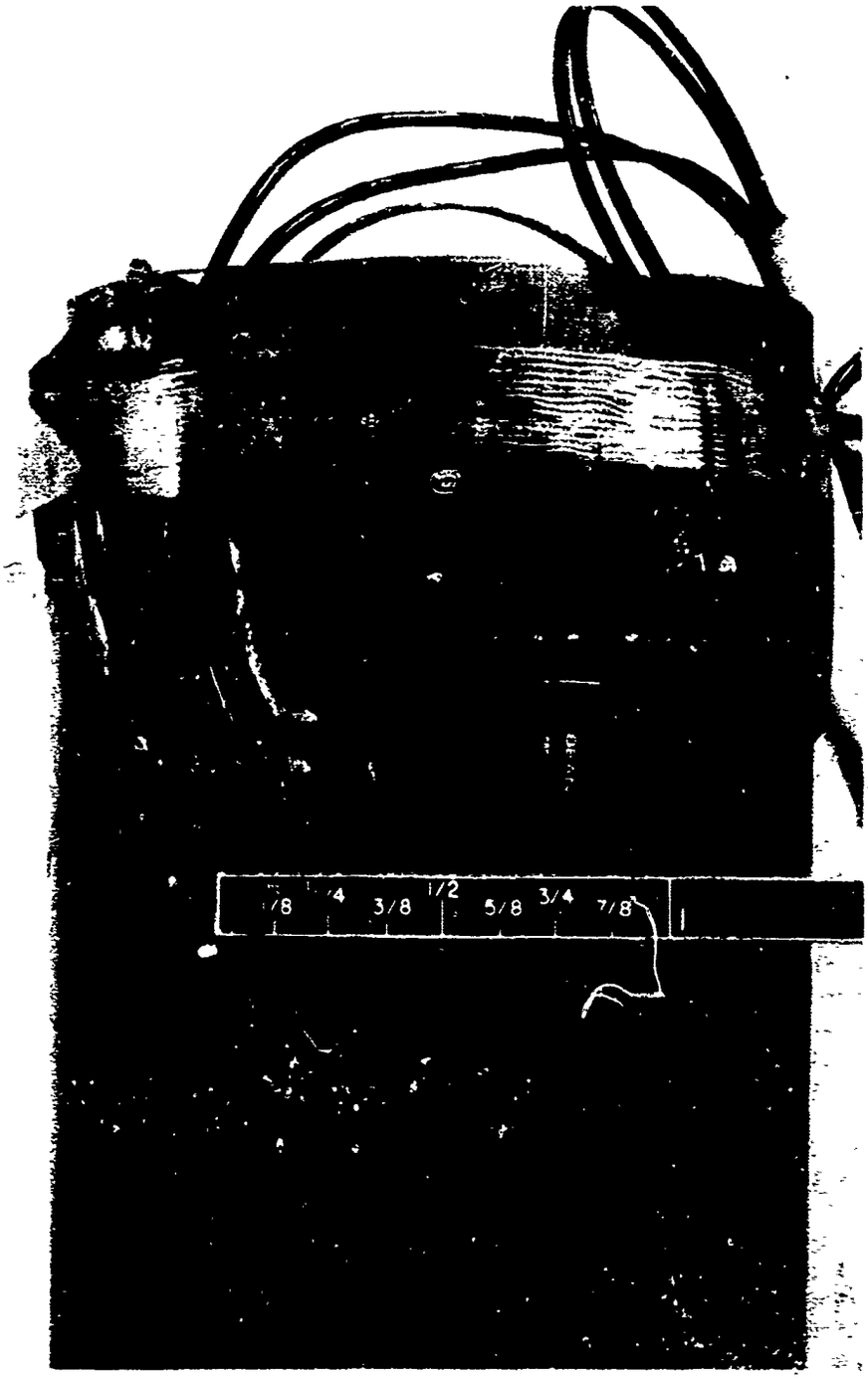

Figure 24 Test Specimen Showing Strain Gages

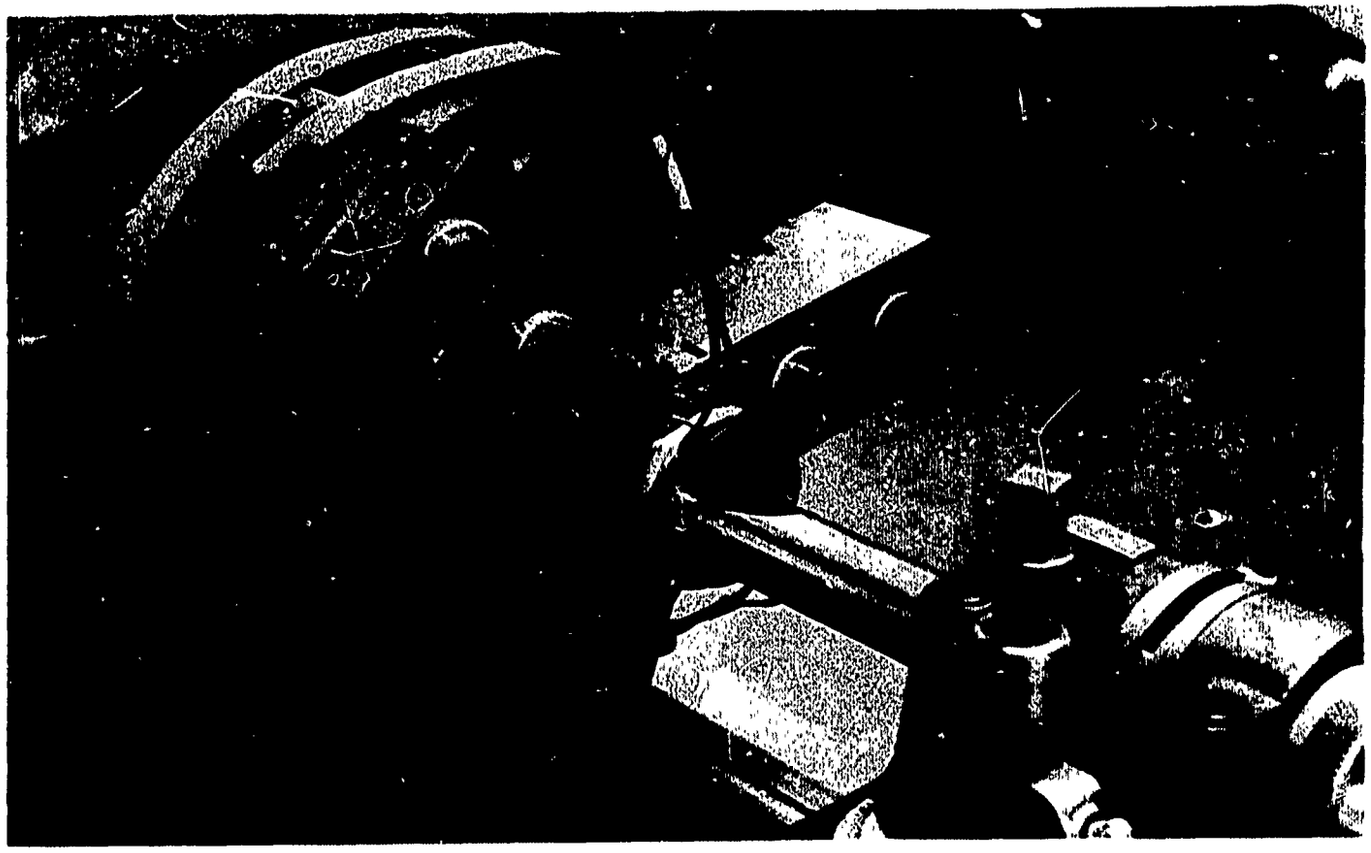

Figure 25 Test Specimen Mounted in Lathe

Figure 26 Test Specimen in Different Stages of Boring Out

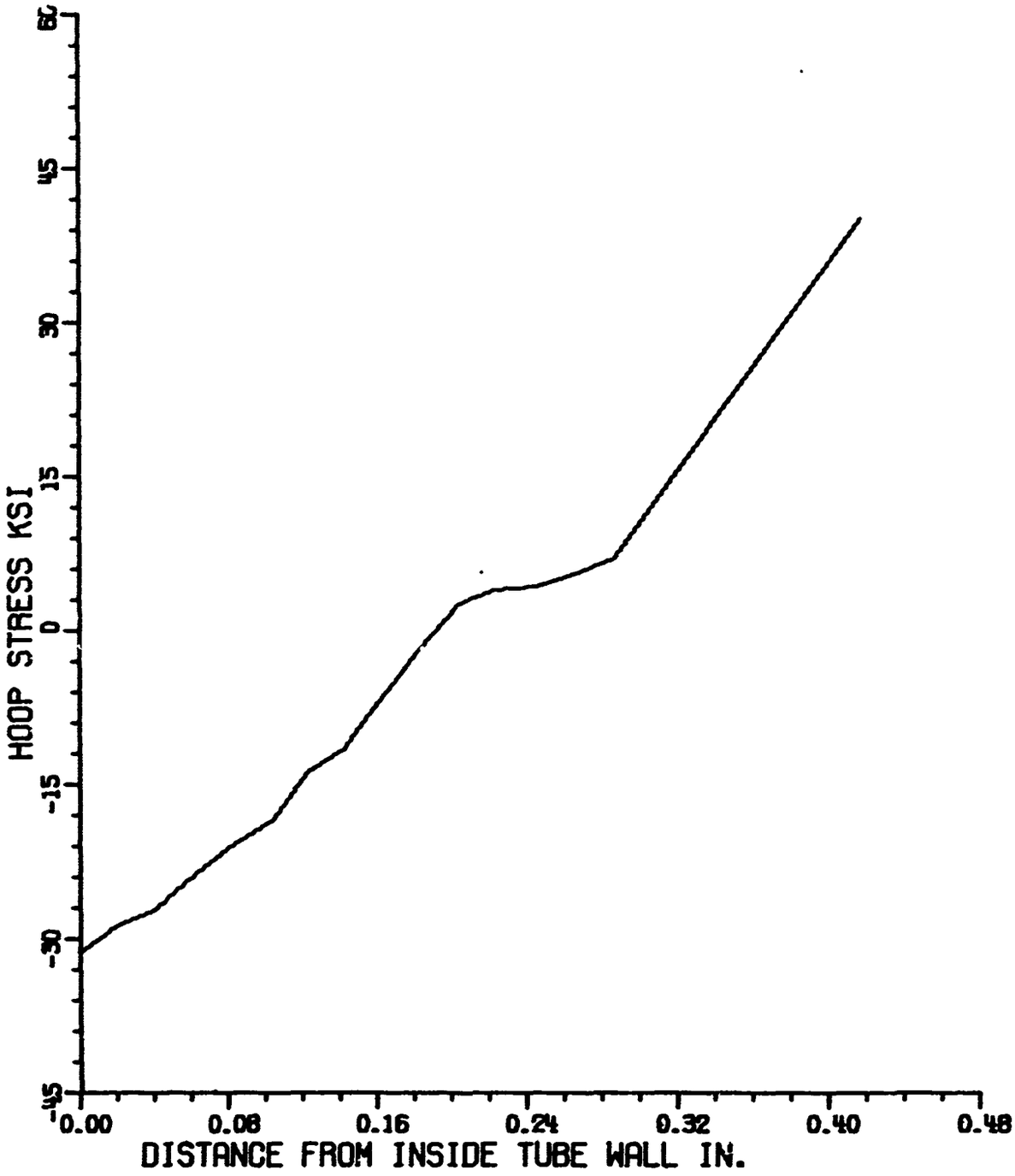

Figure 27 Residual Stress Pattern in Tube

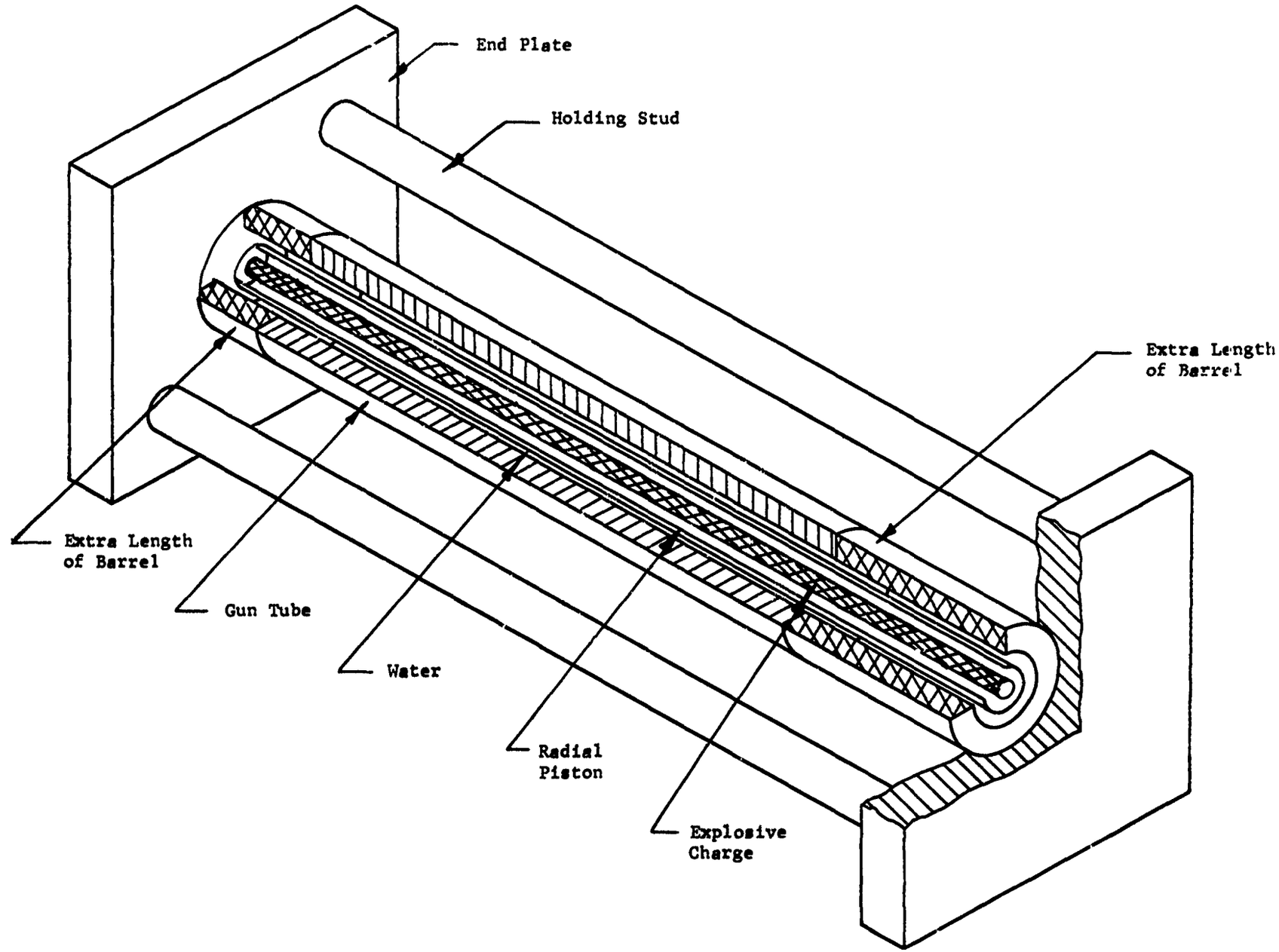

Figure 28 Test Fixture Used to Confine the Ends and Reduce End Effects

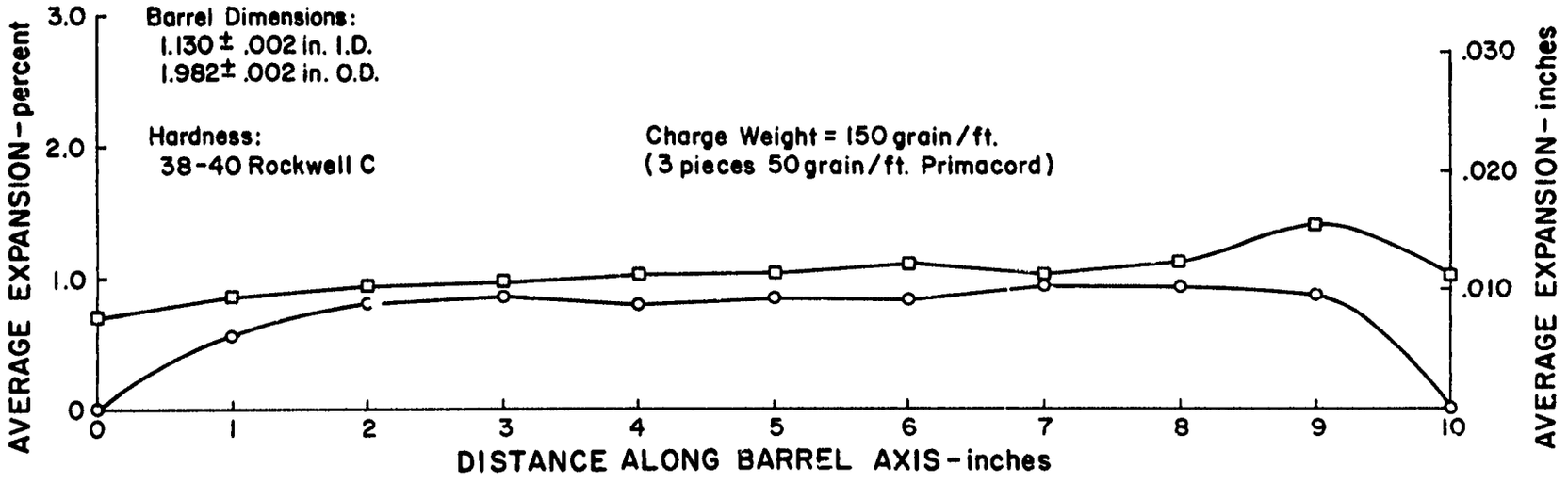

Figure 29 Bore Expansion of 1/5th Scale Tube using Primacord Charge. Upper Curve Obtained using Containment Fixture

stainless steel piston - 52,000 psi
lead piston - 50,000 psi

A tube was expanded without the fixture using the 3/4 inch O.D. stainless steel piston and a piece of 400 grains per foot primacord 10 inches long as the charge. This tube showed a residual deformation of 6.8% which was somewhat higher than expected. The residual stress at the bore was found to be about 74,000 psi. In order to further check this effect two more tubes were expanded, one using the confinement fixture and the other with the ends unconfined. The charge for these two shots was three lengths of 50 grain per foot primacord taped together so that the tendency of the primacord to curl was minimized and a straight explosive charge was obtained. The residual deformation in these two tubes is shown in Figure 29. The residual stress pattern in the wall of the tube expanded in the fixture is shown in Figure 30.

In order to check the scaling laws, a tube 20 inches long which was a 40% model of the breech section of the 152 mm gun tube was expanded using three lengths of 200 grain per foot primacord in a 1½ inch O.D. stainless steel radial piston. The residual deformation at the bore of the tube was approximately 2%. This value is somewhat higher than expected; however, the smaller diameter primacord used in the 20% scale tests is not as efficient as the larger primacord used in the 40% tests. Also, the pressure pulse does not scale exactly, but is expected to be somewhat longer in the larger diameter tube. Both of these effects would tend to produce greater deformation.

This tube was sectioned to obtain specimens for the residual stress checks and to use in making a 40% confinement fixture like that used in the 20% tests. A 40% scale tube was expanded using the fixture with a residual deformation of approximately 2.2%. This tube was sectioned to obtain bore out specimens for residual stress determinations. The residual deformation is shown in Figure 31.

One of the parameters which is very important in controlling the residual stress pattern developed is the ratio of the period of the breathing mode of the tube to the time constant of the decay of the pressure pulse. The manner in which the pressure pulse decays cannot be predicted analytically so the 40% tube was expected to provide an answer as to whether or not the decay time scaled with the breathing mode. The residual stress at the bore of the 40% tube was found to be low, approximately 35,000 psi. This indicates that the time constant of the decay of the pressure pulse is not increasing with the period of the breathing mode when a scale up is made.

While the residual stress determination on the 40% tubes was in progress four tubes were expanded in the fixture using a charge of three strands of 50 grain per foot PETN primacord in a 3/4 inch O.D. stainless steel piston. The repeatability of the residual deformation along the length of each tube was very good. The residual stress determination was held up

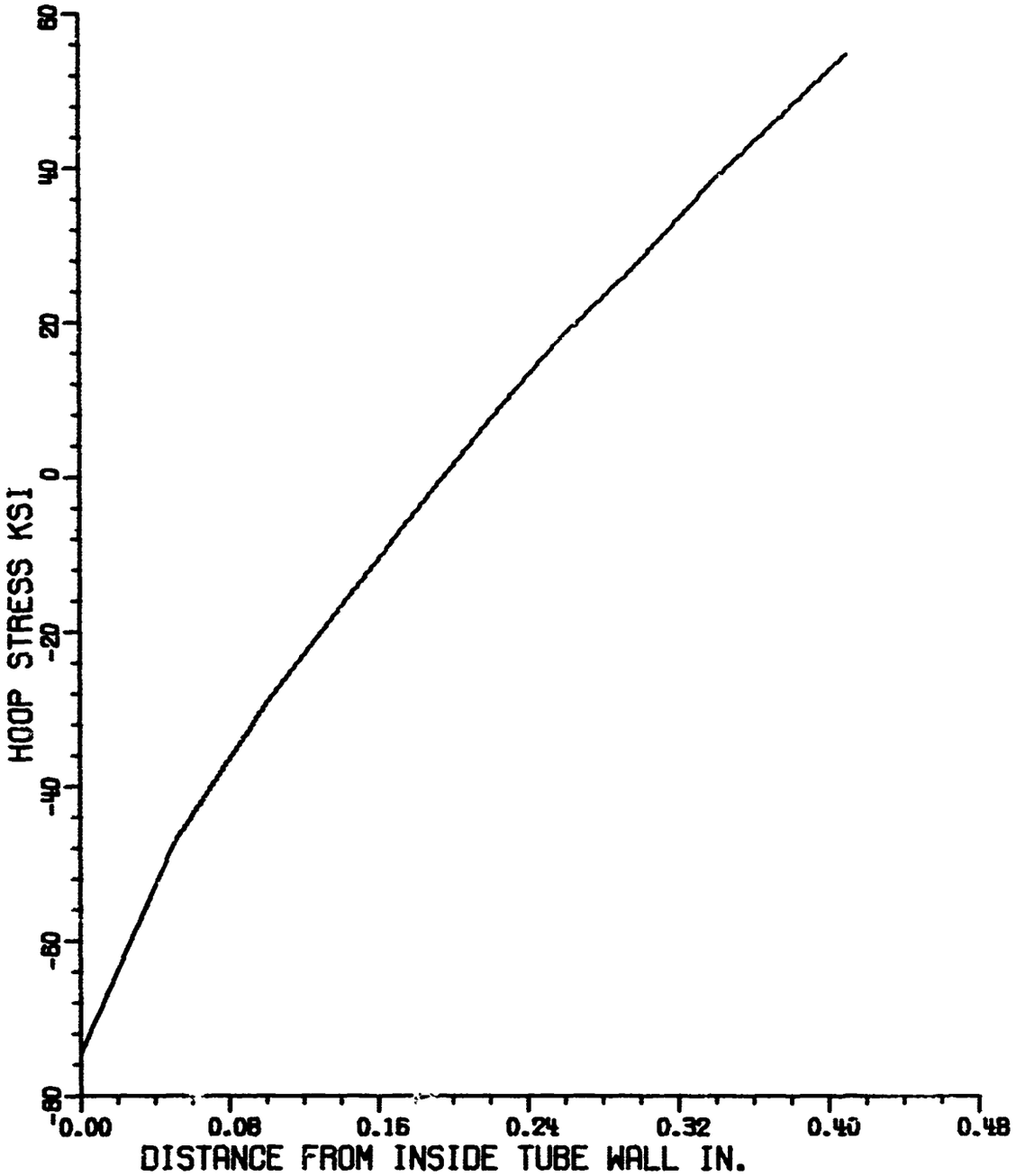

Figure 30 Residual Stress in 20% Tube Expanded in Fixture

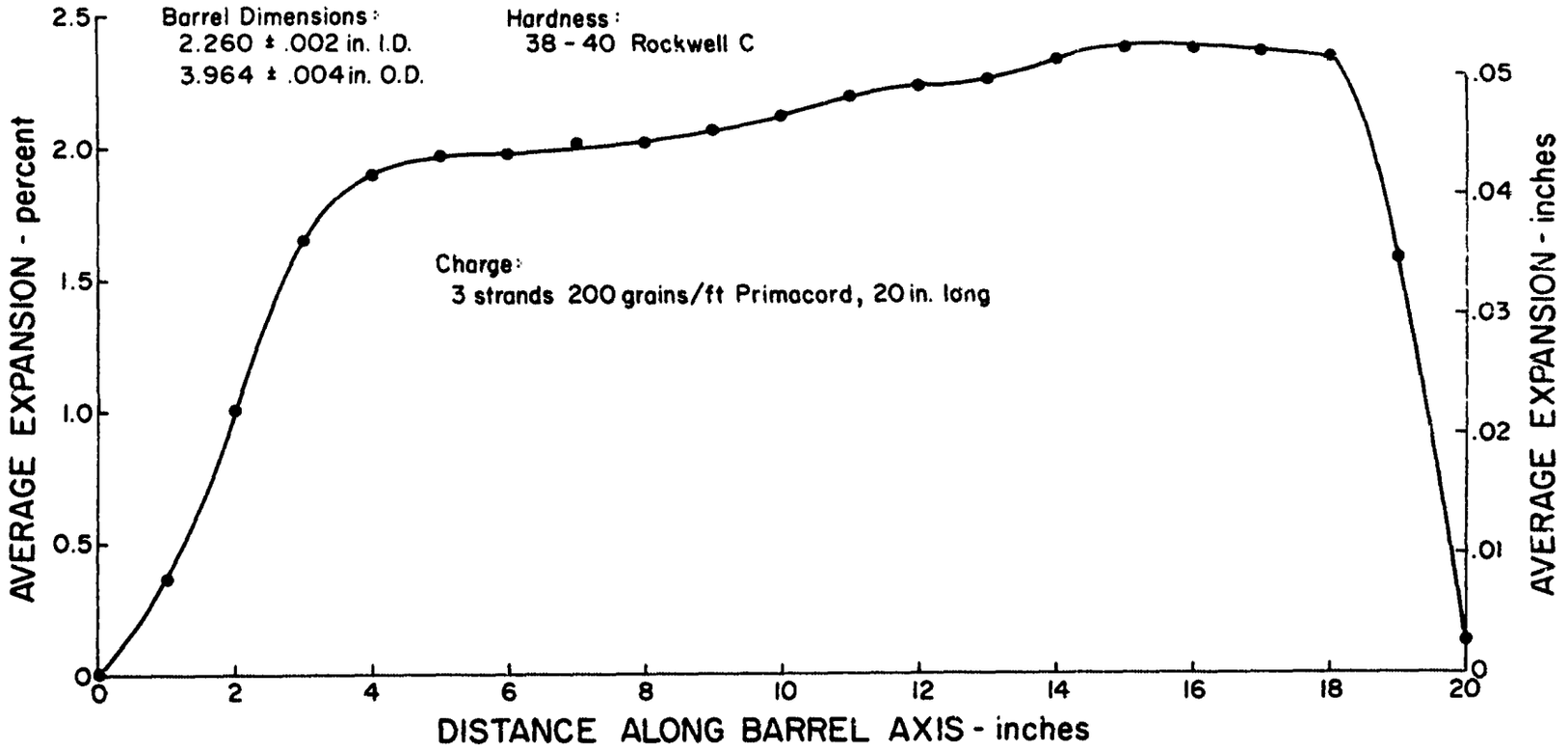

Figure 31 Residual Deformation of 40% Tube

waiting completion of that on the 40% tubes. After the information from the 40% tubes was obtained, it was decided to forgo the residual stress determination on the 20% tubes. Figure 32 shows the residual deformation of the 20% tubes and the first tube expanded in this manner plotted against the distance along the tube from the initiation end of the tube.

Two approaches to reducing the effect of the decay time of the pressure pulse were tried. One was to close the ends of the tube with plugs which would expand and seal the ends of the tube. The fixture used to accomplish this has been shown in Figure 2. The second was to reduce the peak pressure and expand the duration of the pressure pulse. Two different methods of accomplishing this have been tried: 1) the standard explosives with air instead of water inside the piston, and 2) a lower detonation velocity explosive with the piston filled with the explosive.

Results from the test using air surrounding the explosive in the piston indicate that the symmetry, both of the charge itself and of its placement in the piston, is very important when the charge is enclosed in air. Two low detonation velocity explosives were used to check the other approach. A 20% scale tube was expanded using a 3/4 inch O.D., 1/16 inch wall, 304 stainless steel piston filled with SWF-6, a material available from the Trojan Powder Company as a powder. The peak Pressure from this material was apparently not high enough to cause the tube to yield completely. The residual deformation, however, of 0.4% is above the minimum value specified in the Watervliet drawing for tubes made of 170,000 psi material. Figure 33 shows the residual deformation of the 20% tube. The large expansion of the ends is due to using an interference fit in the end seals. Similar tests using SWP-2, a material with a detonation velocity of 9,000 ft/sec as opposed to 7,500 ft/sec for the SWP-6, resulted in a residual deformation of just under two percent, which is the maximum value listed in the Watervliet drawings. The residual stress pattern of the tube expanded using SWP-6 has been checked and the stress at the bore was found to be 106,000 psi. The residual stress determination of the tube expanded using SWP-2 shows the stress at the bore to be 83,000 psi.

In ordering explosives to complete the program it was found that the SWP-2 material was more readily available in a uniform state in this location. The SWP-6 would be available from the factory in Pennsylvania. Figure 34 shows the residual deformation of two tubes expanded using SWP-2 as delivered and after drying in vacuum. There is a definite change in the packing characteristics of the material if it is not absolutely dry. When the material is dry it is fluffier and does not settle in handling. This tendency to settle can be seen in the curve denoted with solid dots. The residual stress at the bores of these tubes was found to be 80,000 and 85,000 psi respectively. Two 40% size tubes were expanded using SWP-2 in a 1½ inch O.D., 0.120 wall, 304 stainless steel tube. The residual deformation was between 0.4% and 0.5% along most of the length of the tubes. This is shown in Figure 35. The residual stress at the bore of the tubes was determined to be 72,000 psi and 70,000 psi respectively.

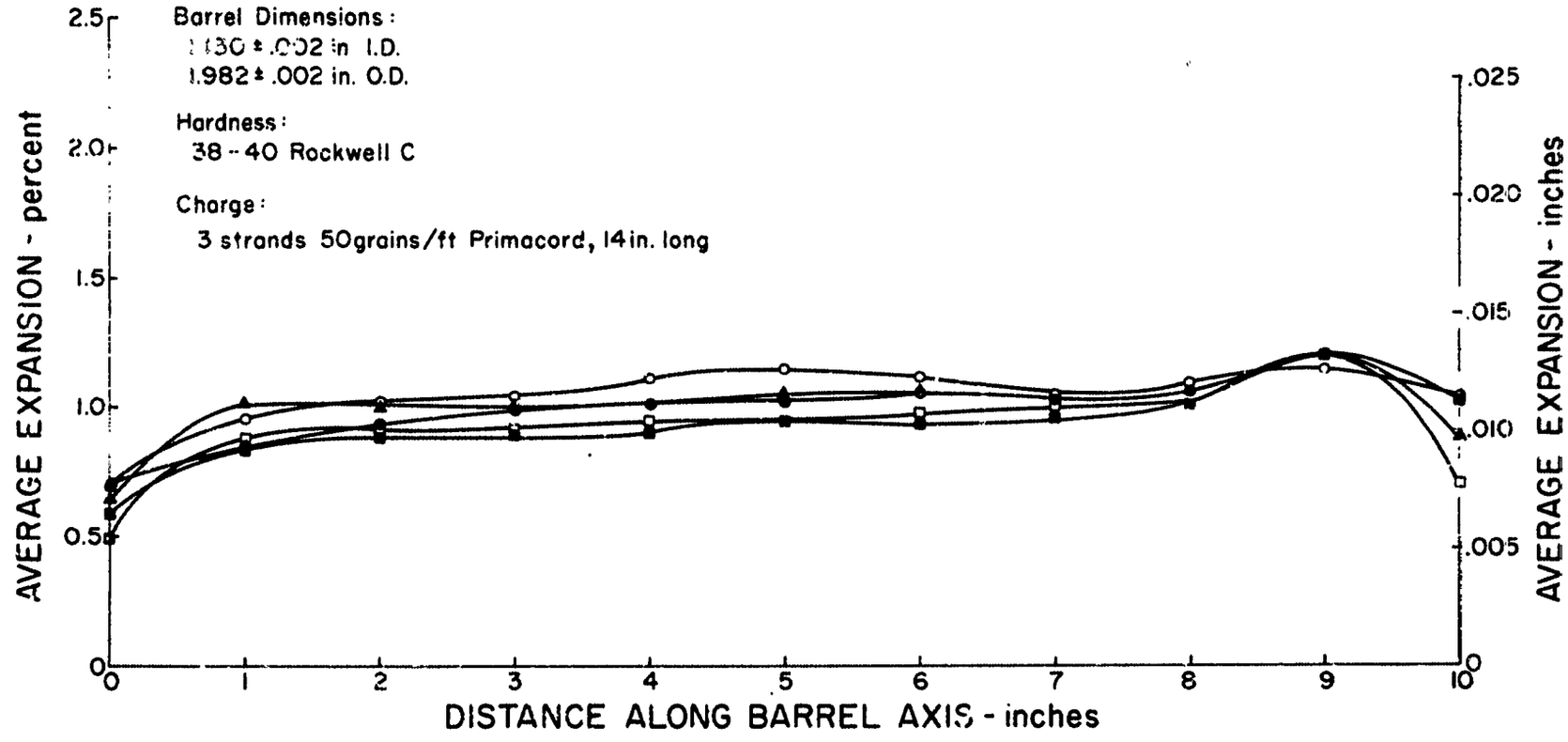

Figure 32 Repeatability of Residual Expansion on 20% Tubes Using Containment Fixture

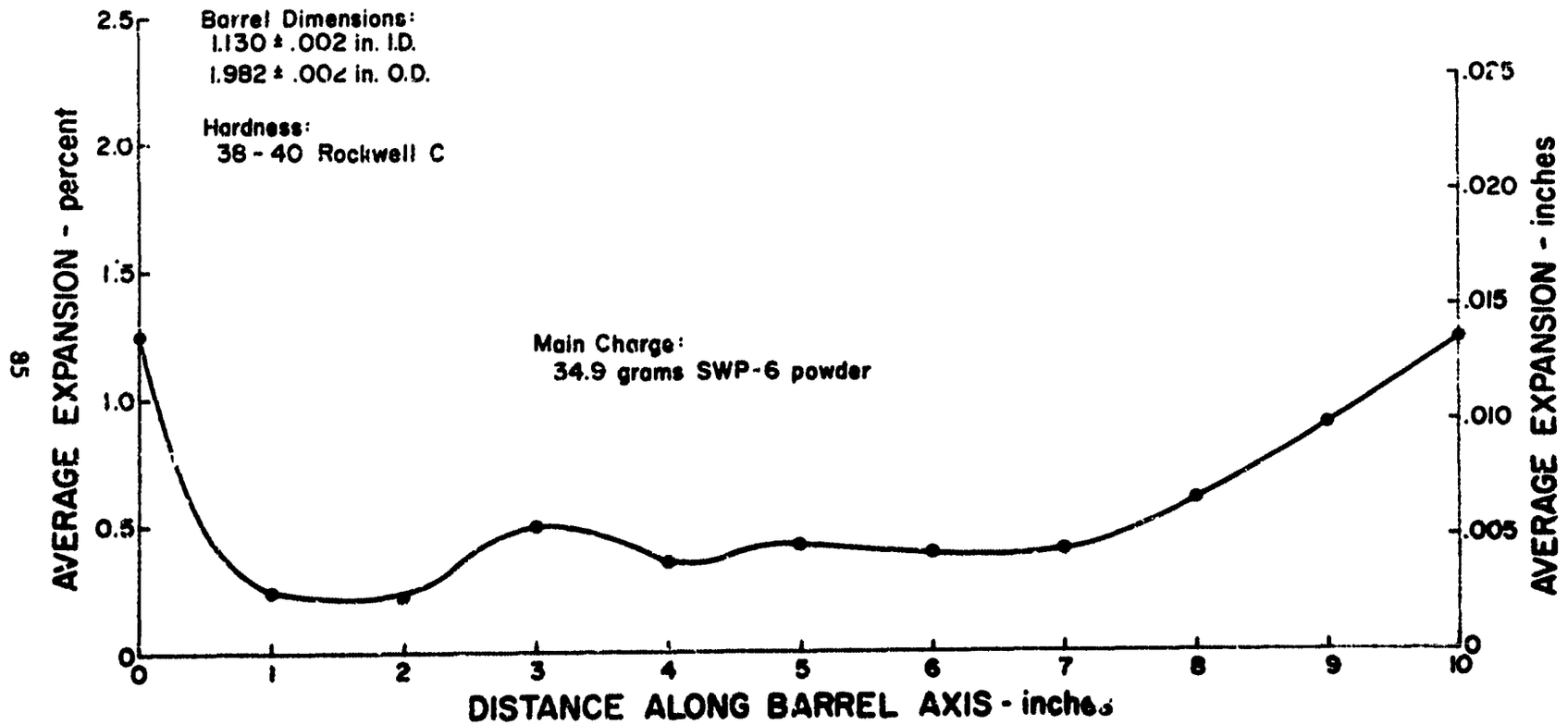

Figure 33 Residual Deformation of 20% Tube Expansion Using SWP-6 Explosive

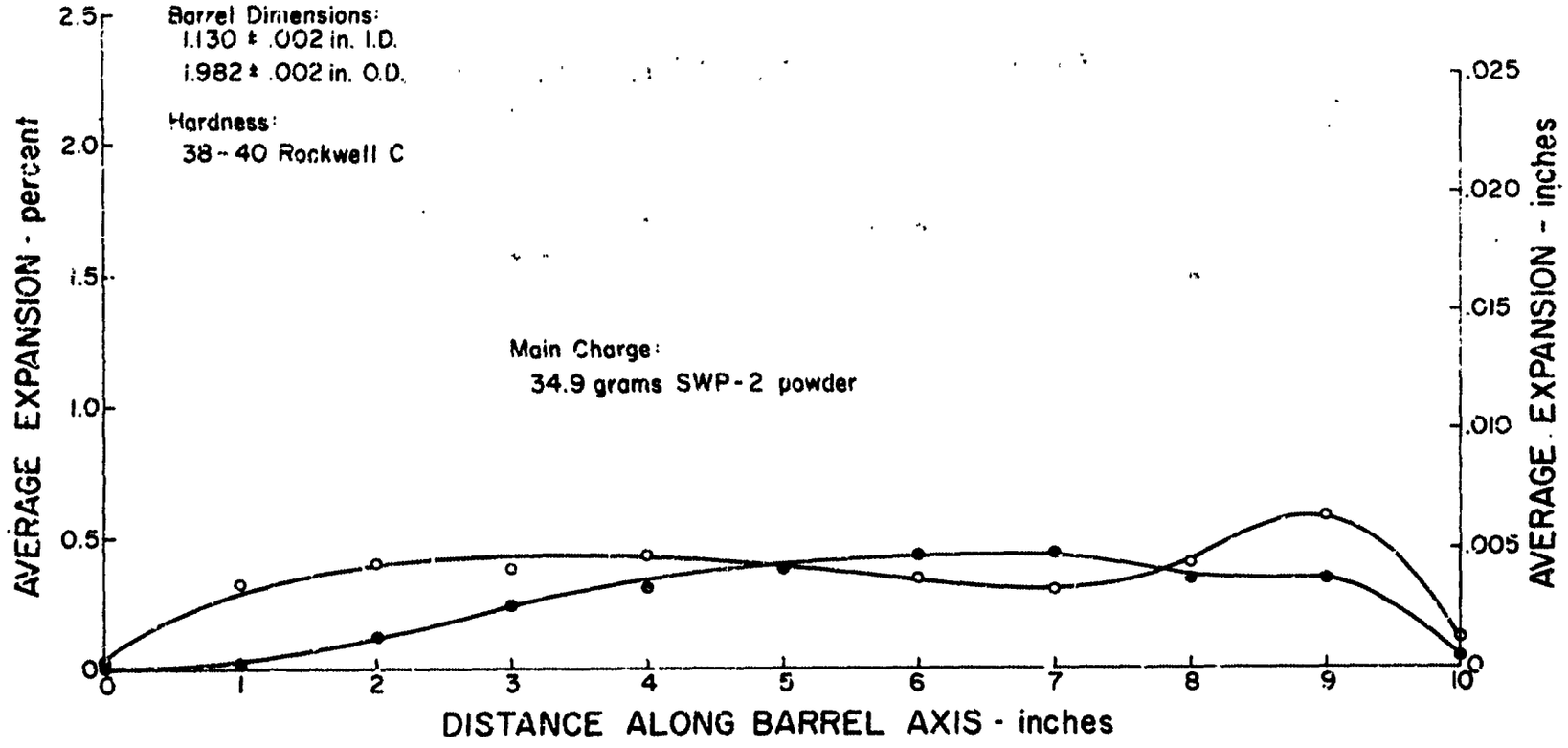

Figure 34 Effects of Packing Density of SWF-2 Powder on Expansion of 20% Tubes

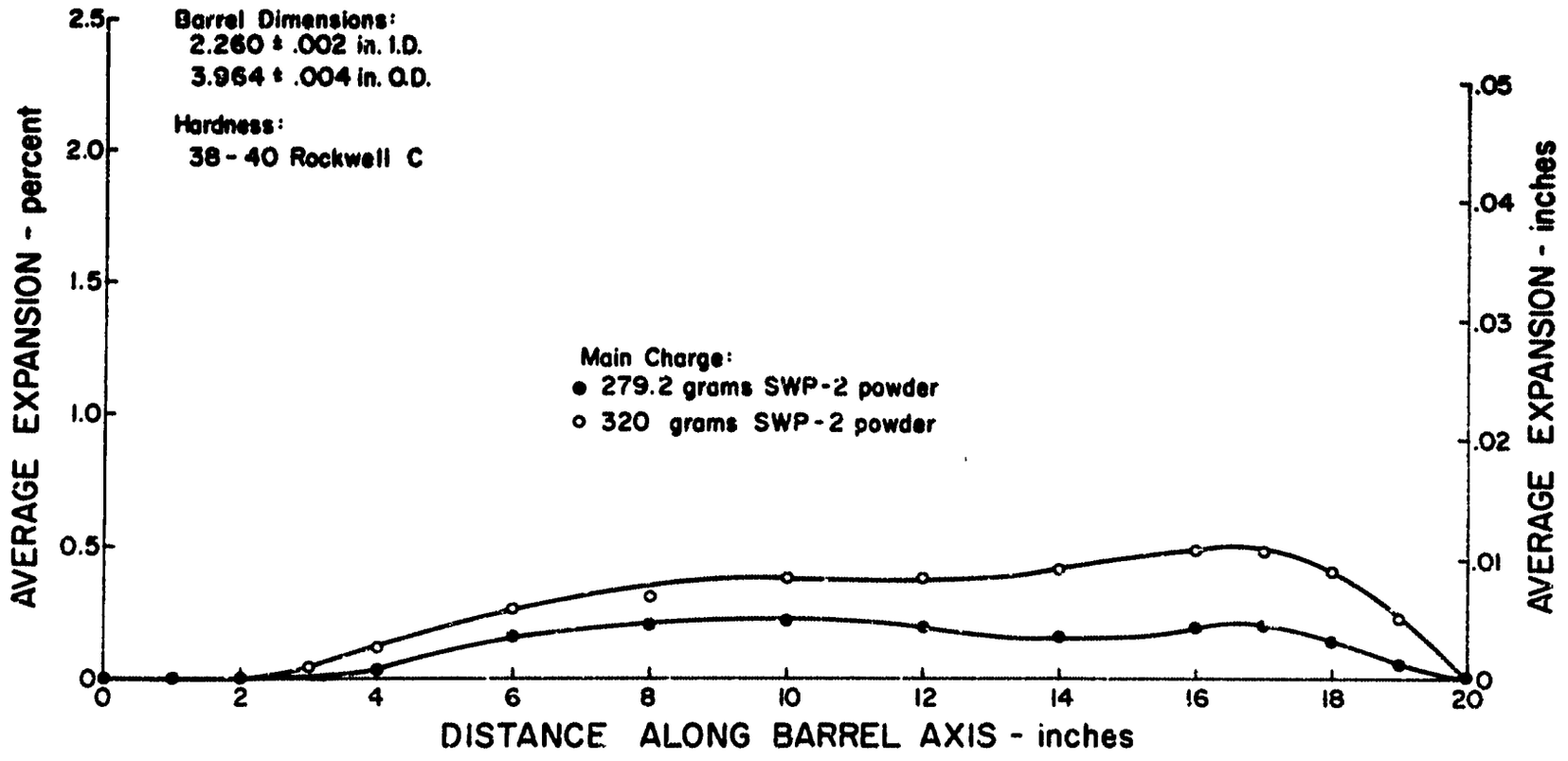

Figure 35 Residual Expansion of 40% Scale Tubes

9. 40% Scale MK81, 152 mm Gun Tube

A. Wall Thickness Effects

A 40% scale model of the MK81, 152 mm gun tube was obtained according to the specifications shown in Figure 36. The previously described bore expansion experiments were conducted on tubes representative of 20% and 40% scale models of the breech section. In the complete gun tube the wall thickness varies from a maximum at the breech to a minimum at the muzzle. Additional experiments were conducted on tube sections with wall thicknesses as represented at A, B, and C as shown in Figure 36. Tubes of these thicknesses were expanded with the same charge as was used for expanding the breech section. The results, along with the data from a breech tube expansion, are shown in Figure 37. As can be seen, the expansion of tubes of thickness B and C are outside the specification limits. In order to bring the expansions into the specification limits, another barrel of thickness C was expanded with a reduced charge. The charge reduction was accomplished by placing a plastic sleeve inside the radial piston which reduced the charge diameter. It can be seen from Figure 37 that the reduced charge brought the expansion into the desired range of expansion.

A radial piston-explosive charge combination was designed for the 40% scale model charge utilizing the data derived from the aforementioned tests. The charge utilized for expanding the breech section proved satisfactory for both the breech thickness and thickness A and was therefore used in the full length charge. The reduced charge proved satisfactory for the muzzle end, thickness C, therefore establishing the charge size there. The charge utilized for expanding the breech section was excessive for thickness B. Based on Figure 37 and ease of fabrication considerations, it was therefore decided to use the reduced charge from thickness C to thickness B and a linearly increasing charge diameter from thickness B to thickness A. The charge used for expanding the 40% scale model MK81, 152 mm gun tube is shown in Figure 38. From Figure 39, it can be seen that the full length charge performed satisfactorily.

B. Explosive Autofrettage Procedure

The following procedure may be used to autofrettage 40% scale models of the MK81, 152 mm gun tube.

1. Powder Charge

The powder charge is 474 grams of SWP-2, an explosive available from the Trojan Powder Company. This explosive must be dry in order to pack to the proper density and yield the correct detonation velocity.

2. Radial Piston

The radial piston is used to contain the powder charge and transmit the pressure from the detonation products to the gun tube walls

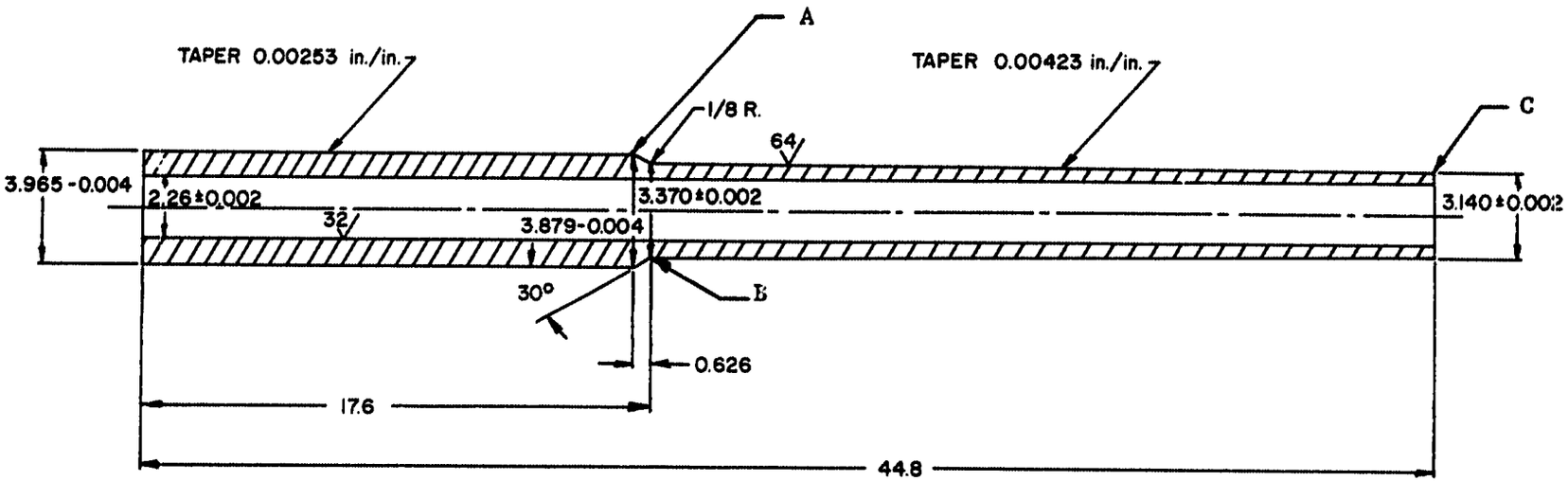

Figure 36 Drawing of 1/2.5 Scale 152 mm Barrel 4340 Steel Heat Treated to 160,000 psi Minimum Yield

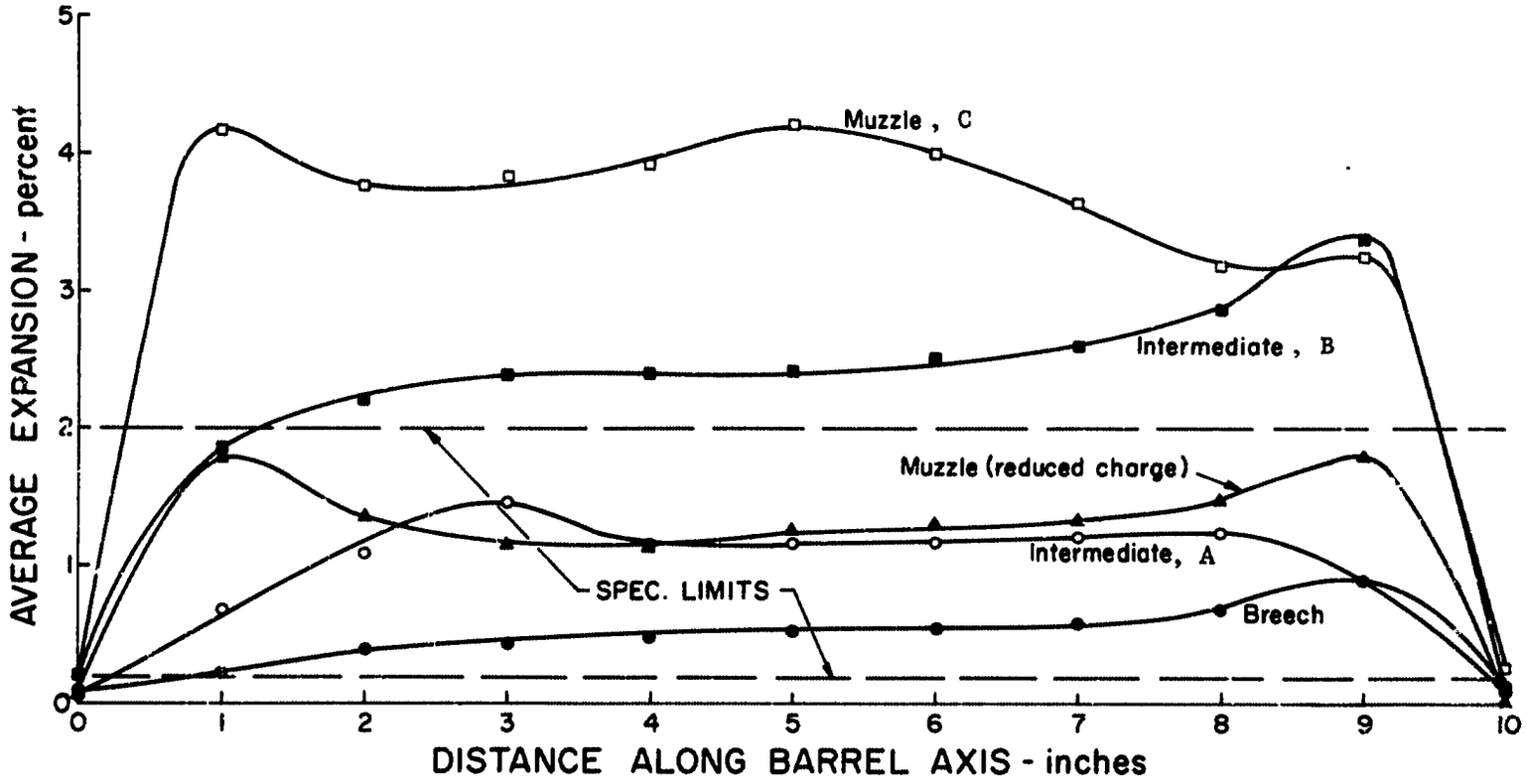

Figure 37 Effect of Tube Wall Thickness on Expansion

through the intervening fluid medium (water). A sketch of the assembled piston with the powder charge in place is shown in Figure 38. The piston is made of 304 stainless steel 1.5 O.D. by 0 ' wall thickness. Stainless steel was used in this and previous te 'nce it was readily available; however, other cheaper material such as mild steel would be suitable for the radial piston material. No attempt was made to optimize the piston material. A plastic sleeve is used to reduce the amount of powder the piston contains per inch in that portion of the piston opposite the thinner parts of the gun tube.

3. Assembly (See Figure 38)

(a) The first step in assembling the piston is to install the sleeve to line one end of the piston. A full size sleeve may be held in place with cement, or a plastic tube of reduced diameter may be centered in the piston and the surrounding void filled with casting resin.

(b) The primacord booster is cut longer than the piston tube and is then pinned in place in the small end seal which fits the end with the plastic liner. This seal is then cemented in place and the cement is allowed to dry.

(c) The piston tube is grounded and the primacord is stretched tight and centered in the piston while the charge of SWP-2 is poured into the piston. The piston is tapped with a rubber mallet to ensure proper packing of the powder charge

(d) The 3/4 inch long foam plug is slipped over the primacord and forced down into the piston.

(e) The seal plug is slipped over the primacord and cemented in place flush with the ends of the piston.

(f) The primacord is trimmed flush with the end seals at both ends and the cut ends of the primacord are sealed with duco cement or another suitable sealer. A small piece of detasheet may be cemented to the primacord at the end of the piston with the plastic liner to insure reliable detonation of the charge.

4. Assembly of Fixture

(a) Make sure the end plugs fit over the ends of the piston without requiring too much pressure to force in.

(b) Set the bottom end plug (the one without the cap hole) into the recess in the lower block of the fixture.

(c) Coat inside bore of tube with a wetting agent such as Kodak Photo-flow.

(d) Lay a bead of rubber caulking compound around the recess in the lower block.

Total Length of Charge - Tube Length + 1½"

Total Length of Liner to be Adjusted so the Center of Taper is Opposite the Center of Shoulder on Tube - 28-5/16"

Main Charge - 474 grams SWP-2

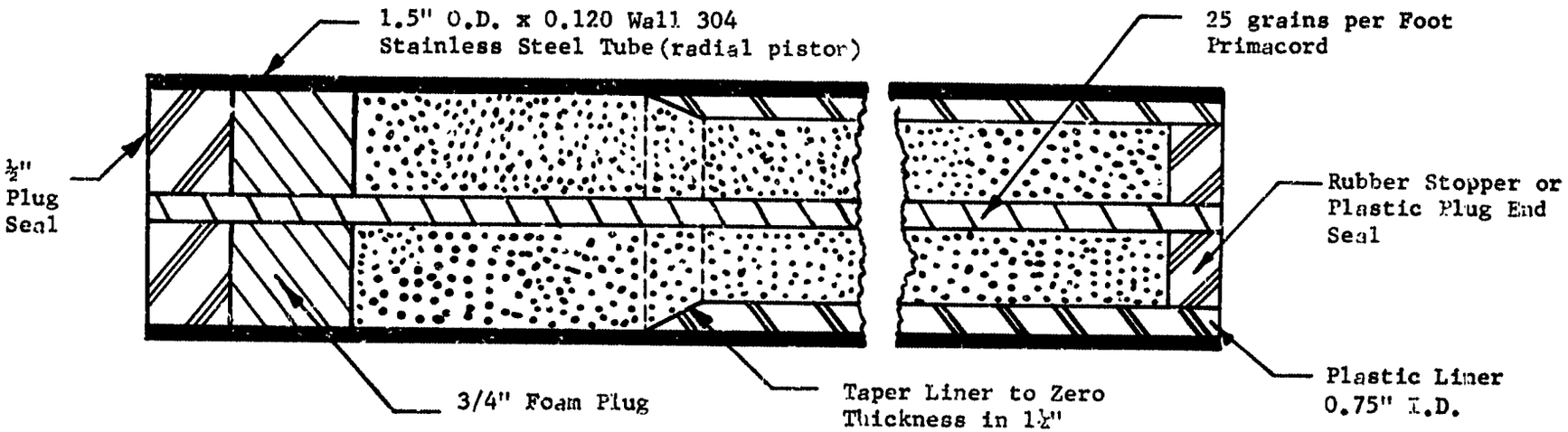

Figure 38 Charge to Autofrettage Tube

(e) Put the gun tube in place with the breech end down. Make sure the caulking compound is squeezed out all around the tube so a waterproof seal is obtained. (Assembly could be accomplished in the horizontal position, however filling the tube with water is accommodated by having it in the vertical position.)

(f) Coat outside of piston with Photo-flow.

(g) Place piston in gun tube and make sure it goes down into the end plug.

(h) Fill gun tube with water.

(i) Place upper end plug over piston and start into bore of gun tube.

(j) Feed cap wire through the hole in the upper block so that the cap is in the plug recess.

(k) Lower upper block down onto gun tube making sure the cap is in the hole provided for it in the upper plug.

(l) Tighten bolts all around taking care that the water seal at the bottom is not broken.

(m) The deflector plate should be placed so that the stream of water from the cap wire hole is directed toward an area where the water will not damage anything.

The assembly is now complete. The shot may be made by placing the assembly into the pool and detonating the charge using usual precautions.

C. Experimental Results

The scale gun tube was expanded as in the foregoing procedures. The residual deformation along the tube is shown in Figure 39. This tube was heat treated so the hardness checked at Rockwell C 42 which indicates the material is at the upper limit of the strength range. The residual deformation of the bore of the tube in the breech section is thus above the minimum values. The residual stress in this tube was checked in a section taken from the breech 3 inches from the end of the tube and was found to be 76,000 psi.

Utilizing the process developed at the University of Denver, an additional two 40% scale 152 mm gun tubes were autofrettaged at the Martin Marietta Denver Division. Bore and outer diameter measurements along with hardness data were obtained prior to autofrettage by Martin Marietta personnel. Hardness readings of Rockwell C 42 for both barrels indicated that the barrels were at the upper limit of the strength range. Once the two barrels had been autofrettaged and allowed to reach thermal equilibrium, bore and outer diameter data were obtained. The bore expansions are shown as curves #2 and #3 in Figure 39. It can be seen that the expansion for the three barrels is quite similar except for barrel three at the muzzle end. The excessive growth in

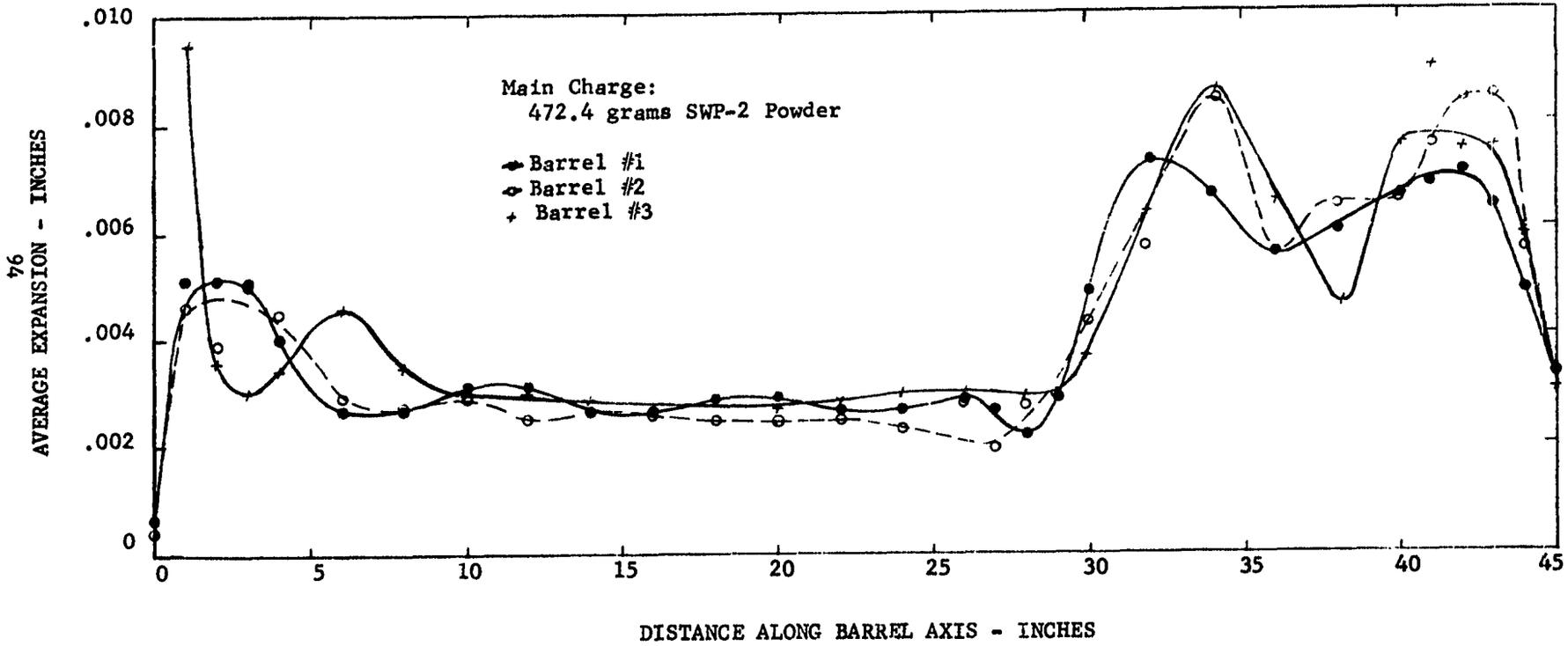

Figure 39 Residual Deformation Along the Bore of 40% Scale MK 81, 152 mm Gun Tubes

the diameter at the muzzle end is a direct result of a fixture failure. The end plug which fits in the muzzle expanded during the autofrettage process, resulting in an over expansion of the bore at that point. This problem could be circumvented had a stronger material been utilized for the end plug.

Once the bore expansion data had been acquired, the barrels were sectioned and prepared for the residual stress determination. The Sachs boring out method, as described in IV.7, was used to obtain the required strain data. Having obtained this strain data, the computer program previously listed was employed to yield the residual stress at the bore. These values of residual stress were 78,100 psi and 80,900 psi for barrels two and three respectively.

10. Full Size 105 mm Gun Tube Breech Section

A breech section of a 105 mm gun tube was explosively autofrettaged using the techniques previously derived. The tube had a nominal bore diameter of 3.80 in., a nominal outer diameter of 7.41 in., and a nominal length of 50 in. Since this gun tube was a 105 mm breech section, the process developed for the 152 mm gun tube was not directly scaleable to the 105 mm gun tube. The scale factor for scaling the bore diameter of the 40% scale model 152 mm gun tube to the bore diameter of the 105 mm gun tube was calculated as 1.675. Using this scale factor, the wall thickness of the 105 mm gun tube was found to be greater than that resulting from scaling down the wall thickness of the 152 mm gun tube. In checking the standards for 304 stainless steel tubing, it was found that the closest standard tube had an outer diameter of 2.50 in. and a wall thickness of 0.250 in. Due to the additional wall thickness in both the radial piston and the 105 mm gun tube, a suitable charge had to be designed. Using the 1.675 scale factor, the following parameters were calculated:

$$n = 1.675$$

$$\text{Charge Diameter} = 2.11 \text{ in.}$$

$$\text{Wall Thickness (radial piston)} = 0.201 \text{ in.}$$

$$\text{Outer Diameter (radial piston)} = 2.512 \text{ in.}$$

$$\text{Length of Charge} = 53.45 \text{ in.}$$

These parameters would be the exact requirements had the wall thickness of the 105 mm gun tube been scaleable. Since the 105 mm gun tube was thicker, the SWP-2 was packed to a slightly higher density and 100 grains per foot primacord was utilized instead of the 70 grains per foot as calculated. Both changes resulted in a slightly higher explosive charge which would partially compensate for the increased wall thickness in the 105 mm gun tube and the radial piston. Based on the test results shown in Figure 37, it was anticipated that the bore expansion of the 105 mm gun tube would fall within the acceptable limits for the 152 mm gun tube.

A radial piston-charge was fabricated along with a holding fixture similar to the fixture shown in Figure 2. The procedure in sections 2, 3, and 4 was modified for use with the 105 mm gun tube and the tube was shot.

After the 105 mm gun tube was expanded, the residual deformation was measured and is shown in Figure 40. It can be seen that the residual deformation is well within the 0.2% to 2.0% expansion range used for 152 mm gun tubes. Once the bore expansion data was obtained, the barrel was sectioned and prepared for the residual stress determination. Using the Sach's boring out method and the computer program, the residual stress at the bore of the 105 mm gun tube was found to be 82,700 psi.

V. RESULTS AND CONCLUSIONS

The analysis indicates that decay rate and peak pressure produced by the explosion must be controlled in order to obtain residual compressing dynamically which is the same magnitude as that obtained statically. By using a radial piston to contain the explosive and selecting the proper explosive characteristics, it has been demonstrated that residual stresses of the proper magnitude can be obtained. The experiments conducted on both the 152 mm configurations and the 105 mm configuration indicated that the process can be scaled with predictable results. In addition, the proper expansion of the 105 mm gun tube breech section indicates that the charge parameters are not hypercritical in successfully achieving residual stresses of the correct magnitude. The technical feasibility of explosively autofrettaging cannon barrels has thus been demonstrated.

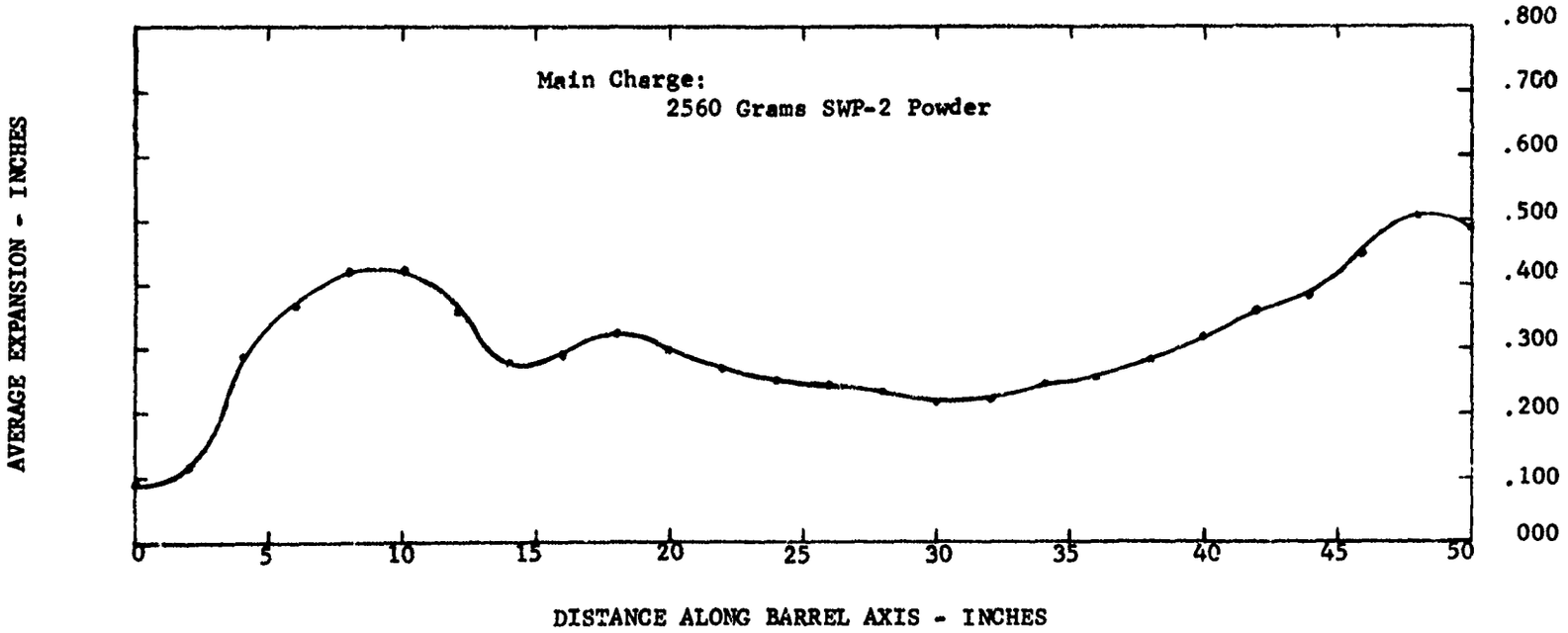

Figure 40 Residual Deformation Along the Bore of the Breech Section of a 105 mm Gun Tube

Unclassified

Security Classification

DOCUMENT CONTROL DATA - R & D

(Security classification of title, body of abstract and indexing annotation must be entered when the overall report is classified)

1 ORIGINATING ACTIVITY (Corporate author)

Martin Marietta Corporation
Denver Division
Denver, Colorado

Denver Research Institute
University of Denver
Denver, Colorado

2a. REPORT SECURITY CLASSIFICATION

Unclassified

2b. GROUP

3 REPORT TITLE

Explosive Autofrettage of Cannon Barrels

4 DESCRIPTIVE NOTES (Type of report and inclusive dates)

Final Report - April 24, 1969 to February 24, 1971

5 AUTHOR(S) (First name, middle initial, last name)

Knight, R. E.; Kaplan, M. A.; Fay, R. J.; Ching, L. K. W.; Mote, J. D.

6 REPORT DATE	7a. TOTAL NO OF PAGES	7b. NO. OF REFS
February 1971	97	

8a. CONTRACT OR GRANT NO	9a. ORIGINATOR'S REPORT NUMBER(S)
DAAG46-69-C-0061	
b. PROJECT NO	AMMRC CR 70-25
D/A 1T062105A328	
c. AMCMS Code 5025.11.29400	9b. OTHER REPORT NO(S) (Any other numbers that may be assigned this report)
d.	MCR 70-421

10 DISTRIBUTION STATEMENT

This document has been approved for public release and sale; its distribution is unlimited.

11 SUPPLEMENTARY NOTES	12. SPONSORING MILITARY ACTIVITY
	Army Materials and Mechanics Research Center Watertown, Massachusetts 02172

13 ABSTRACT

The object of this program was to determine the feasibility of autofrettaging cannon barrels with explosives. The study involved determining the applicability of, the reliability of, and the scaling laws associated with the process. The results of this study provide the basis for the establishment of specifications and procedures for the explosive autofrettage of 152 mm gun barrels. The study consisted of mutually supportive experimental and analytical programs conducted concurrently.

An experimental process was undertaken to determine the expansion produced at the bore of a tube, which modelled the breech section of the 152 mm gun tube, due to different amounts of explosive material along the bore of the tube. It was found that the explosive process could be controlled to produce the desired residual bore expansion.

Using results of the analysis to make changes in the experimental approach, a method of expanding the tubes explosively was developed which gave acceptable results in both the 20% and 40% models of the breech section and also with a 40% scale model of the entire M81, 152 mm gun tube. The process was scaled up and applied to a breech section of a 105 mm gun tube.

DD FORM 1 NOV 68 1473 REPLACES DD FORM 1473, 1 JAN 64, WHICH IS OBSOLETE FOR ARMY USE.

Unclassified

Security Classification

14 KEY WORDS	LINK A		LINK B		LINK C	
	ROLE	WT	ROLE	WT	ROLE	WT
Strain Rate						
Residual Stress						
Explosive Autofrettage						
Scaling Laws						
Stress Analysis						
Autofrettage						
Gun Barrels						
Model Tests						

AD - 718 817

ERRATA

The following corrections should be made to report AMMRC CR 70-25 entitled "Explosive Autofrettage of Cannon Barrels" dated February 1971.

p. 13 Line 12 should read:

following elastic loading. The evaluation of 1.31 at $t = t_o$ shows that

p. 32 Equation 5.2 should have } after $- \frac{I_n}{P_s}$.

p. 33 Equation 5.5 should have] after $- \eta_n]^2$.

p. 34 Line 28 should read:

The stress field in the plastic region $a \leq r \leq \lambda$ depends on the sign of

p. 37 Equation 7.4 should have] after

$$\left[\frac{\frac{1}{r^2} + \frac{1}{b^2}}{\frac{1}{a^2} - \frac{1}{b^2}} \right] .$$

Lines 13 and 14 should read:

... If $t = t_j$ at the end of reyielding, then behavior for $t = t_j$ is ...

p. 73 Lines 25 and 26 should read:

used. The residual stress pattern in the tube expanded using the lead piston inside the bore was determined...

p. 97 The ordinate of Figure 40 should read:

AVERAGE EXPANSION - PERCENT